Experimental Analysis of Infectious Passenger Isolation System for Aircraft

by

Ian David Darrah

B.S., Kansas State University, 2016

A THESIS

submitted in partial fulfillment of the requirements for the degree

MASTER OF SCIENCE

Department of Mechanical and Nuclear Engineering
College of Engineering

KANSAS STATE UNIVERSITY
Manhattan, Kansas

2018

Approved by:

Co-Major Professor
Dr. Mohammad H. Hosni

Approved by:

Co-Major Professor
Dr. Byron W. Jones

Copyright

Abstract

Limiting the spread of infectious airborne diseases and airborne pathogens is an important consideration in aircraft environmental control system design. However, when a passenger suspected of having a highly contagious disease or very dangerous disease is identified in flight, it is desirable to further isolate the individual from other passengers. A research project was conducted to explore an isolation system that can be stored in a small space and deployed in flight if needed. This device is referred to as an "Expedient Passenger Isolation System" abbreviated as ISOPASS. The ISOPASS is a portable, negative-pressure isolation system that can be installed over a section of seats quickly by a flight attendant during flight. A prototype proof of concept ISOPASS was evaluated in this study. Measurements were conducted in a full-scale, 11-row mock-up of a wide-body aircraft cabin, as well as a 5-row section of a narrow-body aircraft cabin. Heated mannequins to simulate the thermal load of passengers inside the cabin were seated in the mockup. Carbon dioxide was used as a tracer gas and was mixed with helium to maintain neutral buoyancy in air. The tracer gas was used to simulate airborne pathogen spread and was injected at the breathing level at a seat within the ISOPASS. Tests were conducted with and without the ISOPASS in place. Matched pairs were used to mitigate potential statistical problems. Matched pair tests were completed with gaspers turned on and off. Measurements were repeated three times for each gasper setting and for each ISOPASS condition. Concentration measurements were taken at the breathing level inside the ISOPASS at the seat next to the injection source; at the seat across the aisle adjacent to the ISOPASS; and at a seat far away from the ISOPASS near the front of the cabin. The with- and without-ISOPASS matched pair tests clearly show the ISOPASS prototype is highly effective at providing isolation

in each aircraft cabin used in the study. Additionally, it was determined that the use of gaspers makes no measurable difference in the containment effectiveness of the ISOPASS.

Table of Contents

List of Figures

List of Tables

Acknowledgements

I would like to thank my thesis advisors Dr. Jones and Dr. Hosni for their help and guidance throughout this project as well as in my planning and my coursework for this Master's degree. Special thanks to Dr. Jones for always being available to assist with the numerous technical issues I faced while completing this project as well as providing good advice when I was unsure of what to do. Special thanks also go to Dr. Hosni for pushing me to try my hardest even when things get tough.

I would also like to thank Dr. Bennett and Dr. Fenton for serving on my thesis committee and providing their valuable comments on this thesis, as well as providing their advice and support.

Finally, I would like to thank my parents and my brother along with the rest of my family for all of their love and support throughout my Master's program. I could not have made it without their encouragement and advice. Thanks for being there for me.

Chapter 1 - Introduction

Aircraft air quality and passenger health impact a large population on a daily basis. The elevated altitude, low humidity, close proximity, and airborne contaminants affect passenger comfort and can contribute to the spread of disease. Because of this, aircraft air quality, cabin airflow, and ventilation continue to be major considerations in aircraft design and disease control solutions.

The Air Transport Center of Excellence for Aircraft Cabin Environmental Research (ACER) was formed to address these issues of aircraft air quality, airflow, and ventilation in commercial aircraft cabins. The ACER lab researches indoor air quality and fluid transport in aircraft cabins using experimental data collection along with mathematical models and Computational Fluid Dynamics (CFD) analysis and other investigative methods. Previous research conducted by ACER include the ventilation effectiveness of the Boeing 737 and 767 mock-up cabins (Patel, 2017), examination of the airflow distribution and turbulence in the longitudinal direction of the cabin mock-ups (Shehadi, 2015), the effect of passenger loading and ventilation air on airflow patterns (Madden, 2015), the effect of gaspers on airflow patterns (Anderson, 2012), ventilation air and passenger loading effects on airflow wake effects (Trupka, 2011), longitudinal particulate dispersion (Beneke, 2010), numerical models for predicting transport (Jones, 2009), and movement of tracer gas and particulate contaminants (Lebbin, 2006).

The research presented in this thesis focuses on the effectiveness of the ISOPASS prototype at containing airborne contaminants and preventing their spread around the aircraft cabin. Both a mock-up of a Boeing 767 cabin and a section of an actual Boeing 737 cabin are used in this research. Carbon Dioxide is used as a tracer gas, and is mixed with helium to achieve

neutral buoyancy in air. This tracer gas is injected from a point source inside the cabin inside the ISOPASS location, and the air is sampled at several different locations throughout the cabin to determine the concentration at each location. A test was ran for both ISOPASS on and ISOPASS off conditions taken in matched pairs, and for each gasper condition, gaspers on and gaspers off. Each test was repeated at least three times.

Chapter 2 - Background and Literature Review

The large number of passengers that use air travel each day results in increased exposure to airborne contaminants and raises concern over the safety and well-being of the passengers on board the aircraft. To combat this, the aircraft is equipped with temperature control, pressurization, ventilation, and filtration systems to provide a comfortable and safe environment for the passengers. Additionally, regulations are in place to insure the aircraft's environmental systems provide a safe environment both in design and maintenance of the aircraft.

2.1 Required Conditions in Commercial Aircraft

Many elements of the aircraft cabin's environment is regulated by the Federal Aviation Administration (FAA). These include cabin pressure, thermal comfort and temperature difference across the cabin, ventilation, and CO_2, CO, and O_3 concentration. While humidity may affect passenger comfort and health, the FAA does not regulate humidity.

2.1.1 Air Quality Standards

As stated in FAA regulations section 25.841, the minimum allowable cabin pressure altitude for non-emergency conditions is 8,000 ft (2,440 m) at any point during the flight (FAA 2010). Compartment temperatures must be within 5 °F of each other and adequate ventilation to each compartment as required by FAA regulations, section 25.831. While the FAA does not specify the acceptable temperature or humidity ranges for aircraft cabins, "reasonable passenger comfort" is required. The ideal temperature range for comfortable working and living is defined by NASA as 40 to 60 °F (4 to 16 °C), and the ideal relative humidity ranging from 25 to 70 percent (NASA, 1994). Additionally, section 25.831 also specifies that CO_2 concentration must

not exceed 0.5 percent by volume (sea level equivalent) in any normally-occupied compartment, and that CO must not exceed 50 parts per million (ppm). Ozone concentration must not exceed "0.25 parts per million by volume, sea level equivalent, at any time above flight level 320; and 0.1 parts per million by volume, sea level equivalent, time-weighted average during any 3-hour interval above flight level 270".

In addition to the requirements set by the FAA, ASHRAE also implements standards for commercial aircraft air quality. The target temperature range for both in-flight and ground operation should be 65 to 75°F, and the temperature should not exceed 80°F while in flight at any point. The operative temperature should not exceed 80°F for ground operations if no in-flight entertainment systems are present or operating, and should not exceed 85°F if all such systems are in operation (ASHRAE, 2018). While the FAA requires that the temperature variance is less than 5°F from compartment to compartment, ASHRAE also requires that the horizontal temperature variation across a temperature control zone be within 8°F, and the vertical temperature variance within a seat be within 5°F as well (ASHRAE, 2018). ASHRAE does not impose any requirements for RH, as minimum RH restrictions may negatively affect the safe operation of the aircraft and may conflict with the fresh air ventilation requirements (ASHRAE, 2018). Because the maximum RH allowable by safety considerations is actually lower than the upper limits of RH for occupant comfort, ASHRAE does not impose any restrictions on the upper limit of the RH range (ASHRAE, 2018). Slight increases in RH in the aircraft cabin may have a positive impact on occupant health and comfort (ASHRAE, 2016).

2.1.2 Ventilation Requirements and Standards

The FAA requires that commercial aircraft provide at least 0.55 lb/min of fresh air per occupant, as stated in section 25.831. At a cabin altitude of 8,000 ft, this is equivalent to 10 ft^3/min (0.283 m^3/min) (ASHRAE, 2007). Additionally, ASHRAE standard 161 requires a minimum of 15 ft^3/min (0.425 m^3/min) and recommends a minimum of 20 ft^3/min (0.566 m^3/min) per person. The 15 ft^3/min minimum requirement may be met with either 100% fresh air or a mixture of fresh and recirculated air. At least 7.5 ft^3/min per person must be outside air, assuming a ventilation effectiveness of at least one (ASHRAE, 2018).

Most modern aircraft supply extra ventilation with recirculated air in addition to the minimum required fresh air per occupant. To reduce the spread of contaminants through the cabin, the recirculated air goes through high efficiency particulate air (HEPA) filters before returning to the cabin. While not mandated by the FAA, HEPA filters are essential for the health and safety of the occupants, removing most of the airborne contaminants in the recirculation air before it is mixed with the fresh air and supplied back into the cabin.

2.2 Airflow Design

The central ventilation system in commercial aircraft is designed to generate highly lateral flow in the cabin. Such a circulation would contain the contaminated air to just a few rows, and greatly reduce the spread of disease along the total length of the cabin (Madden, 2015). Twin-aisle and single-aisle aircraft cabins are both utilized in this study. For each cabin, supply air enters through linear diffusers located in the ceiling down the center of each aircraft. In addition to the central ventilation, gaspers located above the passengers provide personal

ventilation. Air for the gaspers is taken from the central ventilation duct and does not provide any additional ventilation to the cabin as a whole. After circulating through the cabin, the air is exhausted through vents near the floor at the sides of the aircraft. The ventilation system diagrams for the single-aisle Boeing 737 and the twin-aisle Boeing 767 are shown in Figures 2.1 and 2.2.

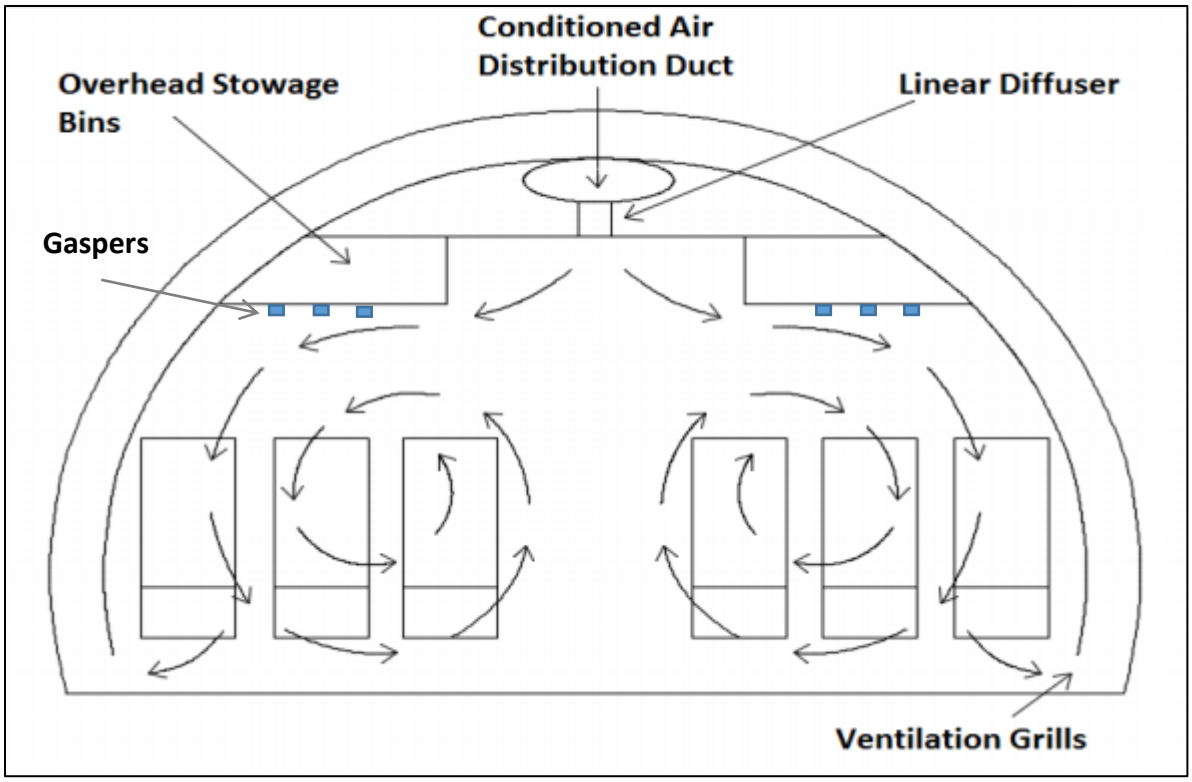

Figure 2.1 Design Airflow Pattern Inside a Boeing 737 Cabin (Patel, 2017)

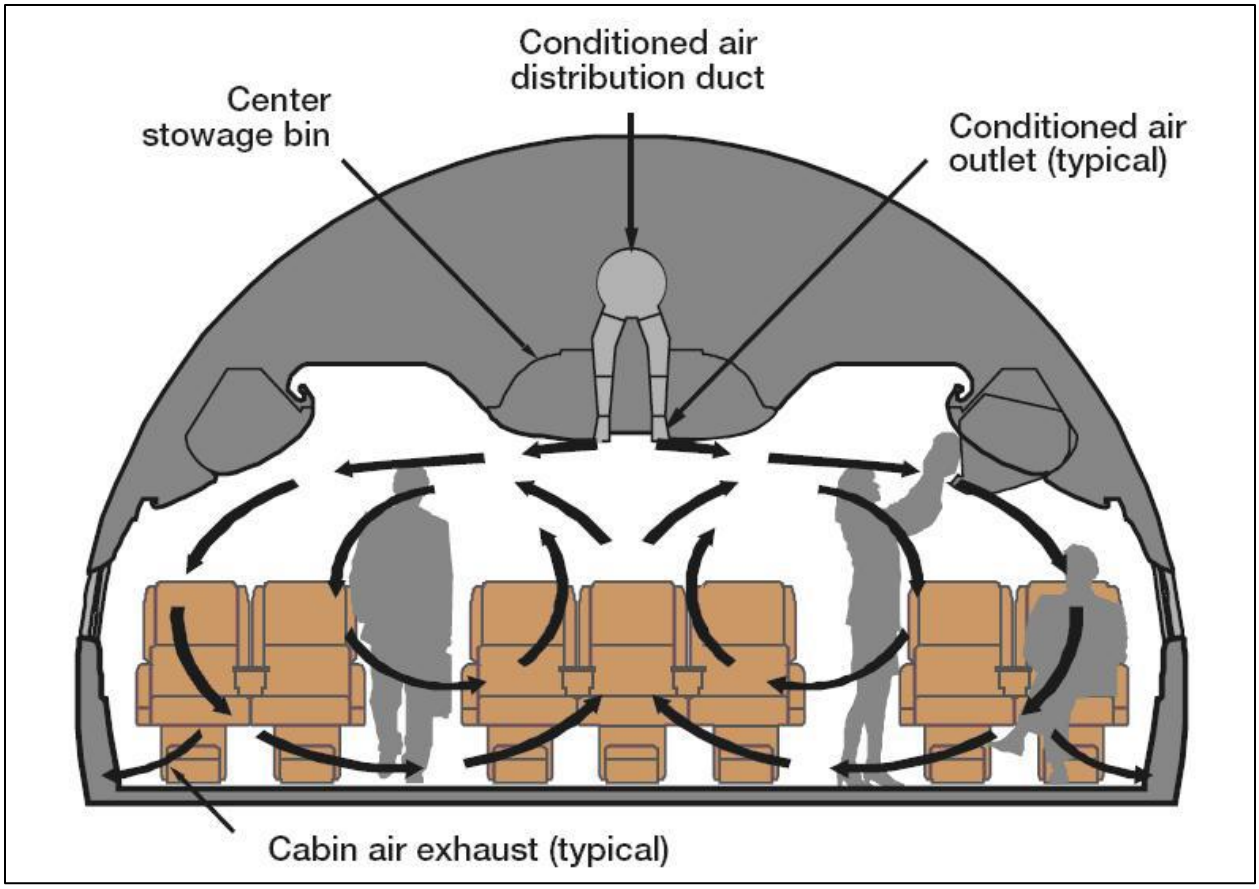

Figure 2.2 Design Airflow Inside a Boeing 767 Cabin (Hunt & Space, 1994)

2.3 Isolation and Disease Control

Personal isolation to control the spread of contagious airborne diseases is not a new concept. Rooms used for isolation are equipped with a blower to create negative pressure in the room, with a filtration system to purify the air before returning it to the outside. Mobile isolation systems exist as well. These range in design from a portable isolation room with an aluminum frame and clear vinyl walls to isolation systems designed to fit over a hospital stretcher. Each of these systems utilize HEPA filters and generate a negative pressure inside the chamber to provide appropriate airflow direction. However, each of these isolation solutions is large and impractical for use in an aircraft cabin.

Current disease control measures for commercial aircraft while in flight involves precautionary measures and avoiding direct contact with the infected passenger as best as possible. The CDC recommends frequent handwashing, minimizing contact with possibly contaminated surfaces, and avoiding contact with bodily fluids; along with gloves and facemasks when possible. Additionally, the CDC recommends moving the sick passenger to keep them at least 6 feet away from other passengers (CDC, 2017). Of course, this is not always a possibility, especially on smaller aircraft. Likewise, the World Health Organization (WHO, 2008) recommends relocating the infected passenger to a seat away from others and to use facemasks when possible, by both the sick passenger and the flight attendant that is attending to them (WHO, 2008). The International Civil Aviation Organization repeats these recommendations and adds disinfecting the affected areas around the infected passenger and disposal of any contaminated supplies or equipment (ICAO, 2009). At the moment, there is no way to reduce the spread of the contagion beyond basic hygiene and disinfectant procedures.

While there is no existing research on negative pressure isolation systems for in-flight aircraft applications, research has been done on personal ventilation systems for disease control in commercial aircraft cabins. One such study by the University of Denmark utilized a system which directs air from the seat back in front of the passenger and collects in through a suction system integrated into the seat back at the sides of the passenger's head, which is then exhausted before recirculating to the cabin. This personal ventilation system was found to reduce the average background concentration of the tracer gas by up to 42% in the cabin mock-up, with a flowrate of 10 L/s (Melikov & Dzhartov, 2012).

Chapter 3 - Experimental Test Facility

The test facility features a mock-up of a Boeing 767 cabin and a section of an actual Boeing 737 cabin. During testing, each cabin is equipped with thermal mannequins to replicate human thermal output, the tracer gas injection source, and CO_2 analyzers for measuring the tracer gas concentration. Each cabin is supplied with conditioned fresh air. The details of this facility are covered here.

3.1 Boeing 767 Mock-up Cabin

The Boeing 767 mock-up cabin simulates the actual cabin, and the interior geometry is designed to Boeing specifications. The cabin section has 11 rows of seats, with the middle three rows equipped with gaspers. This mock-up was built inside of a large wooden structure, as shown in Figure 3.1. The dimensions of this structure are 32 ft. (9.75 m) long x 24 ft. (7.32 m) wide x 16 ft. (4.88 m) tall. In addition to the mock-up itself, the structure features hallways along each side, a crawlspace underneath, and the ductwork and air distribution system for the cabin. Two exhaust fans located at the top of the south face of the structure maintain neutral pressure. The east hallway houses the CO_2 and helium mass flow controllers and associated equipment, as well as the data acquisition system (DAQ) and a vacuum pump and valve system used to maintain the gas analyzers at their proper flowrates. The west hallway houses the gas analyzers and the control system for the coughing mannequin.

Figure 3.1 767 Mock-up Structure and Air Supply

Figure 3.2 Hallways and Crawlspace - Boeing 767 Mock-up (Beneke, 2010)

3.1.1 Cabin Geometry

The 767 mock-up has a length of about 30.9 ft. (9.41 m) and a width of 15.5 ft. (4.72 m). The mock-up contains 11 rows of seats, with two aisles. The cross-sectional diagram of the 767 mock-up is shown in Figure 3.3. The equations relating to the cabin profile design were derived by Lebbin (2006) and provide greater detail.

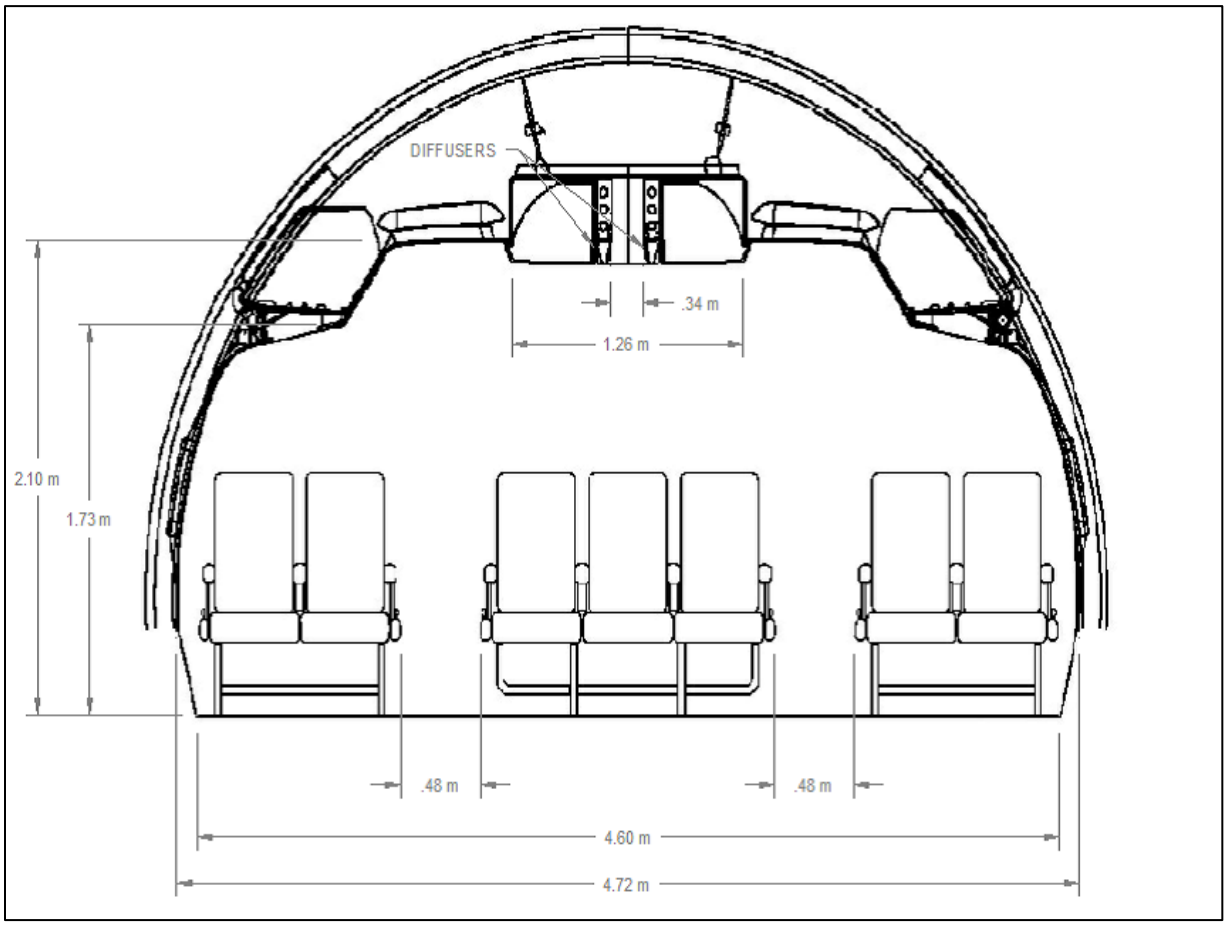

Figure 3.3 Boeing 767 Cabin Cross-Section (Trupka, 2011)

The 767 cabin has 11 rows of seats in a 2-3-2 configuration, separated by two aisles. The rows are numbered from the front of the cabin at the southern wall to the back of the cabin at the northern wall. The columns are labeled A thorough G from left to right. The cabin layout and dimensions are specified in Figure 3.4.

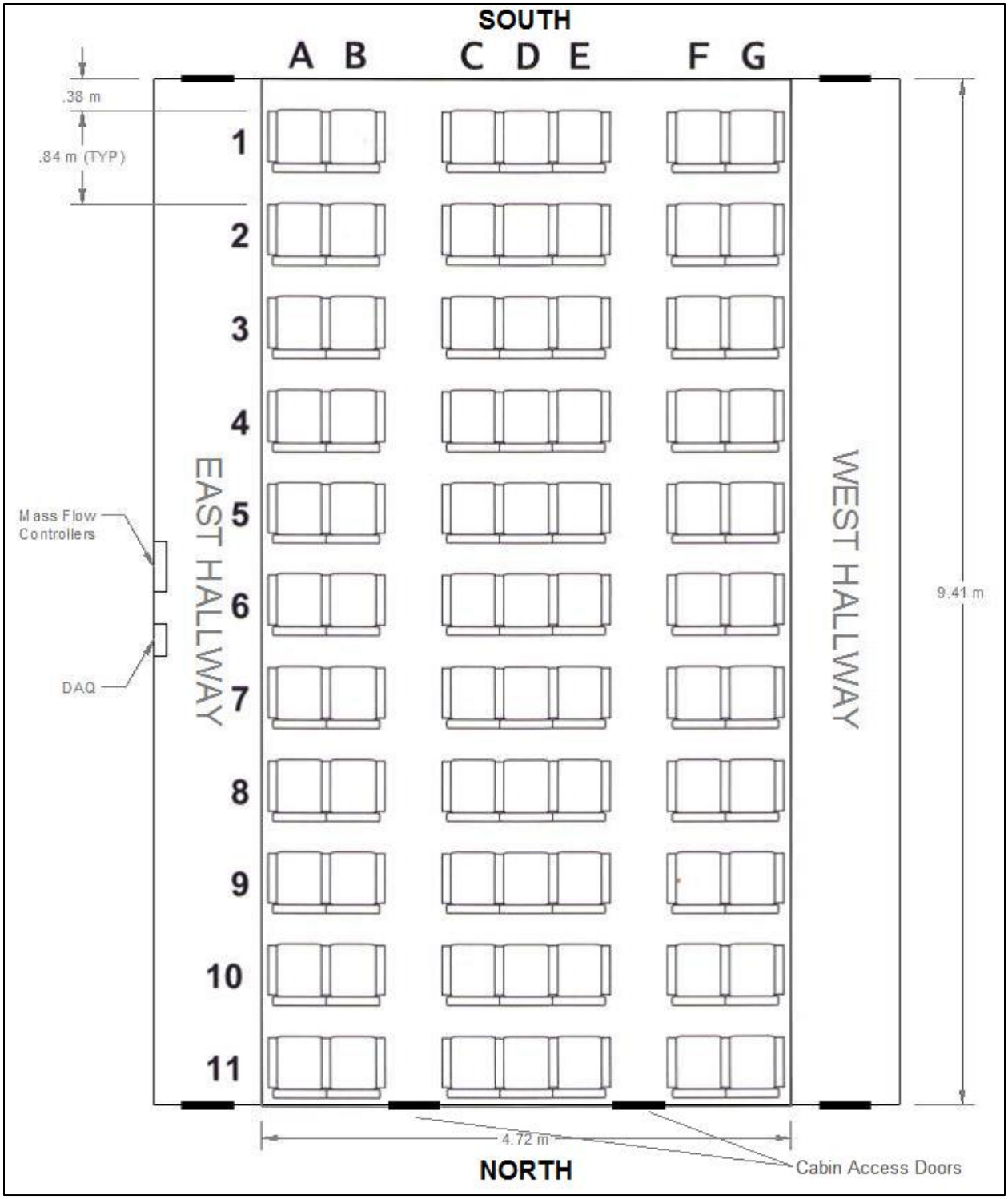

Figure 3.4 Boeing 767 Cabin Layout (Trupka, 2011)

After entering the cabin through the central diffuser, as diagramed in Figure 2.2 and Figure 3.3, the air is ventilated through evenly spaced gaps at the base of the cabin sidewalls. The air is ventilated into the hallway and is eventually drawn out by the exhaust fans as shown in Figure 3.1. The ventilation gaps for the 767 mock-up are shown in Figure 3.5 and 3.6.

Figure 3.5 Ventilation Gaps Inside 767 Mock-up (Patel, 2017)

Figure 3.6 Ventilation into the Hallway, 767 Mock-up

3.1.2 Boeing 767 Seat Geometry

The Boeing 767 utilizes a 2-3-2 seat layout with two aisles dividing the seating sections. The mock-up uses seats from an actual 767 aircraft and has 11 rows, for a total of 77 seats. The dimensions of both the 3-seat and 2-seat sections are diagramed in Figure 3.7 and 3.8, respectively. Additionally, the seat dimensions from the side are provided in Figure 3.9. The aisles between them are 1.58 ft (0.48 m) wide, and the front of the cabin is 1.25 ft (0.38 m) from the first row of seats as show previously in Figure 3.4.

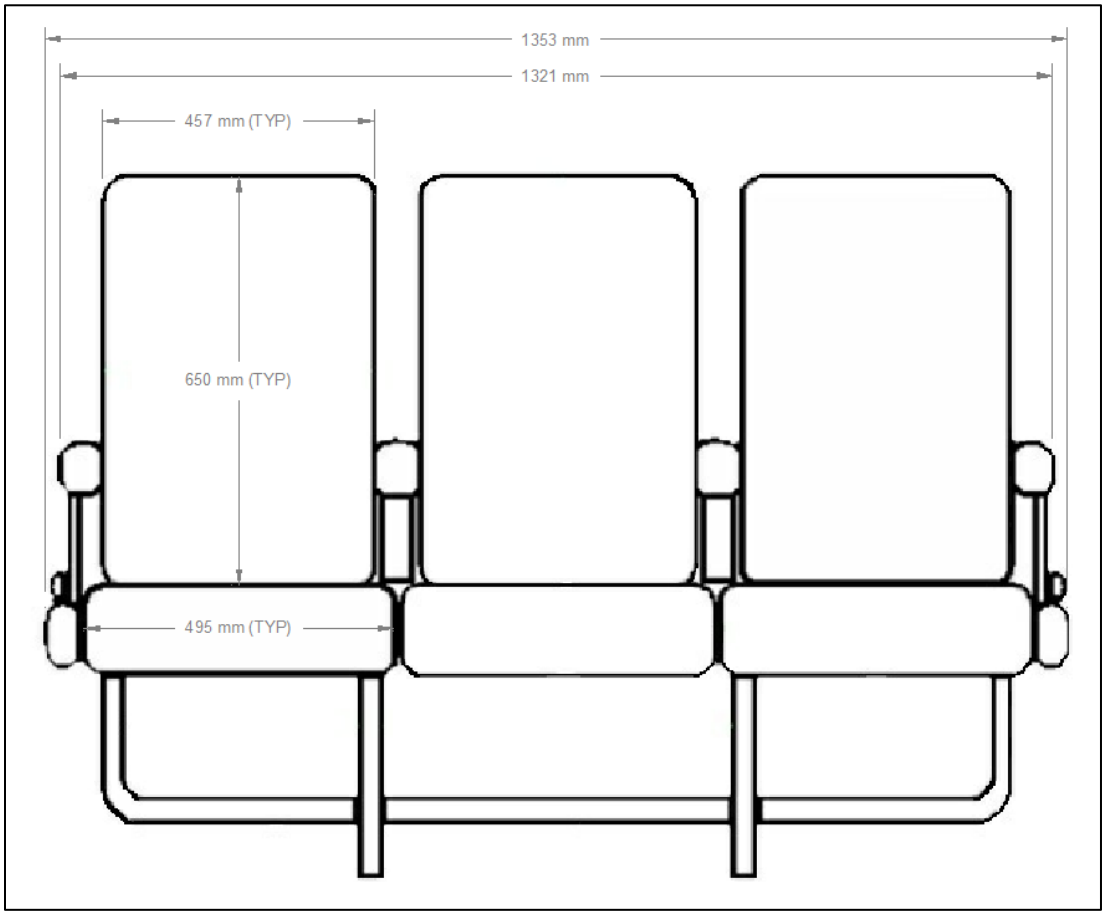

Figure 3.7 Boeing 767 Center Seat Dimensions (Trupka, 2011)

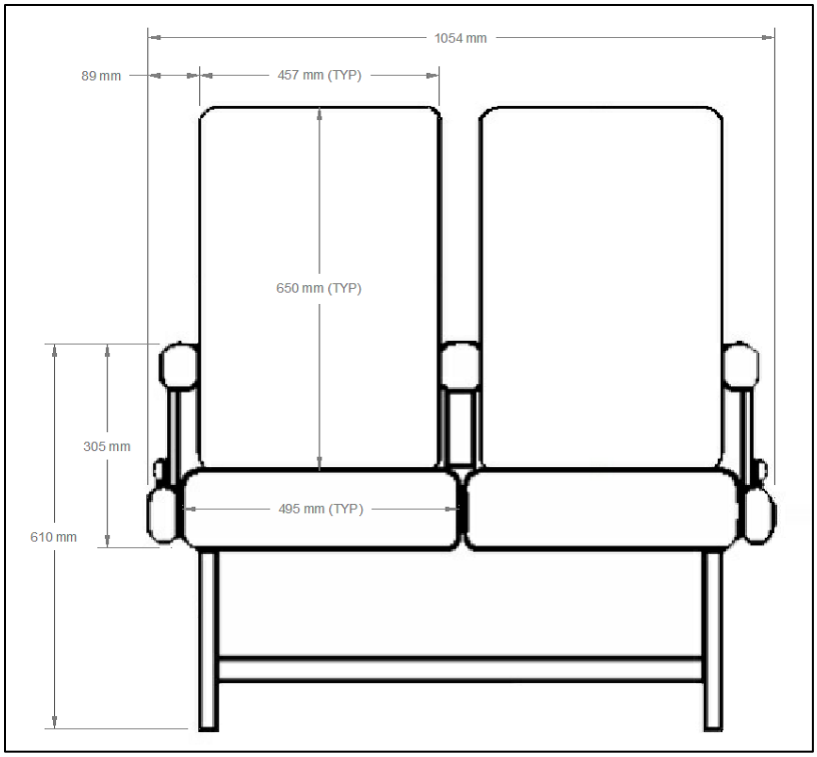

Figure 3.8 Boeing 767 Side Seat Dimensions (Trupka, 2011)

Figure 3.9 Boeing 767 Seats Side View Dimensions (Trupka, 2011)

3.2 Boeing 737 Mock-up Cabin

The Boeing 737 mock-up is a section of an actual cabin, and utilizes the original ventilation system and gaspers. Unlike the 767 mock-up, the 737 cabin has a gasper for each seat in the mock-up. The cabin section has 5 rows of seats in a 3-3 arrangement with an aisle down the middle between them. The dimensions of the cabin section are 18.3 ft. (5.6 m) long x 11.8 ft. (3.6 m) wide x 9.2 ft. (2.8 m) tall. The 737 cabin is not enclosed by a structure like the 767, but just exhausts out into the environment. The CO_2 and Helium mass flow controllers and associated equipment, as well as the Data Acquisition System (DAQ) and a vacuum pump and valve system for the CO_2 analyzers are still located in the east hallway of the 767 structure. The CO_2 analyzers are mounted to the front wall of the 737 cabin on the outside.

Figure 3.10 Boeing 737 Mock-up Cabin (Patel, 2017)

3.2.1 737 Cabin Geometry

The 737 mock-up has an interior length of about 15.85 ft. (4.83 m) and a width of 9.33 ft. (2.84 m). The cross-sectional diagram of the 737 mock-up with more detailed dimensions is shown in Figure 3.11.

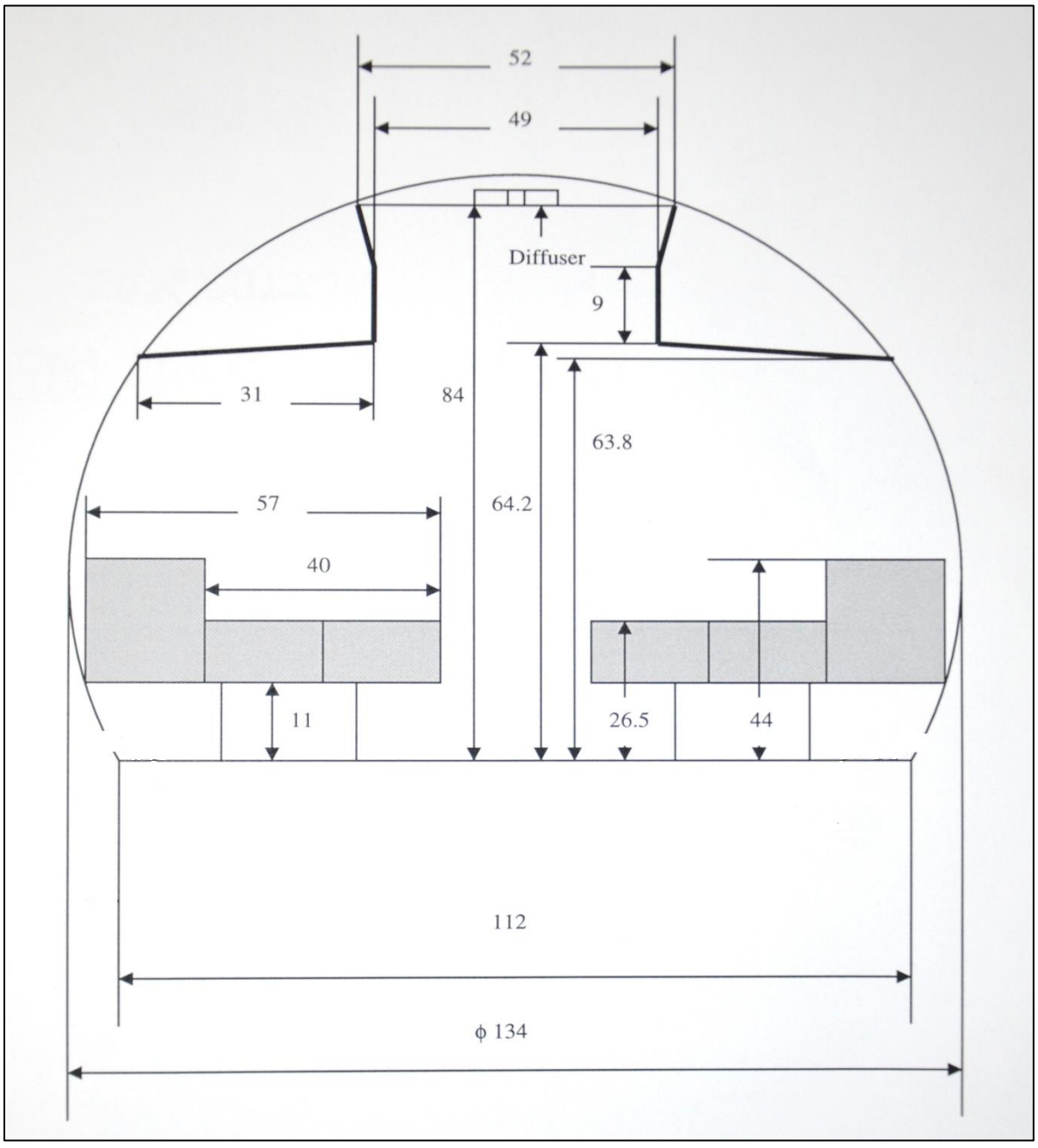

Figure 3.11 Boeing 737 Cabin Cross-Section (Mo, 2012)

As previously mentioned, the 737 cabin has 5 rows of seats in a 3-3 configuration, separated by a single aisle. The rows are numbered from the front of the cabin at the northern wall to the back of the cabin at the southern wall. The columns are labeled A thorough F from left to right. The cabin layout and dimensions are specified in Figure 3.12.

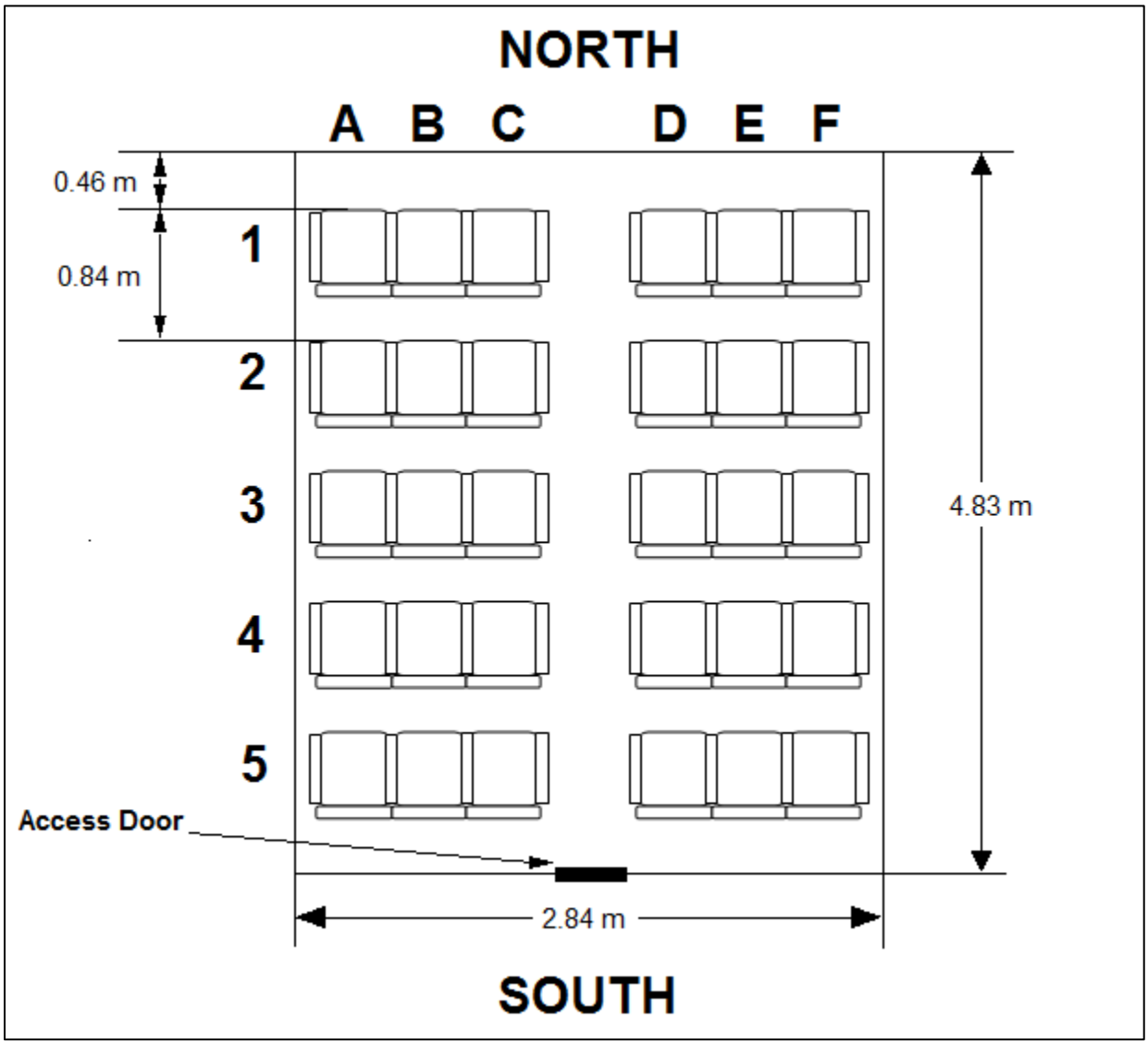

Figure 3.12 Boeing 737 Cabin Layout (Patel, 2017)

After entering the cabin through the central diffuser, as diagramed in Figure 2.1 and Figure 3.11, the air is ventilated through ventilation grills at the base of the cabin sidewalls. The air is ventilated out directly into the environment of the lab. The ventilation grills for the 737 cabin section are shown in Figure 3.13.

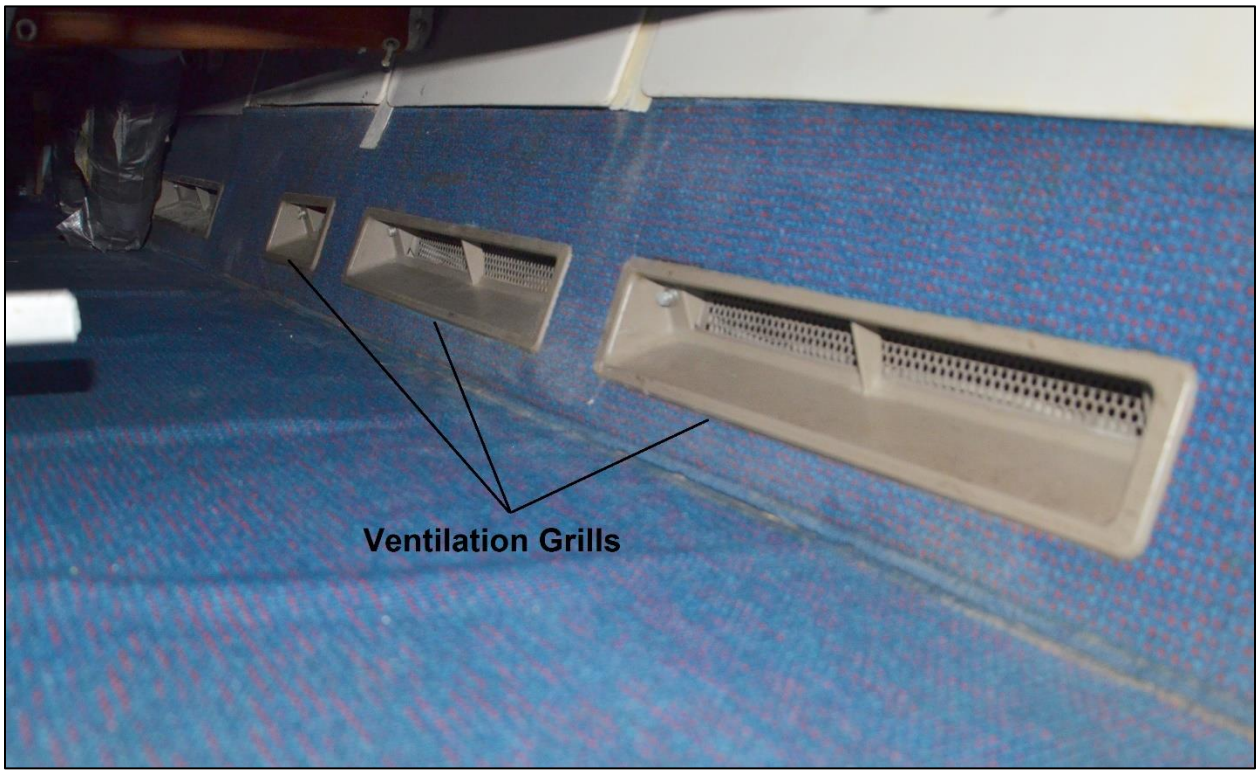

Figure 3.13 Ventilation Grills Inside Boeing 737 Cabin (Patel, 2017)

In the 737 cabin, the walls are segmented by evenly spaced ribs. The specific design of the area behind the ventilation grill is an important consideration when forcing a higher flowrate of air through the vent, to ensure that the increased flow won't overwhelm the ventilation system and blow exhausted air back into the cabin. The structure behind the ventilation grill in the 737 is diagramed in Figure 3.14.

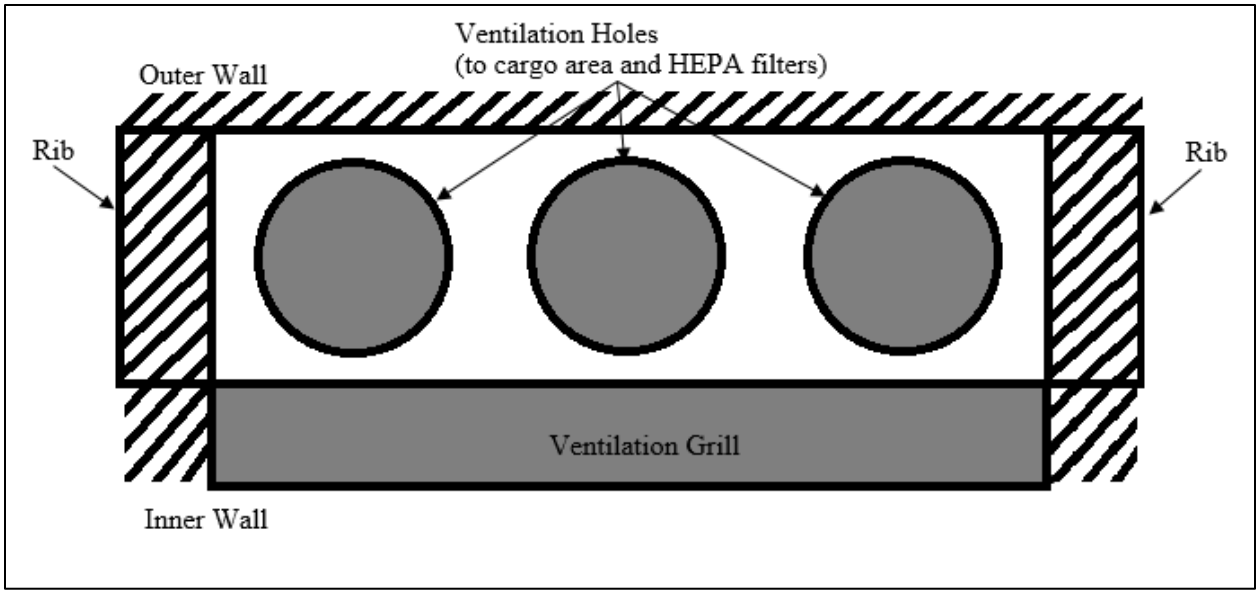

Figure 3.14 737 Ventilation Section Diagram

3.2.2 Boeing 737 Seat Geometry

Like the 767 mock-up, the 737 section uses seats from an actual 737 aircraft. The 737 cabin section has 5 rows in a 3-3 seat configuration, for a total of 30 seats. The dimensions of a three-seat section are diagramed in Figure 3.15. Additionally, the seat dimensions from the side are provided in Figure 3.16. The aisle between the seats is 1.54 ft (0.47 m) wide, and the front of the cabin is 1.5 ft (0.46 m) from the first row of seats as show previously in Figure 3.12. The rows are 2.75 ft (0.84 m) apart.

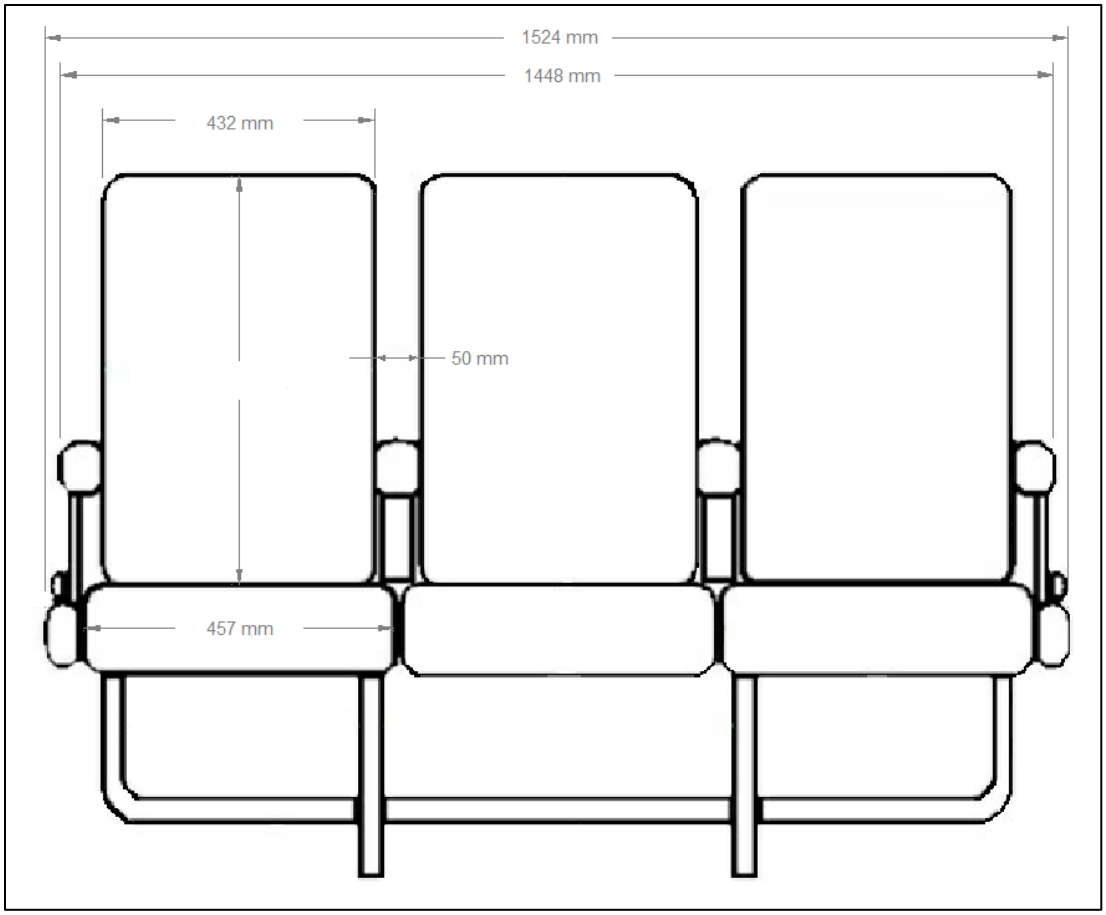

Figure 3.15 Boeing 737 Seat Dimensions (Patel, 2017)

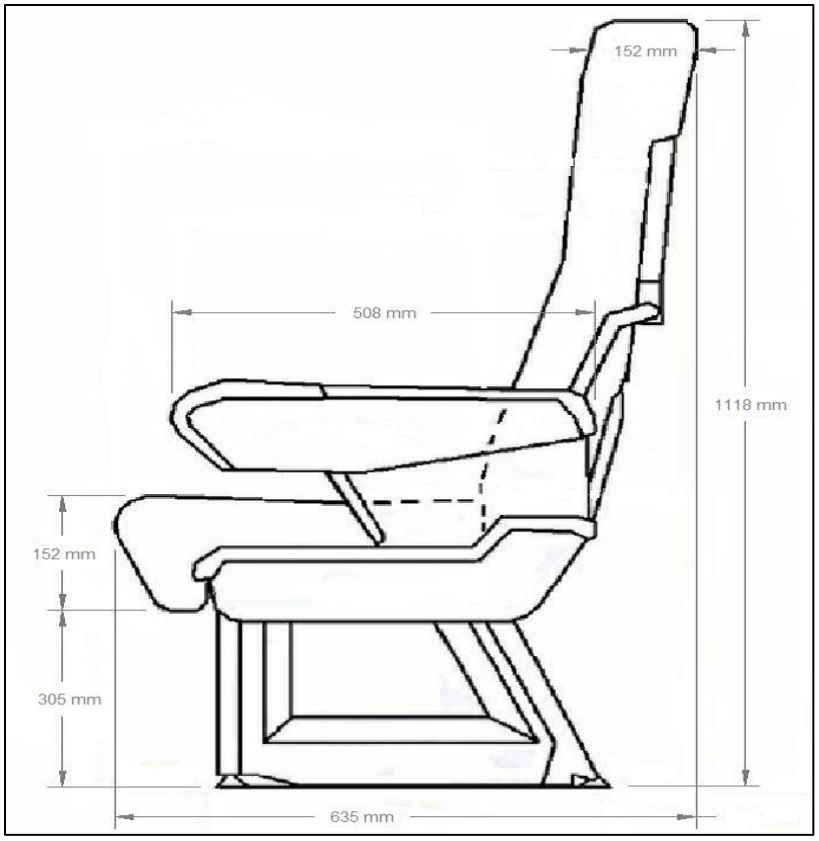

Figure 3.16 Boeing 737 Seat Side View Dimensions (Patel, 2017)

3.3 Thermal Mannequins

The thermal output of the occupants has a significant effect on the airflow patterns inside the aircraft cabin. To simulate a partially filled cabin, heated mannequins were installed. Each mannequin was uniformly wrapped with heater wire on the arms, legs, chest, and head. Each mannequin is pluged in to a 115 V outlet and generates about 102 W (348 BTU/hr) of heat. This accounts for the average sensible thermal output of a resting adult, 70 W (238 BTU/hr) (ASHRAE, 2013), plus additional heat from in-flight entertainment systems, avionics, and personal electronics such as laptops. Both the 767 and 737 cabins were half-loaded with the heated mannequins, spread evenly.

As a safety precaution, a thermostat was equipped inside the cabin. If the temperature inside the cabin exceeds the set temperature, the power to the mannequins will be shut off.

Figure 3.17 Boeing 767 Mock-up with Mannequins

3.4 Air Supply System

The air supply system supplies the mock-up cabins with conditioned air to simulate a real aircraft environment and meeting FAA ventilation requirements. The 767 cabin, with 77 seats, is supplied with 1400 CFM (40 m^3/min) of conditioned air. The 737 cabin, with 30 seats, is supplied with 600 CFM (17 m^3/min) of conditioned air. Fresh air is drawn in from outside and passes through the dehumidifier unit and into the air conditioner, which maintains the air at 60 °F (15.6 °C). The air is then delivered to the cabin. For these tests, the dehumidifier was not used. Additionally, only fresh air is used for these tests, no recirculated air is used.

3.4.1 Ductwork

The blower in the dehumidifier unit draws outside air through the rectangular ductwork connected to the lab wall. Once the air has passed through the dehumidifier unit, it moves through more ductwork and through the air conditioning system. A chiller and hot water system is used to regulate the temperature, and an electric heating coil is used to fine-tune the temperature to maintain 60 °F (15.6 °C). From there, the air moves through the ductwork to a T-gate, where it is delivered to the correct cabin. Each cabin's ductwork will be covered in the next sections.

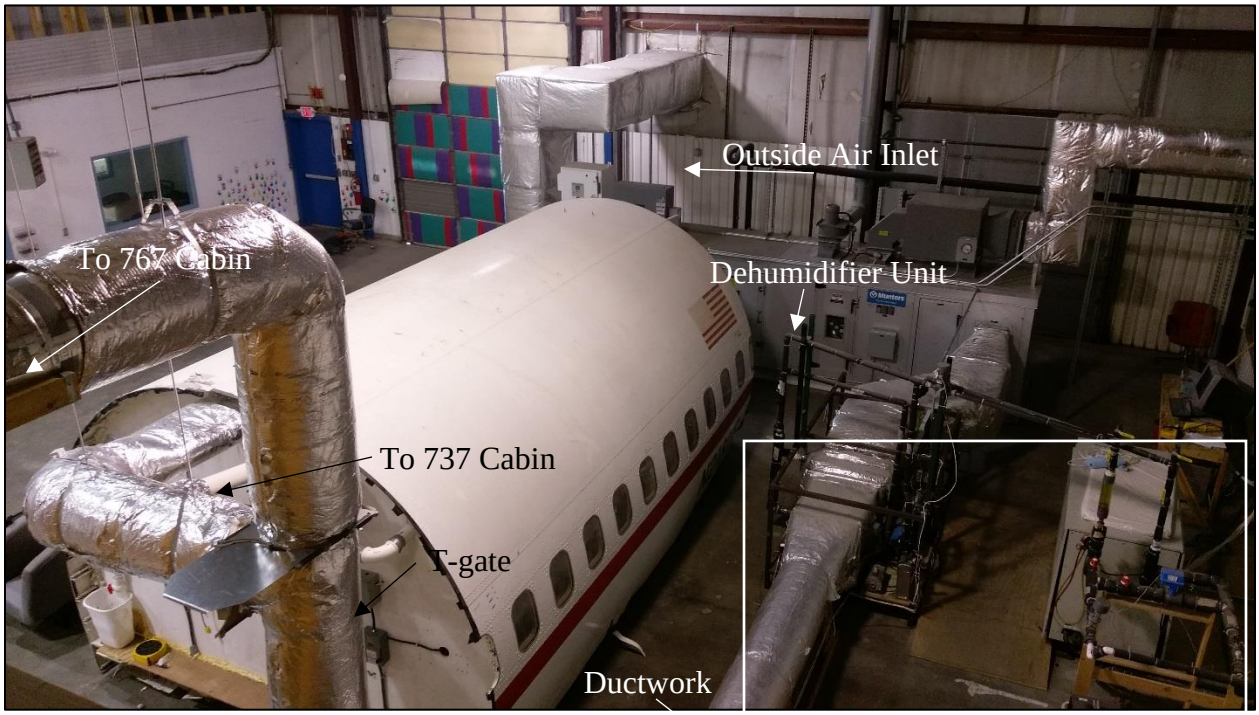

Figure 3.18 Ductwork for 737 and 767 Mock-up Cabins

3.4.1.1 Boeing 767 Mock-up Cabin Ductwork

The 767 mock-up cabin ductwork is connected to the main air supply by a tapered transition duct. The cabin air supply duct starts at 0.82 ft (0.25 m) in diameter and reduces in

diameter over the length of the cabin. It is a section of duct from the air supply system of an actual 767 aircraft. The linear diffusers are connected to the supply duct by flexible tubes spaced evenly down the length of the cabin. The connection to the diffusers is shown in Figure 3.19. A blower pulls conditioned air from the supply duct and delivers it to the gaspers via a separate PVC duct and connections. The gaspers are maintained 2" H_2O pressure to meet the design specifications. The gasper fan and connections are shown in Figure 3.20.

Figure 3.19 Boeing 767 Mock-up Supply Duct and Diffuser Connection (Patel, 2017)

Figure 3.20 Boeing 767 Mock-up Gasper Fan and Connection

3.4.1.2 Boeing 737 Mock-up Cabin Ductwork

The 737 mock-up cabin ductwork is connected to the main air supply by a transition duct that changes shape from the circular duct to the flattened shape used in the 737. The 737 mock-up uses its original ductwork, sealed at the end to deliver all of the supplied air to the cabin through the diffuser. The linear diffuser is connected directly to the base of the supply duct. The supply duct and connection to the diffuser is shown in Figure 3.21. A blower pulls conditioned air from the supply duct and delivers it to the gaspers using the original gasper ducts and connections, sealed at the ends. Separate PVC ductwork connects the blower to these original ducts. As in the 767 mock-up, the gaspers are maintained 2" H_2O pressure to meet the design specifications. The gasper fan and connections are shown in Figure 3.22.

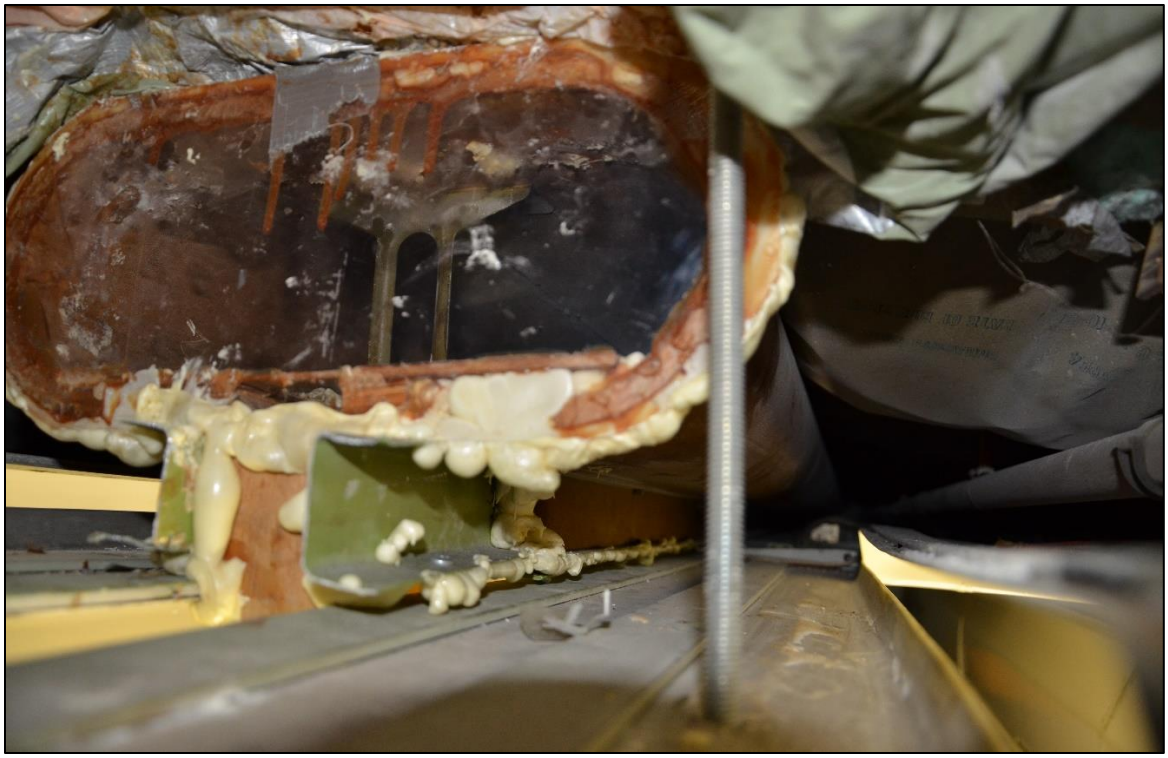

Figure 3.21 Boeing 737 Mock-up Supply Duct with Diffuser Connection (Patel, 2017)

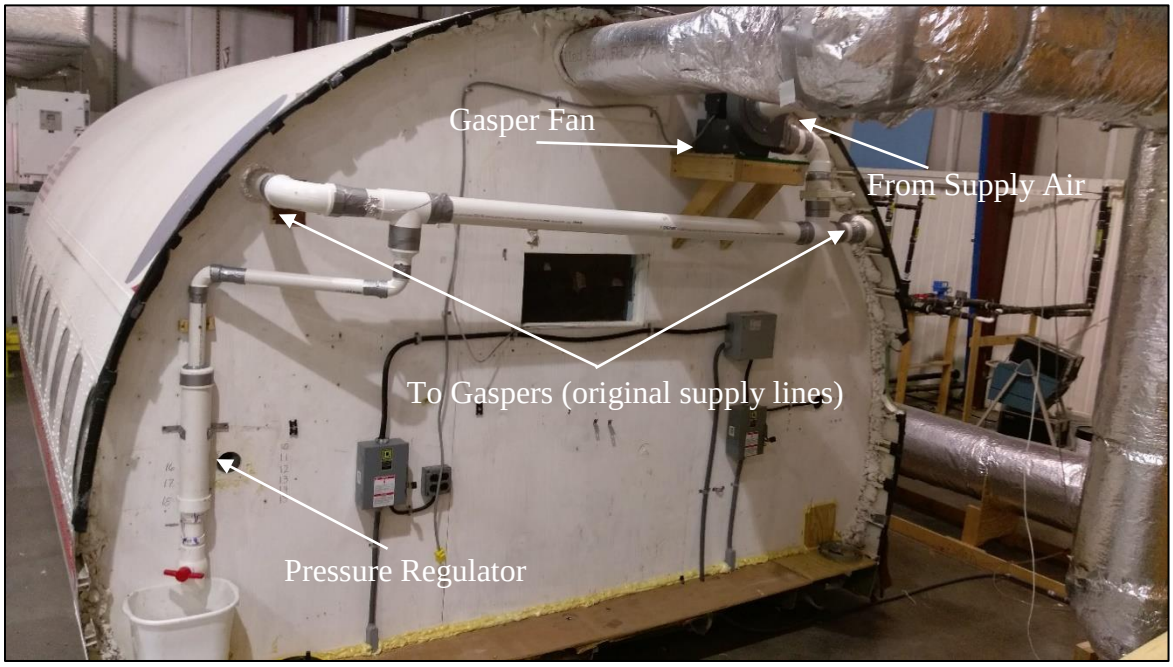

Figure 3.22 Boeing 737 Mock-up Cabin Gasper Fan and Connections

3.4.2 Air Conditioning System

The air supply system provides the mock-up cabins with fresh air, drawn in from the outside by the blower. The air then passes through the dehumidifier and on to the chiller and heater system. The air conditioning system includes the blower, dehumidifier, water chiller and hot water heater for rough tuning the temperature of the air, and an electric heater for fine tuning. The schematic flow diagram of the air conditioning system is shown in Figure 3.23. For the testing conducted in this study, the dehumidifier was not used.

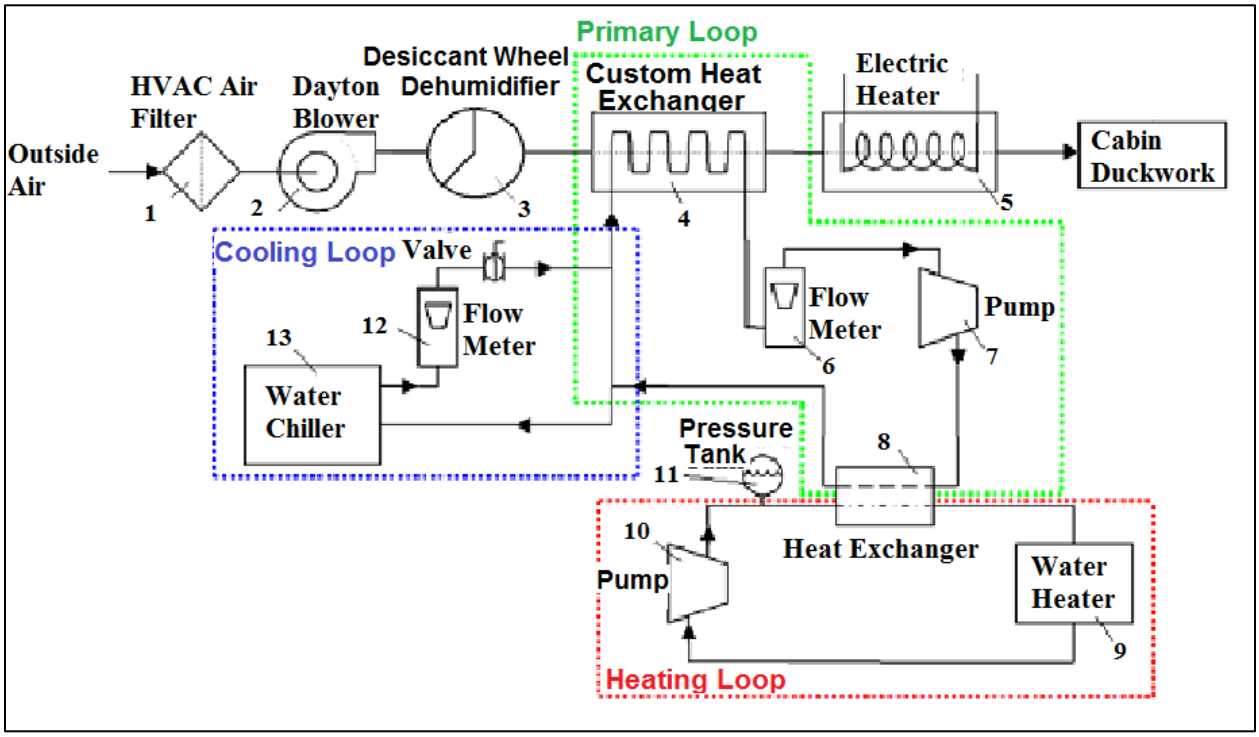

Figure 3.23 Schematic Flow Diagram of the Air Conditioning System (Madden, 2015)

The specific equipment used in the air conditioning system is detailed here, as described by Patel (2017):

1. Air Filters

- Glass Floss Z-line series
- 2 parallel filters 24” × 24”

2. Blower/Supply Fan

- Model # Yaskawa GPD315/V7 VFD
- 12 ¼" Dayton Blower at 3 hp

3. Dehumidifier

- Model # Munters ICA-0750-020
- Desiccant dehumidifier type
- Maximum Flow Rate: 1500 ft^3/min

4. Heat Exchanger

- Custom made: 24" × 24"

5. Electric Heater

- Model # AccuTherm DLG-9-3
- 220 V, 3 phase

6. Flow Meter

- Model # Omega FL7204
- Water Range: 40 GPH

7. Pump

- Model # Marathon CQM 56C34D212OF P

8. Heat Exchanger

- Model # Alfa Laval CB27-18H T06

9. Water Heater

- Model # Rheem GT-199PVN-1
- Temperature Range: 100° to 180° F
- Gas Input Range: 19,000 to 199,900 btu/hr

- 120 V, 60 Hz

10. Pump
    - Model # FHP C4T34DC35A26
11. Pressure Tank
    - Model # Dayton 4MY57
    - Capacity: 6.5 gallons
    - Precharge Pressure: 30 psi
12. Flow Meter
    - Model # King 7205023133W
    - Flow range: 1 to 200 GPM
13. Commercial Water Chiller
    - Model # AccuChiller LQ2R15
    - PV-B311 Condensing coils

The total system is divided into three loops: the cooling loop, and the heating loop, and the primary loop (Figure 3.23). The cooling loop brings the temperature of the air down to about 50 °F, and is only used when the temperature of the processed air is below 50 °F. The cooling loop uses an industrial water chiller to adjust the temperature of the air. Likewise, the heating loop brings the temperature of the air up to 50 °F, and is only used when the temperature of the processed air is below 50 °F. The heating loop uses a natural gas water heater to adjust the temperature of the air. Lastly, the primary loop fine-tunes the temperature of the air to 60 °F and holds the temperature steady at that point.

3.4.3 Control System

The entire air supply system is controlled by a computer using National Instruments LabVIEW software. A screenshot of the LabVIEW program interface is shown in Figure 3.24. The components are connected via Agilent 34970A and National Instruments FP-1000 Data Acquisition (DAQ) units. The control system outputs through the NI FP-1000 DAQ with add-on modules PWM-520 and AO-210 for pulse width modulation and analog voltage output, respectively (Trupka, 2011).

Supply air flowrate is controlled through the LabVIEW software by reading the air speed from a section of duct after the air conditioning and before the mock-up cabins and adjusting the blower speed accordingly. Various temperature levels are also monitored by the LabVIEW software, and provide both additional control and relevant data. The specific control functions of each are given in more detail in Table 3.1.

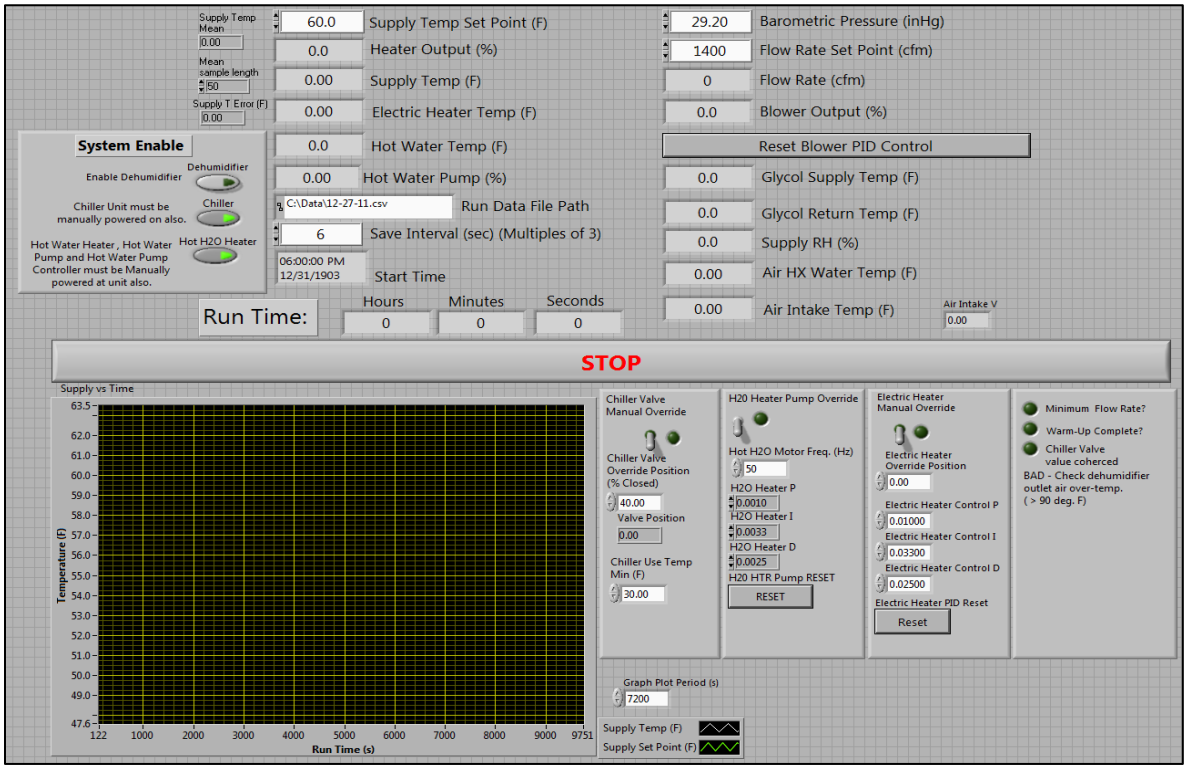

Figure 3.24 Supply Air Control LabVIEW Interface (Madden, 2015)

Table 3.1 Air Conditioning System Control and Feedback Parameters (Madden, 2015)

Feedback	Sensor Location	Control
Supply Air Temperature	Cabin Inlet Duct	Heater Temperatures
Electric Heater Temperature	Thermistor in Heater	Heating Loop Pump VFD
Hot Water Temperature	Water Heater Exit	Mixing Valves
Supply Flow Rate	Cabin Inlet Duct	Blower VFD
Glycol Supply Temperature	Chiller Exit Line	Duct Heater
Glycol Return Temperature	Chiller Inlet Line	Duct Heater
Supply Relative Humidity	Cabin Inlet Duct	None
Heat Exchanger Temperature	Primary Water Loop	None
Air Intake Temperature	Dehumidifier Inlet	None

3.5 Tracer Gas Injection and Measurement System

Carbon dioxide is used as a tracer gas for every test in this study. CO_2 is an inert gas that is easily detectible, readily available, and much safer to use than other detectible gasses such as carbon monoxide. Helium is mixed with the CO_2 proportionally to maintain neutral buoyancy in the air. The ratio of helium to mix with the CO_2 is determined by setting the molecular weight of the CO_2/helium mixture equal to the molecular weight of the air, assuming standard temperature and pressure. Because we know the desired volumetric flow rate of the CO_2, we can solve the ideal gas law and determine the volumetric flow rate of the He such that the final mixed tracer gas is neutrally buoyant in the air.

The tracer gas is injected from a point source inside the cabin, and CO_2 analyzers sample the air through vinyl tubes placed at various points throughout the cabin. The specific placement of these sampling tubes and the injection point will be covered in Chapter 4.

3.5.1 Tracer Gas Injection

A mixture of CO_2 and He is used as the tracer gas. Both gasses are supplied by Matheson Tri-Gas. The CO_2 is industrial grade and is stored in a 50 lb cylinder with a 4 MPa gage pressure. The He gas is high purity and is stored in a type T cylinder with a 16 MPa gage pressure. Each cylinder is fitted with a pressure regulator. The regulators are adjusted to maintain a 200 kPa outlet pressure for each gas. The gas is delivered to the mass flow controllers via vinyl tubes, designed to break at a lower pressure than the other components of the gas delivery system such as the mass flow controllers in the case of accidental over-pressurization.

The flowrate for each gas is controlled by mass flow controllers located in the east hallway of the 767 mock-up. CO_2 is controlled by an MKS GE250A025105SBV0020 electric mass flow controller, and He is controlled by an MKS 2179A00114CS pneumatic mass flow controller. The mass flow controllers are connected to a MKS PR4000 power supply that controls the flowrates via input from the LabVIEW program. Each gas then passes through a variable area flow meter to verify the actual flowrates before mixing at a brass tee fitting. From there, a ½" vinyl tube delivers the mixed tracer gas to the copper pipe injection point placed inside the cabin. The copper pipe injection point is mounted to the armrest of the seat and is positioned vertically, with the gas entering the cabin at the approximate breathing level of a seated passenger.

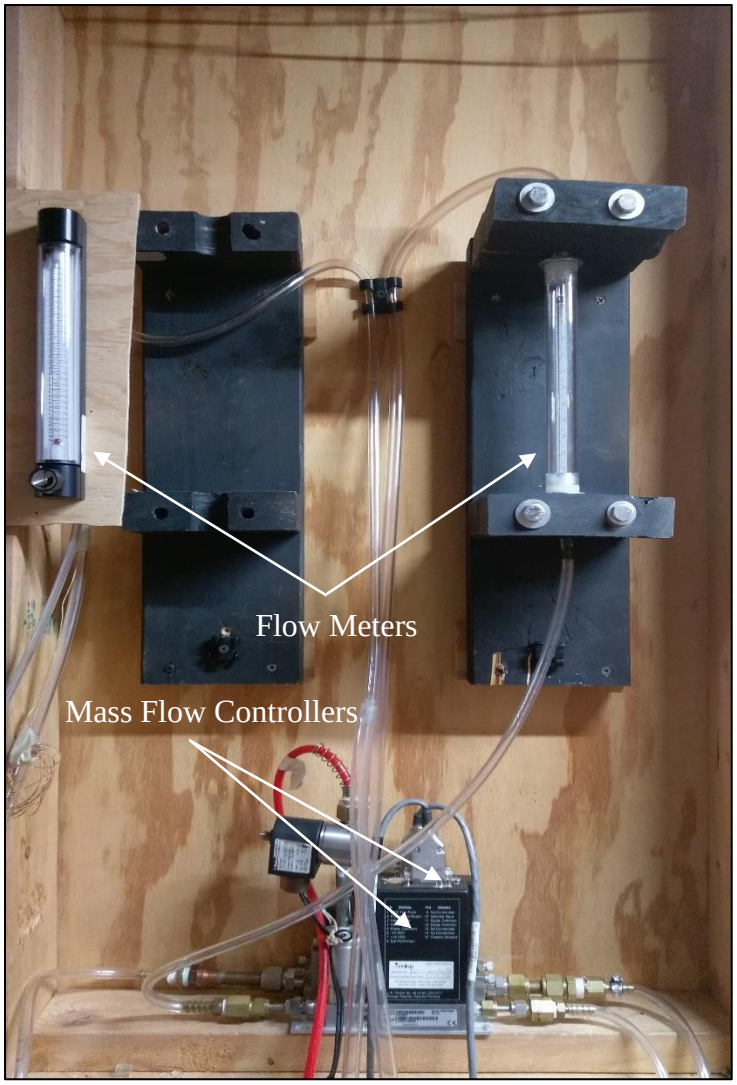

Figure 3.25 Mass Flow Controllers with Flow Meters

3.5.2 Tracer Gas Sampling and Measurement

The air is sampled by four separate infrared CO_2 gas analyzers which measure the concentration of the sampled air. The air is drawn in by the analyzers through vinyl tubes, placed at approximate breathing level at various points throughout the cabin as detailed in Chapter 4. The analyzers output the concentration to the DAQ as a voltage. The voltage received at the DAQ unit is then collected by the LabVIEW program used to control the tracer gas delivery and measurement system and is output to a spreadsheet. Two of the CO_2 analyzers are PP Systems

WMA-4 analyzers, one is a PP Systems WMA-5 analyzer, and one is a custom analyzer that utilizes an Edinburgh Instruments Gas Sampling Card and a 24 V supply with 60 Hz noise filters (Trupka, 2011). The WMA-4 and custom analyzers are calibrated for a range of 0 – 2000 parts per million (ppm), while the WMA-5 analyzer is calibrated for a range of 0 – 3000 ppm. The analyzers use infrared detection method to determine the concentration of the CO_2 in the sampled air. The location of the analyzers depends on which cabin is being used. For testing in the 767 cabin mock-up, the analyzers were mounted in the west hallway of the 767 structure. For testing in the 737 cabin, the analyzers were mounted on the exterior of the north-facing wall of the 737 cabin.

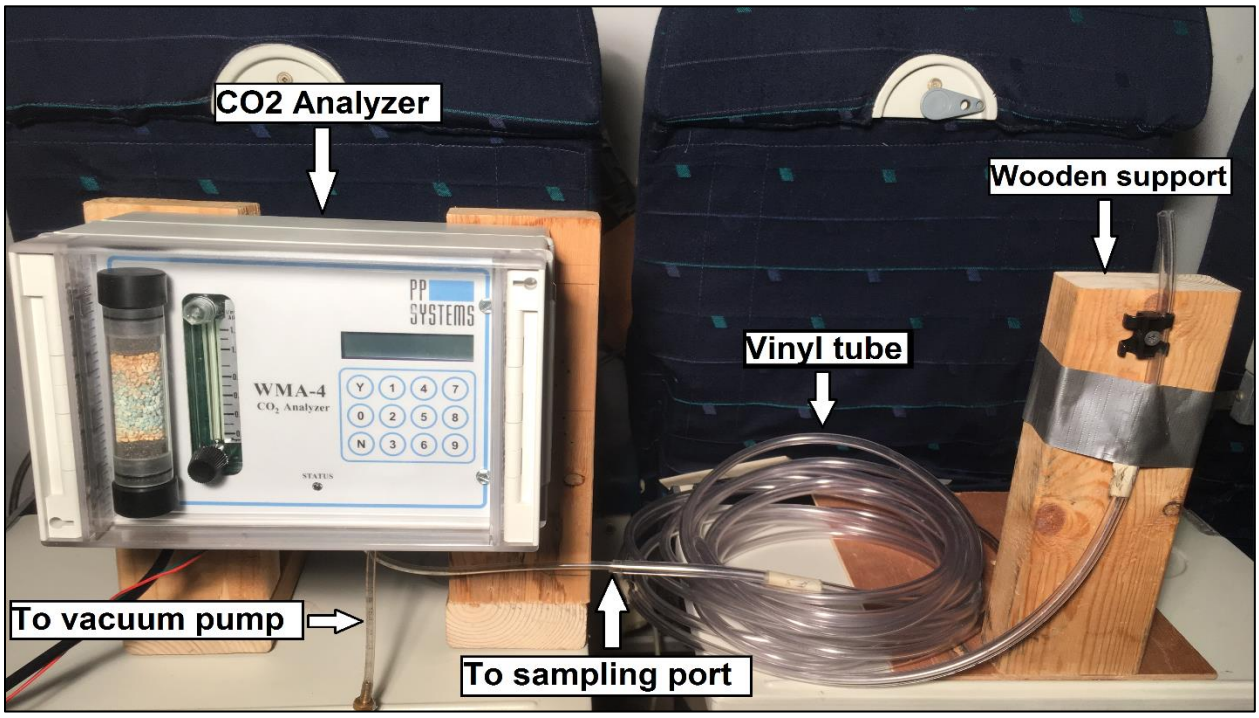

Figure 3.26 CO2 Analyzer with Sampling Tube (Patel, 2017)

Figure 3.27 WMA-4 CO2 Analyzers

Figure 3.28 WMA-5 CO2 Analyzer

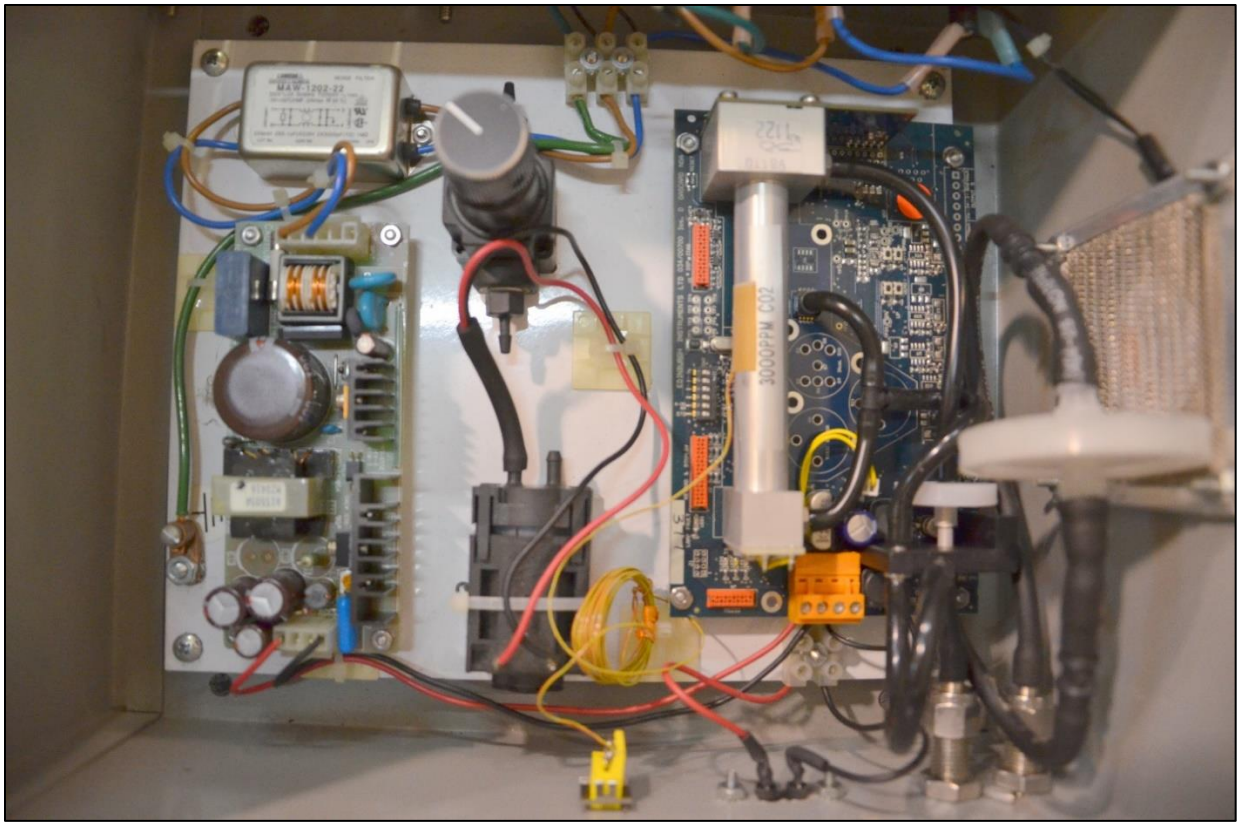

Figure 3.29 Interior of Custom CO2 Analyzer (Patel, 2017)

To draw air from the sampling location through the CO_2 analyzers at a rate of 1 LPM, a vacuum pump is connected to the outlet ports of the analyzers. Since there is a difference in pressure drop between each analyzer depending on the length of the tubes connecting the pump and the analyzers, a balancing system is used to ensure that each analyzer draws in the same flowrate. This system is shown in the figure below. While both WMA-4 analyzers and the custom analyzer require this system, the new WMA-5 analyzer has a different design which requires a lower flowrate and has an onboard pump that is strong enough to draw a sample at the correct flowrate without the need for an external pump.

Figure 3.30 Flow Balancing System for CO2 Analyzers (Patel, 2017)

3.5.3 Control System

The CO_2 and He injection rates, along with the sampling interval and test duration are controlled independently through a computer interface using National Instruments LabVIEW software. In addition to these controls, the LabVIEW program also collects data from the CO_2 gas analyzers and various temperature sensors located inside the cabins. While the LabVIEW software was originally designed to be used with a sampling tree with Scans Per Location, it can be used without the sampling tree by setting the Scans Per Location to 0 and using only the S.S

Delay Scans parameter. The sampling tree was not used for any of the testing in this study. A screenshot of this LabVIEW interface is given in Figure 3.31.

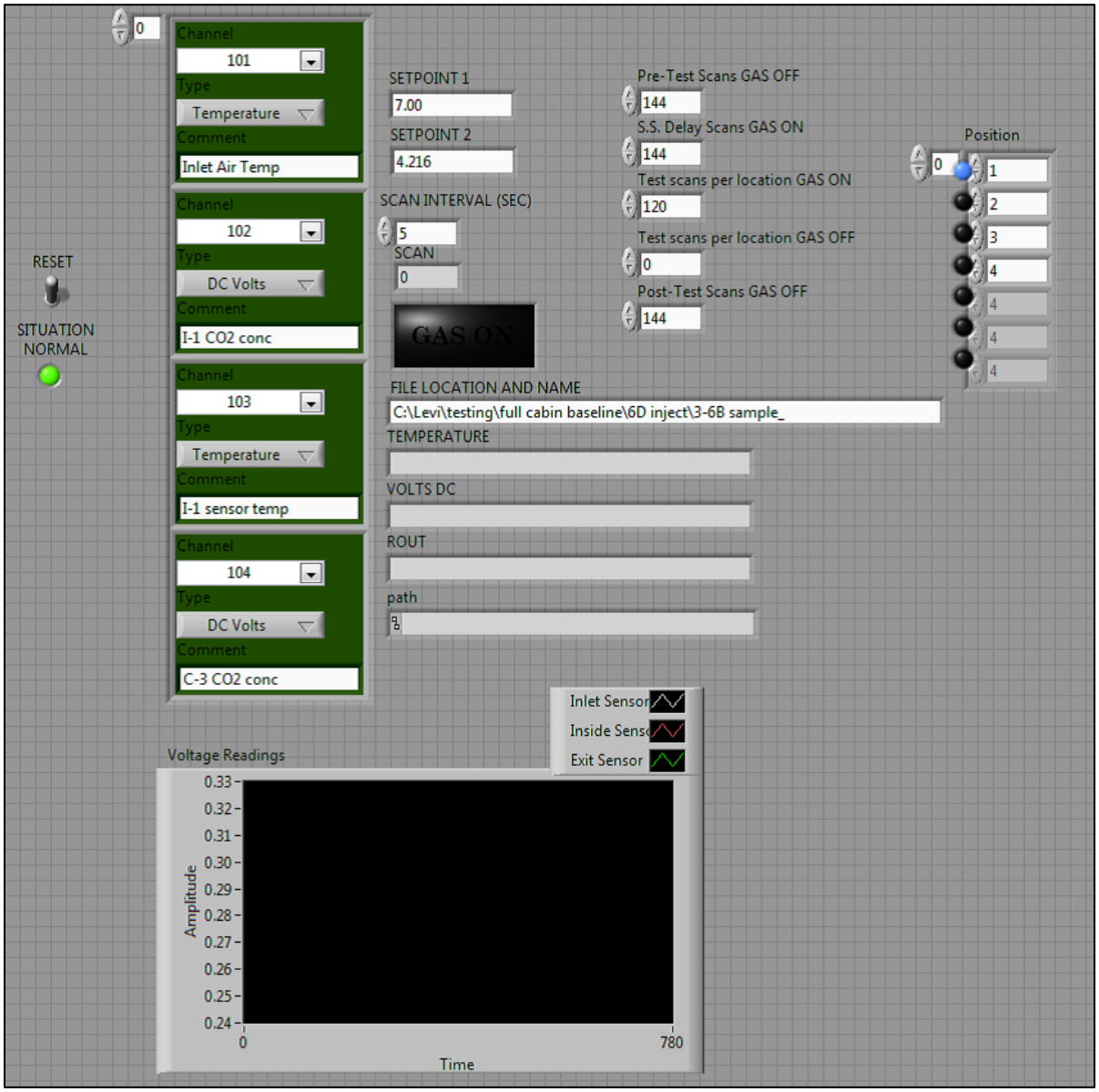

Figure 3.31 Tracer Gas Injection and Sampling LabVIEW Interface (Madden, 2015)

Chapter 4 - Test Procedure and Results

The purpose of this study is to evaluate the effectiveness of the ISOPASS isolation system in containing airborne contaminants. This is accomplished by injecting a tracer gas into the testing area from a point source and measuring the concentration at various locations throughout the cabin. Tests were performed with the ISOPASS on and off, in matched pairs.

4.1 General Experimental Setup

The general experimental setup involves the ISOPASS itself as well as the tracer gas and CO_2 concentration measurement system. The ISOPASS, analyzer calibration, and experiment duration are discussed here.

4.1.1 ISOPASS

The ISOPASS is designed to be installed over two seats by a flight attendant during the flight. It consists of a vinyl enclosure which is secured at the top to the bottom of the overhead bin and to the seat backs and the cabin wall using Velcro. The base of the ISOPASS is held on the floor by weights along the bottom of the skirt, and draped over the exhaust tube. The entrance to the ISOPASS is shut using magnetic strips. The air inside the ISOPASS is exhausted through a pipe placed in the feet area, which draws the air through using a battery powered electric motor and empties into the adjacent exhaust port, as shown in Figure 4.3. From there, the contaminated air passes through the aircraft's HEPA filtration system to remove any airborne contaminants. The ISOPASS exhaust generates a negative pressure inside the ISOPASS, and ventilation air enters through gaps around the corners and base of the ISOPASS. Figure 4.1 and Figure 4.2 show the ISOPASS system in place.

Figure 4.1 ISOPASS Installed in Cabin

Figure 4.2 Inside the ISOPASS

For testing the effectiveness of the ISOPASS at containing airborne contaminants, the tracer gas was injected through a point source inside the ISOPASS. Additionally, an unheated mannequin was placed inside the ISOPASS to occupy a similar volume as an adult passenger.

Figure 4.4 shows the inside of the ISOPASS with the injection source and seated passenger in place.

Figure 4.3 ISOPASS Exhaust Exit, 737 Cabin

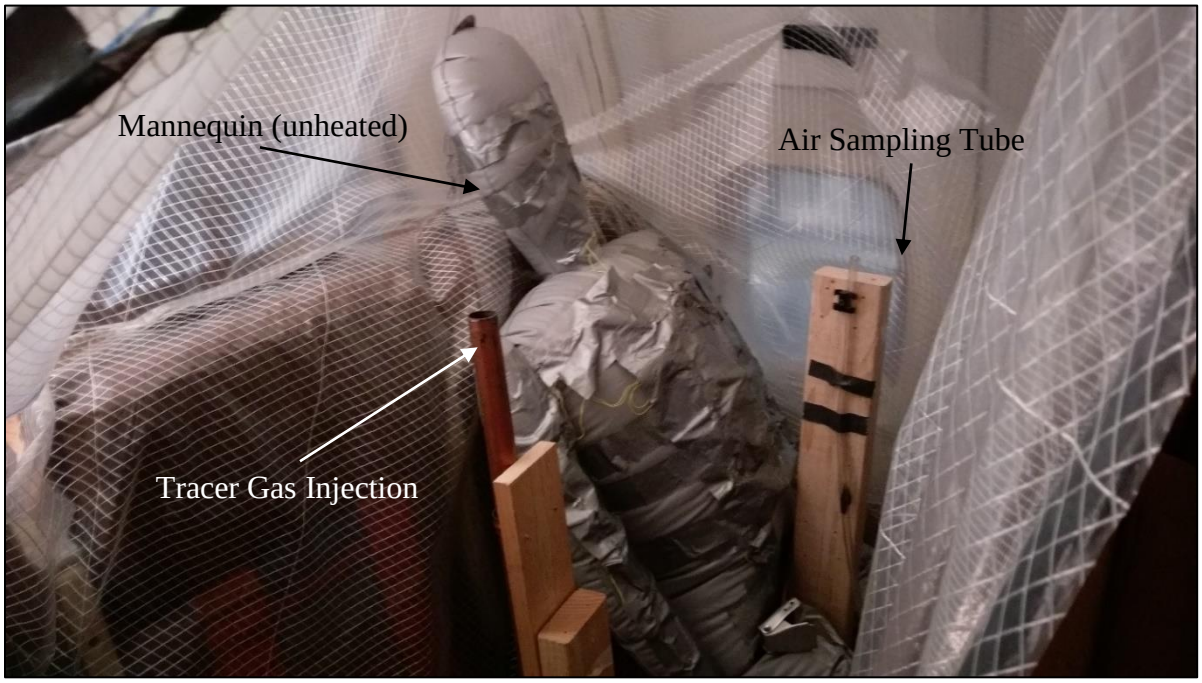

Figure 4.4 ISOPASS with Injection Source and Mannequin

4.1.2 Tracer Gas Measurement

For each cabin, the CO_2 concentration measurements were taken at breathing level for an adult passenger. The sampling tubes were placed level with the headrest of the seat and were held in position by wooden stands placed at the specified seats. Concentration measurements were taken inside the ISOPASS exhaust stream, inside the ISOPASS itself, at the seat across the aisle from the ISOPASS, and several rows in front of the ISOPASS. The specific measurement locations for the 767 and 737 cabins are given in sections 4.2 and 4.8, respectively.

4.1.3 CO_2 Analyzer Calibration

Because the CO_2 concentration data is in voltage, it is important to know the correlation between the received voltage data and the corresponding concentration in parts per million (ppm). For new analyzers and analyzers recently recalibrated by the factory, this is given as a linear relationship over the range of the analyzer. This is the case for the WMA-5 analyzer which was purchased brand new for use in this study. The voltage range of the analyzer is 0 – 2.5 V and the concentration range is 0 – 3000 ppm. Therefore, the correlation between voltage and ppm is the following:

$$C = \frac{3000}{2.5} \times V$$

Where C is the concentration in ppm and V is the voltage.

Because the rest of the analyzers are older and not recently calibrated by the factory, it is important to calibrate them. Calibration gasses with known concentrations of 500 ppm and 2000 ppm of CO_2 were used to calibrate the analyzers. To avoid damaging the analyzers, a pressure regulator was attached to the cylinders.

Each analyzer directly sampled each calibration gas individually for 6 minutes. The average voltage was taken over the last 5 minutes to be sure that the analyzers had reached a stable concentration. The voltage averages were then plotted on a graph and the corresponding linear equation developed by Excel was used to relate the voltage to the concentration in ppm for the duration of the study.

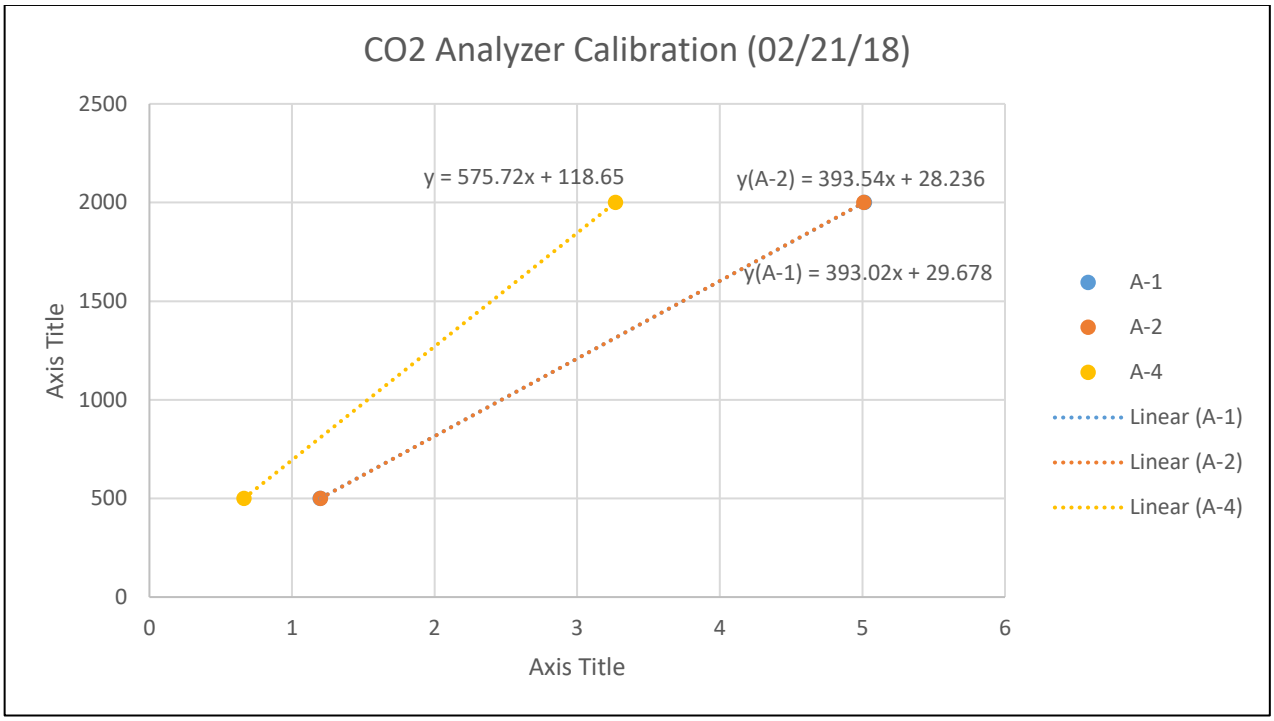

Figure 4.5 CO2 Analyzer Calibration

The calibration, accuracy, voltage range, concentration range, and location of each analyzer is summarized below in Table 4.1.

Table 4.1 Gas Analyzer Summary

Analyzer	Location	Calibration Equation	Voltage Range	Concentration	Accuracy
A-1	Cabin near ISOPASS	$393.02 \cdot V + 29.678$	0-5V	0-2000 ppm	20 ppm
A-2	Inside ISOPASS	$393.54 \cdot V + 28.236$	0-5V	0-2000 ppm	20 ppm
A-3	ISOPASS exhaust	$\frac{3000}{2.5} \cdot V$	0-2.5V	0-3000 ppm	30 ppm
A-4	Far Away from ISOPASS	$575.72 \cdot V + 118.65$	0-5V	0-3000 ppm	60 ppm

4.1.4 Experiment Duration

To properly analyze and compare the results of the tracer gas studies, it was important to allow the system to reach steady state concentration. In order to determine the time required to reach steady state CO_2 concentration, the tracer gas was injected inside the ISOPASS for 30 minutes. After this, the tracer gas injection was stopped, and the computer continued to take readings for an additional 30 minutes. The CO_2 concentrations were measured inside the ISOPASS, inside the ISOPASS exhaust stream, at the seat across the aisle adjacent to the ISOPASS, and in the cabin supply air inlet. The results of the steady state experiment are shown in Figure 4.6. This experiment shows that it took approximately 13 minutes to achieve steady state CO_2 concentration inside the ISOPASS. Similarly, the results show that it took about 7 minutes to return to ambient CO_2 concentration after the gas was turned off. Because it was important to have a sufficient amount of data points after steady state conditions have been reached, the final experiment duration was decided to be 10 minutes of readings before the gas

was turned on, followed by 30 minutes with the gas on, and 20 minutes with the gas off. For each test in this study, he pre-injection average is taken over the first 600 seconds (10 minutes), and the steady-state gas on average is taken over the last 1000 seconds (16.7 minutes) of the tracer gas injection.

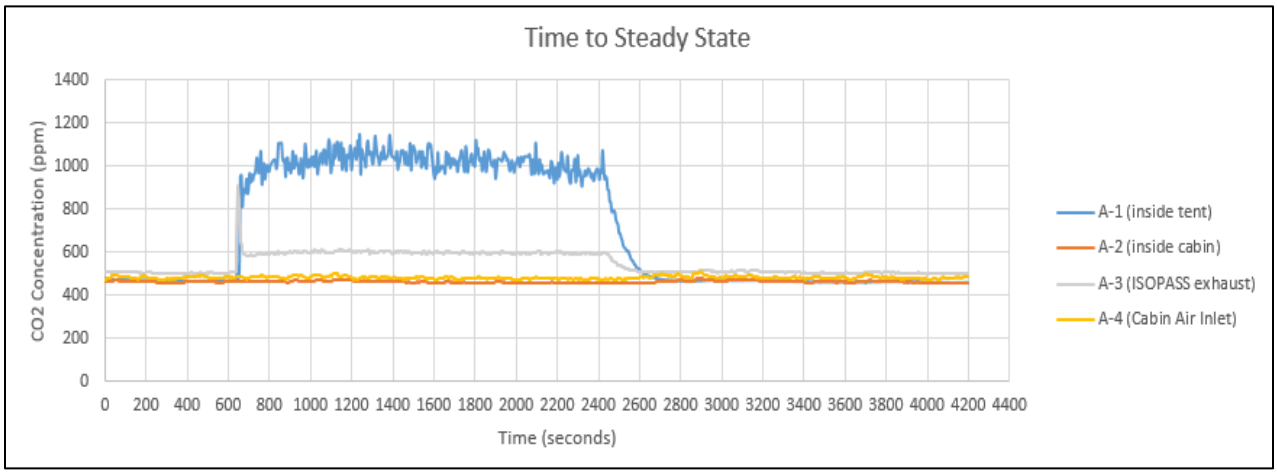

Figure 4.6 Steady State Results in ISOPASS

4.2 Procedure Overview - Containment Effectiveness in 767 Mock-up

To test the containment effectiveness of the ISOPASS prototype within the 767 cabin, tracer gas was injected through a point source at approximate breathing level mounted to a seat within the ISOPASS. Matched pairs were used to mitigate potential statistical problems while verifying repeatability. Tests were conducted with and without the ISOPASS in place. Additionally, matched pair tests were completed for both gaspers on and gaspers off. Each matched pair was repeated three times; 3 repetitions x 2 gasper conditions for a total of 6 matched pairs, or 12 individual tests. For each test, the exhaust fan was set to 60%, with a fresh battery. This corresponds to approximately 160 CFM at the start of the test.

Concentration measurements were taken inside the ISOPASS in the seat next to the injection source, attached to the back of the coughing mannequin (not in use for these tests); in

the seat across the aisle adjacent to the ISOPASS; and far away from the ISOPASS, near the front of the cabin. Each of the sampling tubes were positioned at approximate breathing level. The radial distances between the injection point and the sampling tubes were 14", 44", and 128", as shown in Figure 4.7. The uncertainty of the PP Systems CO_2 analyzers is 1% of the range of the analyzer. This corresponds to 20 ppm for the A-1, A-2, and 30 ppm for the A-3 analyzer. The A-4 analyzer, which was custom built using an Edinburgh Gas Sampling Card, has an uncertainty of 2% of the range. This corresponds to 60 ppm for the A-4 analyzer.

It was determined from the mass balance and stratification confirmation tests later in this chapter that the concentration measured in the ISOPASS exhaust is not an accurate or useful point of data, and therefore not significant for the matched pair tests. For this reason, the ISOPASS exhaust concentration data is excluded from the graphs of the results.

Figure 4.7: 767 Cabin Layout, Sample and Mannequin Locations

4.3 Representative Results and Analysis – Boeing 767 Mock-up Cabin

Presented here are tests that are representative of the overall results for each ISOPASS condition, ISOPASS on and ISOPASS off, and for each gasper condition, gaspers on and gaspers off. Because the results for each repetition are all very similar, any one could have been chosen as the representative result for that particular ISOPASS and gasper condition. Thus, for the sake of this thesis, the result shown is simply the most readable of the three repetitions. Full results for every test are available in the accompanying electronic appendix.

The ISOPASS on tests are conducted with the ISOPASS prototype fully in place in the location specified in Figure 1, and with the flap closed completely. ISOPASS off tests are conducted with the ISOPASS completely removed from the cabin, and the exhaust fan off. The injection point and analyzer locations remain the same between the ISOPASS on and ISOPASS off conditions and are referred to with respect to the ISOPASS whether it is in place or not.

The CO_2 injection rate is approximately 5.0 liters per minute for all tests, with an accompanying Helium injection rate of 3.07 liters per minute. The cabin is half-loaded with thermal mannequins to represent passengers and equipment. Mannequin locations are given on Figure 4.7 as X's.

4.3.1 ISOPASS Off

Testing without the ISOPASS gives a point of comparison when considering the effectiveness of the ISOPASS.

4.3.1.1 Gaspers Off

With gaspers off, the airflow around the cabin is wholly controlled by the central ventilation and the heat from the mannequins. FAA ventilation requirements are typically met

without the need for gaspers, many aircraft do not have them equipped, making these tests realistic in practice. The gaspers off tests are conducted with the gasper fan shut off and the gaspers themselves fully closed.

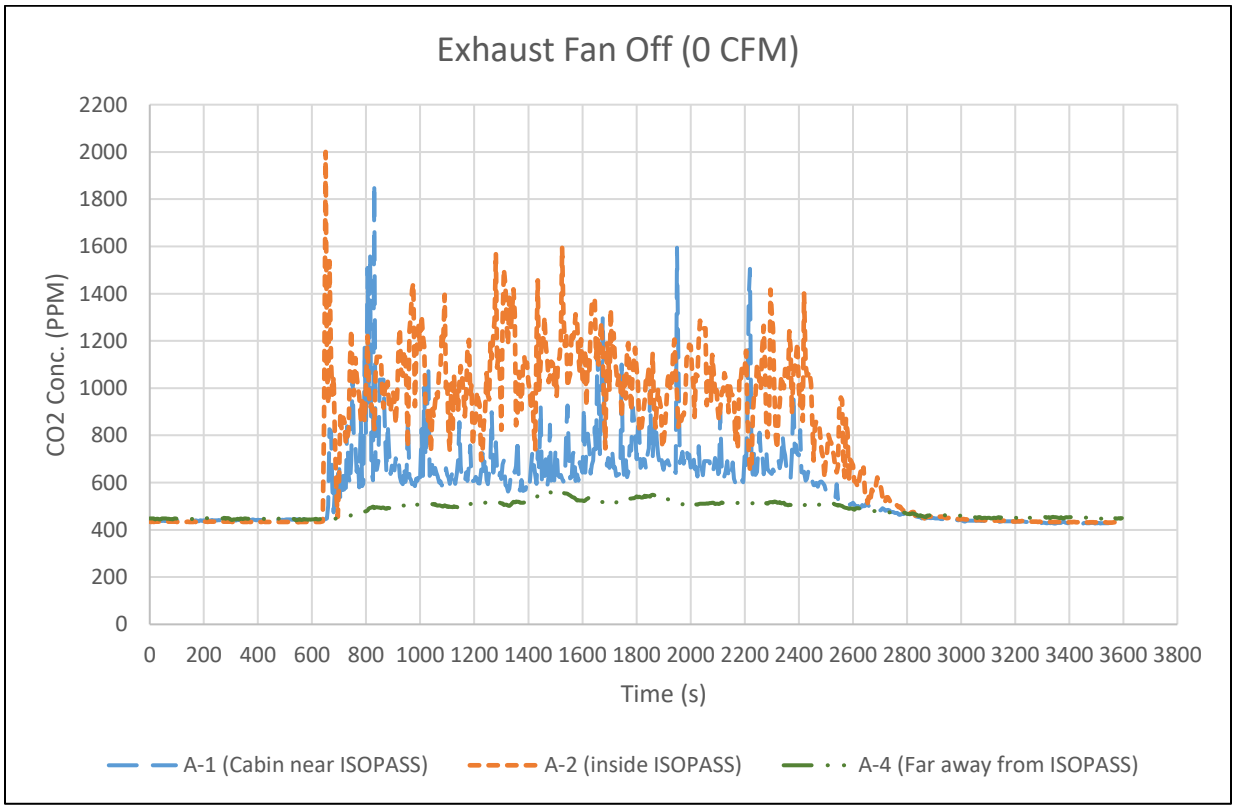

Figure 4.8: ISOPASS Off, Gaspers Off

Average background CO_2 concentrations for the test presented in Figure 4.8, before the tracer gas injection, are as follows:

A-1 (Cabin near ISOPASS):	441 ppm
A-2 (Inside ISOPASS):	434 ppm
A-4 (Cabin Away From ISOPASS):	446 ppm

Once the tracer gas injection began and reached steady state in the cabin, the average concentrations became as follows:

A-1 (Cabin near ISOPASS):	715 ppm
A-2 (Inside ISOPASS):	1050 ppm
A-4 (Cabin Away From ISOPASS):	524 ppm

From this we can see that the concentrations across the cabin increase, as expected. We can define the percent-difference as the change in CO_2 concentration at steady state with the gas injection on with respect to the background prior to the injection. The percent-difference for each sampling location are approximately:

A-1 (Cabin near ISOPASS):	+62%
A-2 (Inside ISOPASS):	+142%
A-4 (Cabin Away From ISOPASS):	+17%

As expected, the ISOPASS off, gaspers off experiments show dispersion of the tracer gas throughout the entire cabin, with the highest percent increase in concentration being nearest to the injection point, and becoming progressively lower at further locations. Even the furthest sampling location sees a noticeable increase in CO_2 concentration, higher than the uncertainty of the measuring device. Results for the ISOPASS Off, gaspers off tests are reasonably consistent. The percent increase is similar for each test, varying slightly depending on actual injection rate as measured by the rotameter.

4.3.1.2 Gaspers On

With gaspers on, airflow patterns may be disrupted and could affect the distribution of the tracer gas through the cabin. The 767 mock-up cabin is equipped with just three rows of gaspers, rows 5, 6, and 7. For the sake of these tests, every gasper in the 767 mock-up cabin was fully opened and directed straight down. Gasper pressure was maintained at 2" H_2O.

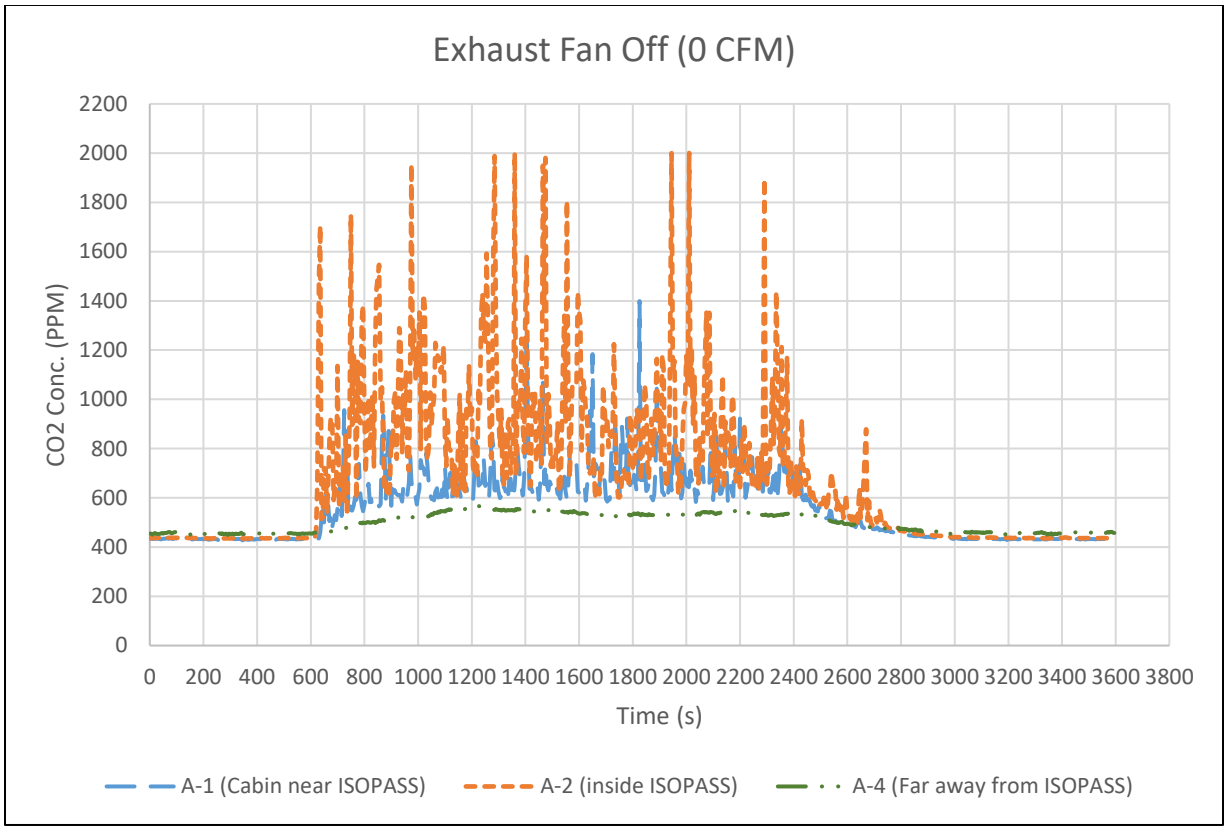

Figure 4.9: ISOPASS Off, Gaspers On

Average background CO_2 concentrations for this test before the tracer gas injection are as follows:

A-1 (Cabin near ISOPASS):	432 ppm
A-2 (Inside ISOPASS):	436 ppm
A-4 (Cabin Away From ISOPASS):	455 ppm

At steady state CO_2 concentration in the cabin, the average concentrations became as follows:

A-1 (Cabin near ISOPASS):	698 ppm
A-2 (Inside ISOPASS):	894 ppm
A-4 (Cabin Away From ISOPASS):	536 ppm

As observed with the gaspers off, the concentrations across the cabin increase. The percent-difference for each sampling location are found to be:

A-1 (Cabin near ISOPASS):	+61%
A-2 (Inside ISOPASS):	+105%
A-4 (Cabin Away From ISOPASS):	+18%

With the ISOPASS off, we do not observe much difference between the gaspers on and gaspers off conditions. Results remain consistent, with a bit more variance from test to test with gaspers on, although this can be attributed to varying airflow patterns in the cabin. Overall, we observe very similar distribution of tracer gas through the cabin for both gasper conditions without the ISOPASS.

4.3.2 ISOPASS On

With the ISOPASS installed in the 767 cabin, we expect that the tracer gas will be contained well, and that there will be a measurable reduction in the percent-increase of CO_2 concentration in the cabin outside of the ISOPASS. For each test, the ISOPASS exhaust fan was set to 60%. Actual exhaust flowrate was measured by a 4” vane anemometer placed in the exhaust stream, and swirl was reduced using metal honeycomb.

4.3.2.1 Gaspers Off

With gaspers off, the source of fresh air to the passenger inside the ISOPASS is from the leakage points around the ISOPASS, such as the corners, slight gaps in the entrance, gaps along the floor where the ISOPASS is draped, etc. Most of the fresh air drawn in by the exhaust fan is around the floor where the exhaust pipe entrance is located, and as a result, tracer gas builds up in the passenger breathing space, eventually being drawn into the top of the exhaust pipe. This causes a high concentration of CO_2 in the upper portion of the ISOPASS and a stratified concentration in the exhaust stream.

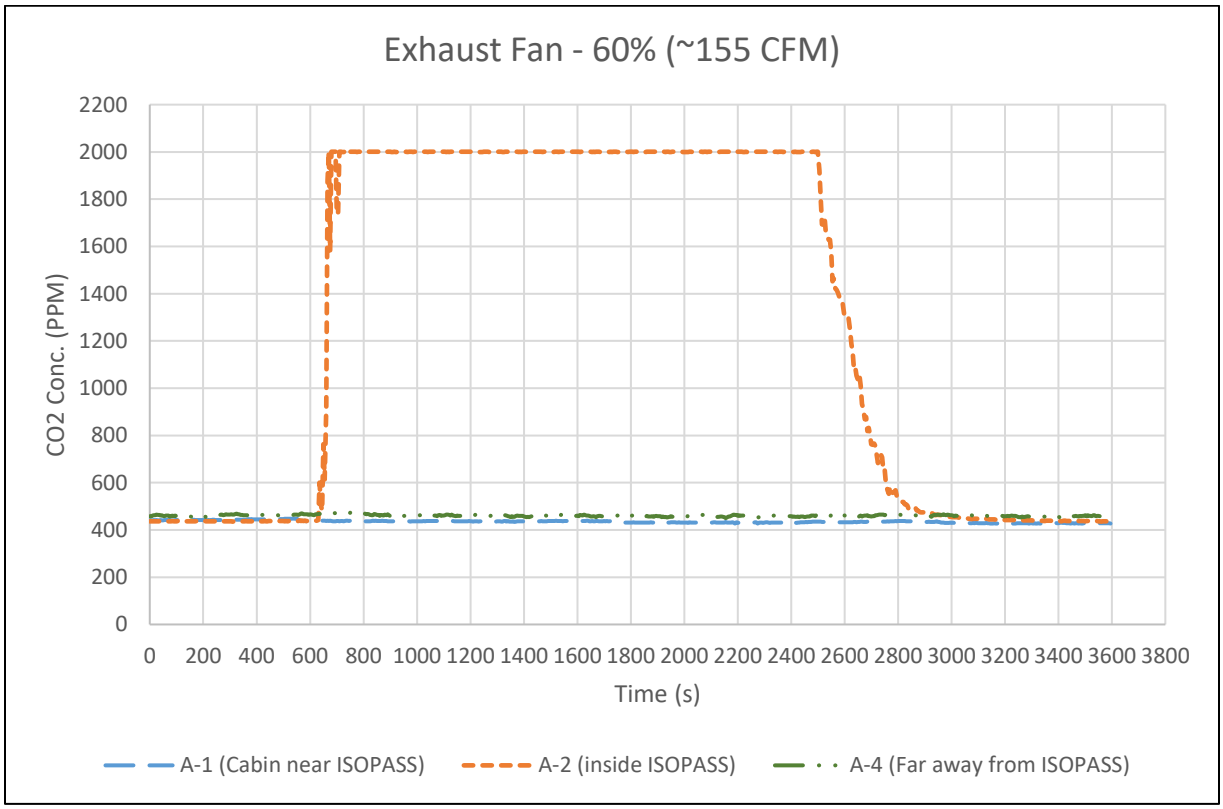

Figure 4.10: ISOPASS On, Gaspers Off

Average background CO_2 concentrations before the tracer gas injection are as follows:

A-1 (Cabin near ISOPASS): 443 ppm

A-2 (Inside ISOPASS): 436 ppm

A-4 (Cabin Away From ISOPASS): 461 ppm

After the tracer gas injection began, and upon steady state CO_2 in the cabin, the average concentrations became as follows:

A-1 (Cabin near ISOPASS): 433 ppm

A-2 (Inside ISOPASS): 2000 ppm (at least)

A-4 (Cabin Away From ISOPASS): 459 ppm

The A-1 and A-2 analyzers peak at approximately 5 volts, which corresponds to 2000 ppm. The actual concentration inside the ISOPASS is likely much higher, but cannot be accurately measured by the equipment. The percent-difference for each sampling location are approximately:

A-1 (Cabin near ISOPASS): -2 %

A-2 (Inside ISOPASS): +358% (at least)

A-4 (Cabin Away From ISOPASS): -1%

The ISOPASS then is very effective at containing the tracer gas injection with the gaspers off. The results are also very consistent. The percent-differences in concentrations outside the ISOPASS never go into the positives, and only vary by about 2% at most. Additionally, this represents a difference of around 10 ppm, which is well within the uncertainty of the analyzers.

4.3.2.2 Gaspers On

While the addition of the gaspers in the ISOPASS does not solve the stratification issue in the exhaust, it does circulate the air around the passenger breathing level better than with just the exhaust alone. The exhaust flowrate is many times higher than the flow rate of both of the gaspers combined, however, with the flowrate of the exhaust at 60% averaging around 155 CFM and the flowrate of both gaspers combined being about 5 CFM. There was still the question as to whether the gaspers would affect the ISOPASS containment effectiveness by forcing some of the tracer gas out of the ISOPASS, changing the airflow patterns in the ISOPASS, etc. Additionally, it is valuable to compare the ISOPASS off, gaspers on data to the ISOPASS prototype and verify the effectiveness ISOPASS model for multiple realistic conditions.

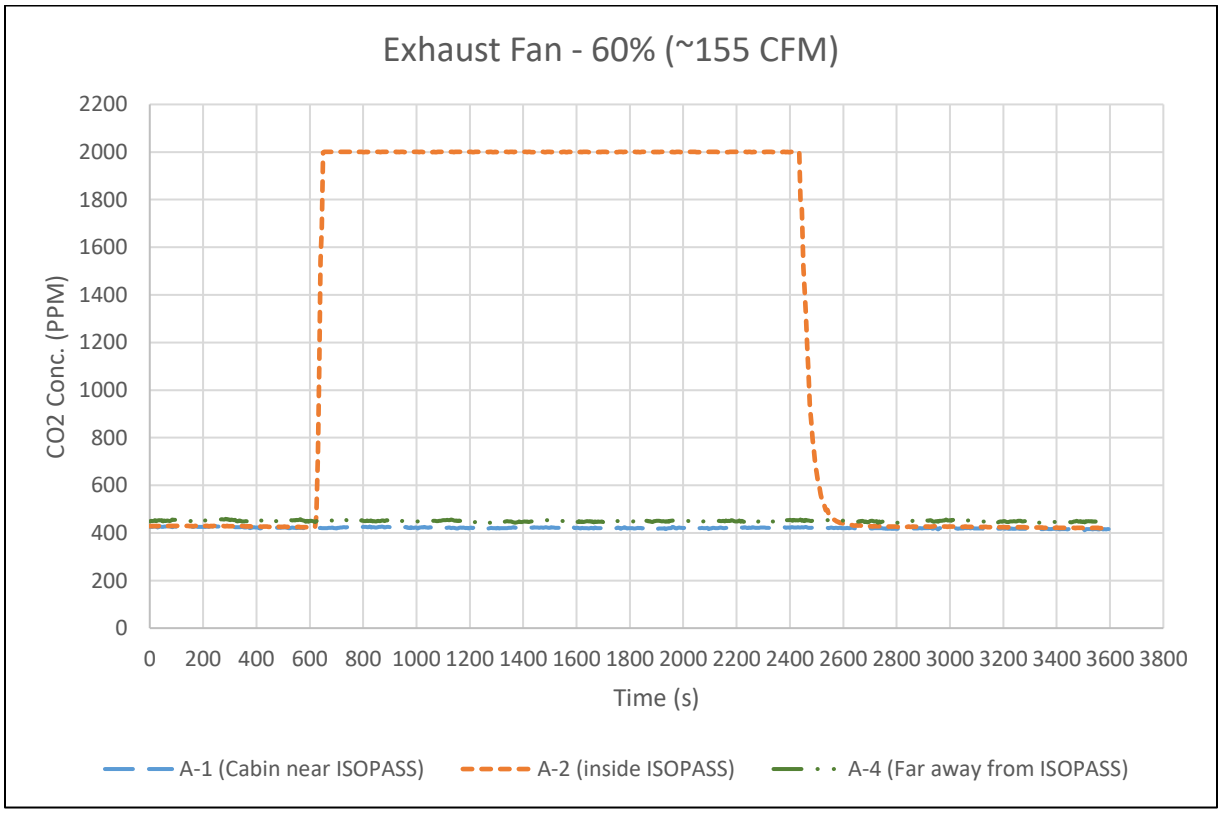

Figure 4.11: ISOPASS On, Gaspers On

Average background CO2 concentrations before the tracer gas injection are as follows:

A-1 (Cabin near ISOPASS):	424 ppm
A-2 (Inside ISOPASS):	428 ppm
A-4 (Cabin Away From ISOPASS):	452 ppm

After the tracer gas injection began, and upon steady state CO2 in the cabin, the average concentrations became as follows:

A-1 (Cabin near ISOPASS):	421 ppm
A-2 (Inside ISOPASS):	2000 ppm (at least)
A-4 (Cabin Away From ISOPASS):	449 ppm

As before, the analyzer sampling from inside the ISOPASS peaks out at approximately 5 volts, although the concentration could be much higher. The percent-difference for each sampling location are approximately:

A-1 (Cabin near ISOPASS):	-1%
A-2 (Inside ISOPASS):	+368% (at least)
A-4 (Cabin Away From ISOPASS):	-1%

The inclusion of gaspers inside the ISOPASS makes no noticeable difference in its containment effectiveness. As with the gaspers-off tests, the results here are remarkably consistent, varying only by a couple percent at most and well within the uncertainty of the CO2 analyzers. As previously mentioned, the passenger may want to open the gaspers to create a more comfortable environment inside the ISOPASS. These tests suggest that this will not impact the performance of the ISOPASS in any measurable way while the ISOPASS itself is fully closed.

4.4 Coughing Mannequin Initial Evaluation

To more accurately simulate a sick passenger inside the cabin, a preliminary evaluation of the coughing mannequin prototype was performed in the 767 cabin mockup. For this initial evaluation, one test was performed without the ISOPASS, and one test was performed with the ISOPASS in place. Each test was performed with the gaspers off. Because this evaluation is just a proof of concept for the coughing mannequin inside the ISOPASS enclosure, the effect of gaspers with the coughing mannequin was not considered. Future research on the coughing mannequin will cover gasper effects.

The coughing mannequin coughs approximately once every 1.25 minutes, with a volume of 4.2 liters per cough. To insure sufficient CO_2 supply, each test was run for 15 coughs. CO_2 was again used as a tracer gas but was not mixed with helium for these tests.

4.4.1 ISOPASS Off

As before, the ISOPASS-off condition provides a point of comparison for the ISOPASS-on condition and overall performance of the ISOPASS prototype.

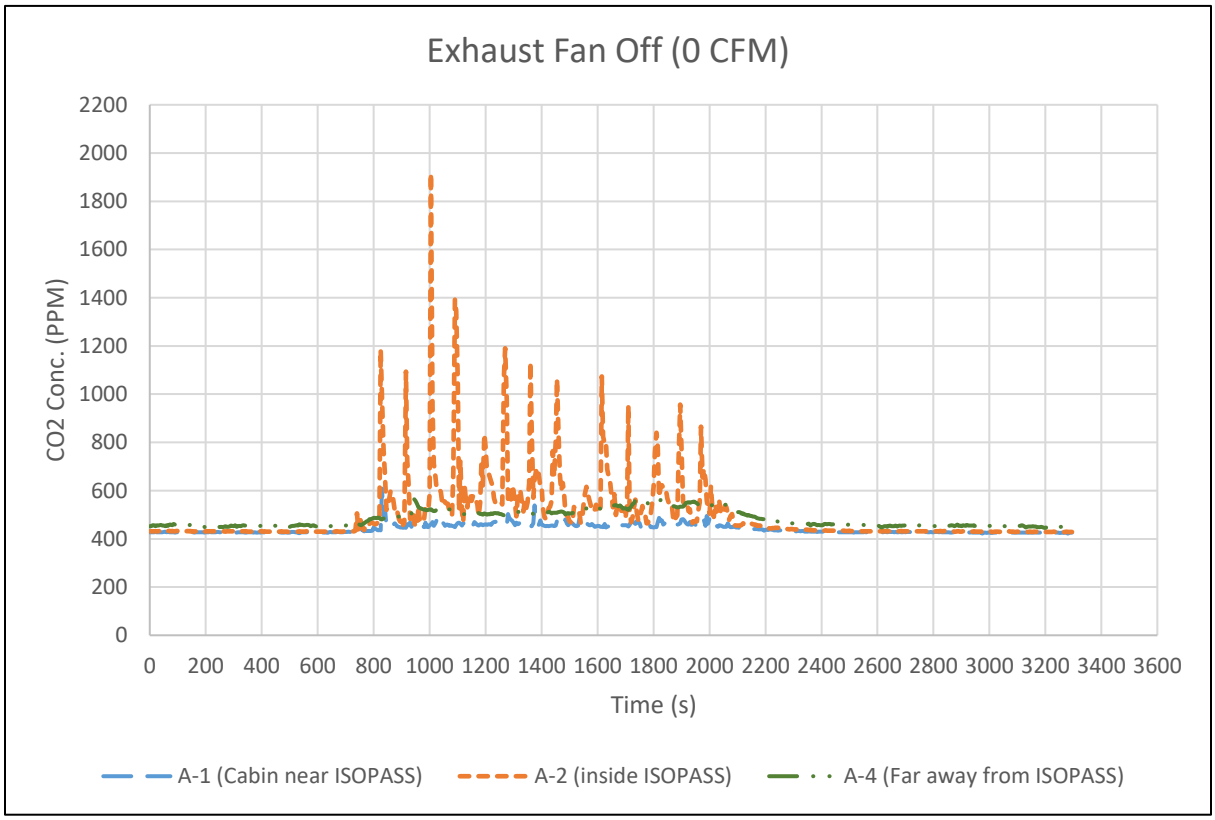

Figure 4.12: Coughing Mannequin, ISOPASS Off

Average background CO_2 concentrations before initializing the coughing procedure were as follows:

A-1 (Cabin near ISOPASS):	427 ppm
A-2 (Inside ISOPASS):	430 ppm
A-4 (Cabin Away From ISOPASS):	454 ppm

Once the coughing began and the tracer gas reached approximately steady state in the cabin, the average concentrations became as follows:

A-1 (Cabin near ISOPASS):	462 ppm
A-2 (Inside ISOPASS):	613 ppm
A-4 (Cabin Away From ISOPASS):	523 ppm

Thus, the percent-difference for each sampling location are approximately:

A-1 (Cabin near ISOPASS):	+8%
A-2 (Inside ISOPASS):	+42%
A-4 (Cabin Away From ISOPASS):	+15%

When compared to the higher and constant injection rate of the matched pair tests in the 767 cabin, the respective percent increases in concentration are lower as would be expected. Perhaps more interesting is the fact that, in this test, the percent increase at the sampling locations adjacent to the source are considerably less than in the matched pair tests, while the percent increase for the sampling location down the cabin from the source remains quite similar. This is likely do to the direction of the cough and may have something to do with the force of the cough as well. Not only is the coughing mannequin pointed horizontally, perpendicular to the adjacent sampling tubes, but it also ‘coughs’ the tracer gas in this direction with some force, rather than trickle out from the injection source into the cabin. This is demonstrated by the peaks in concentration at each coughing event in Figure 4.12.

4.4.2 ISOPASS On

The effectiveness of the ISOPASS at containing tracer gas has already been demonstrated with a point source injection. As previously stated however, the coughing mannequin is a better analogue for a sick passenger, and the effective of the forcefulness of a cough had not yet been evaluated inside the ISOPASS prototype.

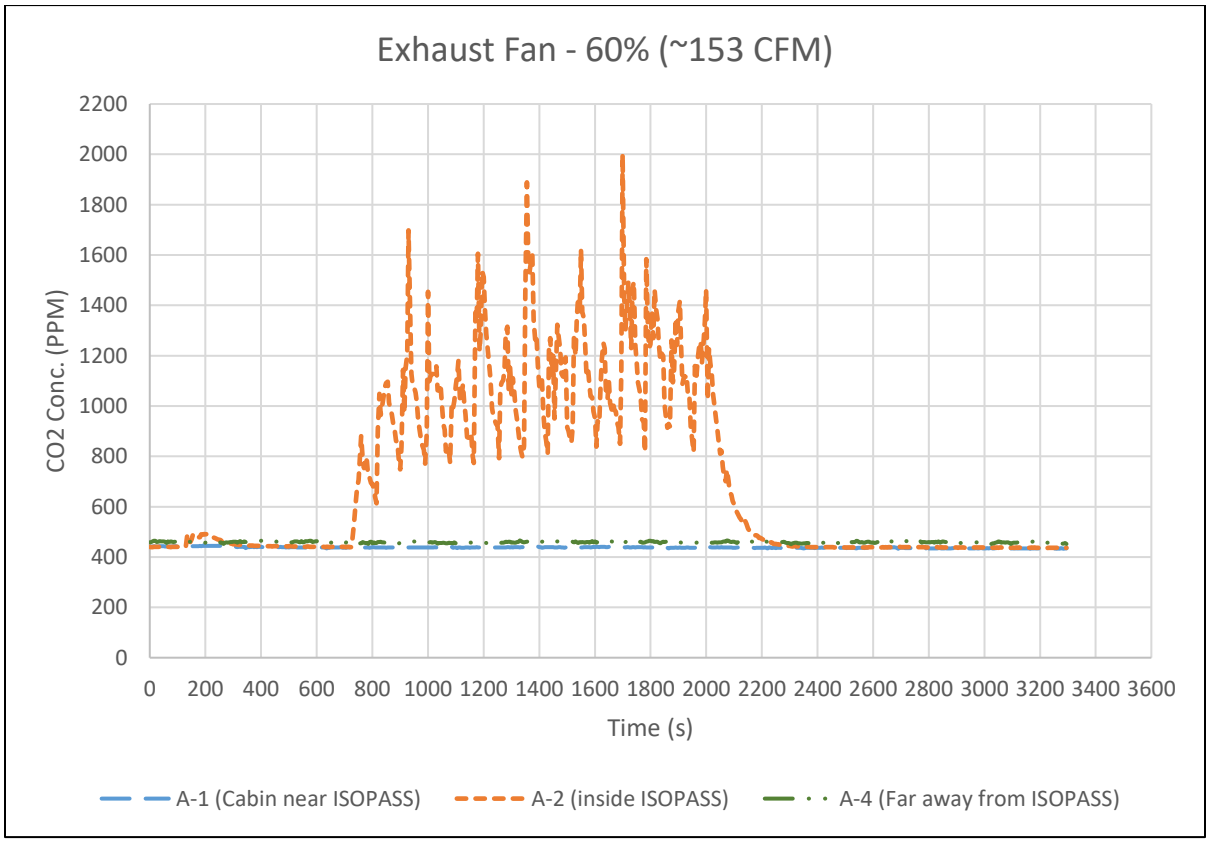

Figure 4.13: Coughing Mannequin, ISOPASS On

Average CO_2 concentrations before initializing the coughing procedure were as follows:

A-1 (Cabin near ISOPASS):	441 ppm
A-2 (Inside ISOPASS):	451 ppm
A-4 (Cabin Away From ISOPASS):	460 ppm

After the coughing procedure began and the tracer gas reached approximately steady state in the ISOPASS and the cabin, the average concentrations became as follows:

A-1 (Cabin near ISOPASS): 438 ppm

A-2 (Inside ISOPASS): 1136 ppm

A-4 (Cabin Away From ISOPASS): 459 ppm

Thus, the percent-difference for each sampling location are approximately:

A-1 (Cabin near ISOPASS): -1%

A-2 (Inside ISOPASS): +152%

A-4 (Cabin Away From ISOPASS): ±0%

These results replicate the results of the matched pair tests in the 767 cabin. Because the injection rate is lower and segmented into individual coughs rather than a continuous injection, the average concentration in the ISOPASS is lower in the ISOPASS-on coughing mannequin test than in the ISOPASS-on matched pair tests. The containment is essentially identical in both, with no measurable quantity of tracer gas escaping the ISOPASS enclosure when fully closed.

4.5 Minimum Exhaust Flowrate

Each of the ISOPASS-on tests in the 767 cabin were performed with the exhaust fan set to 60%. However, factors such as battery longevity, noise, and human comfort may be improved with a reduced fan speed. Additionally, varying the fan speed allows for further analysis of the ISOPASS prototype's performance.

To test the minimum exhaust fan speed required for no leakage, a 3" PVC connection was placed in the entrance of the ISOPASS at breathing level, with the ISOPASS itself sealed around it. This creates a reasonably large controlled leak point. A sample tube was then placed

around the center of the opening, approximately an inch outside the ISOPASS. Other sampling locations remained the same.

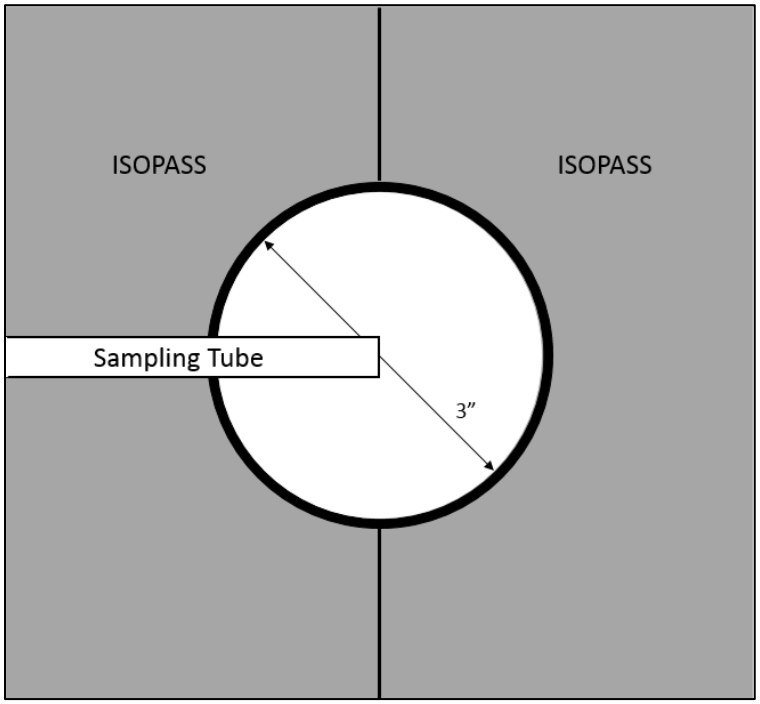

Figure 4.14: Controlled Leak Point Layout

Tests were initially performed with the gaspers off, with the exhaust fan at 0%, 20%, 30%, 40%, and 60%. Later, the same test was performed with gaspers on, focusing on 0% through 40%. The injection rates for every test were set to 5 lpm for CO_2 and a corresponding 3.07 lpm for helium, although the gaspers-off data was taken before we were able to take accurate rotameter readings to verify.

4.5.1 Gaspers Off

Minimum exhaust fan flowrate was initially tested just with the gaspers off. As with the matched pair tests, the gaspers-off condition provides a reasonable baseline for comparison while still being realistic.

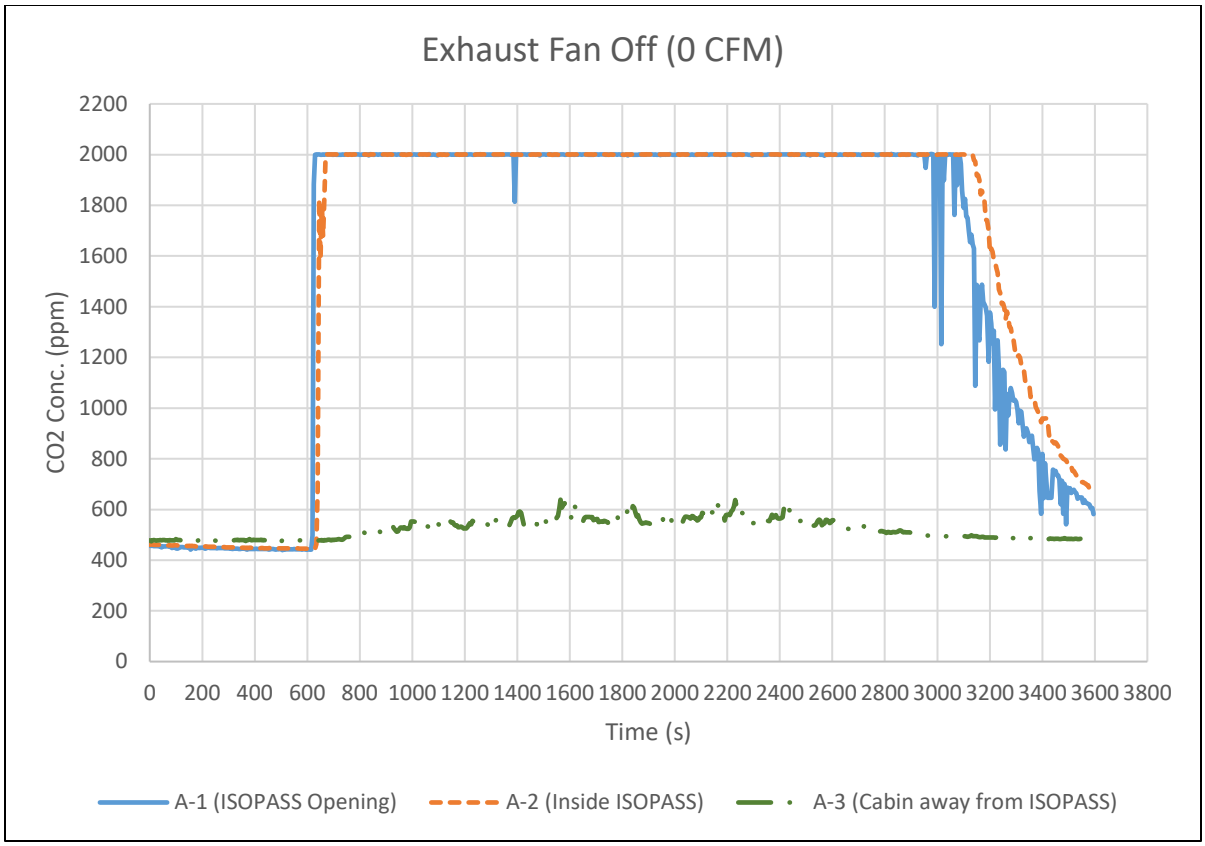

Figure 4.15: Gaspers Off Minimum Exhaust Speed - No Flow

With the ISOPASS in place and the exhaust fan completely turned off, the concentration of CO_2 builds inside the ISOPASS and saturates both the analyzer inside the ISOPASS and the analyzer just outside of the controlled opening. We observe very similar results to the ISOPASS-off experiments further in the cabin. The percent increase in the average CO_2 concentration for the A-3 analyzer down in the cabin is 19%, which is very similar to each of the ISOPASS-off tests. As expected, the ISOPASS is not at all effective at containing the tracer gas with no exhaust ventilation.

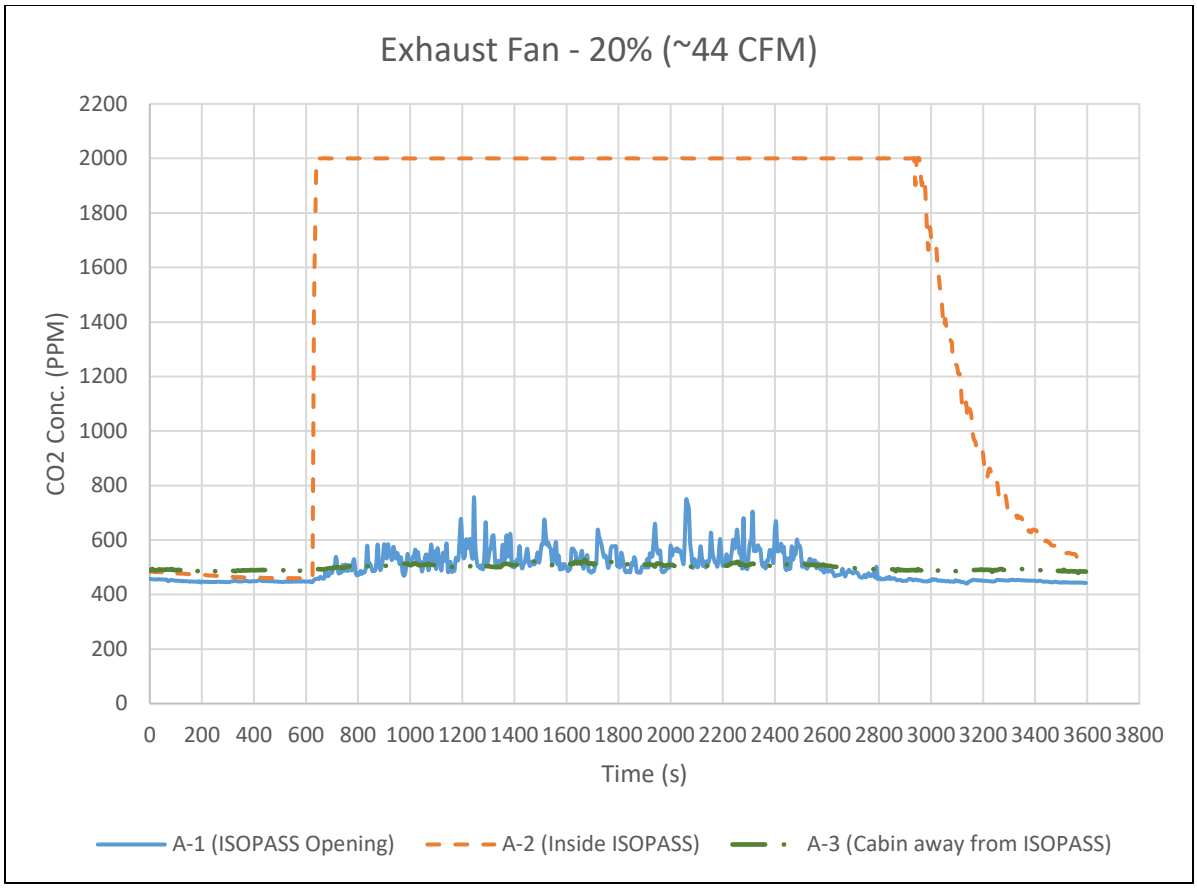

Figure 4.16: Gaspers Off Minimum Exhaust Fan Speed - 20%

At 20%, we see a massive improvement over no exhaust ventilation at all, however we do still observe tracer gas leakage at the controlled opening, and a slight increase in concentration in the cabin. The percent increase at the opening is 20% and the increase in the cabin is just 5%.

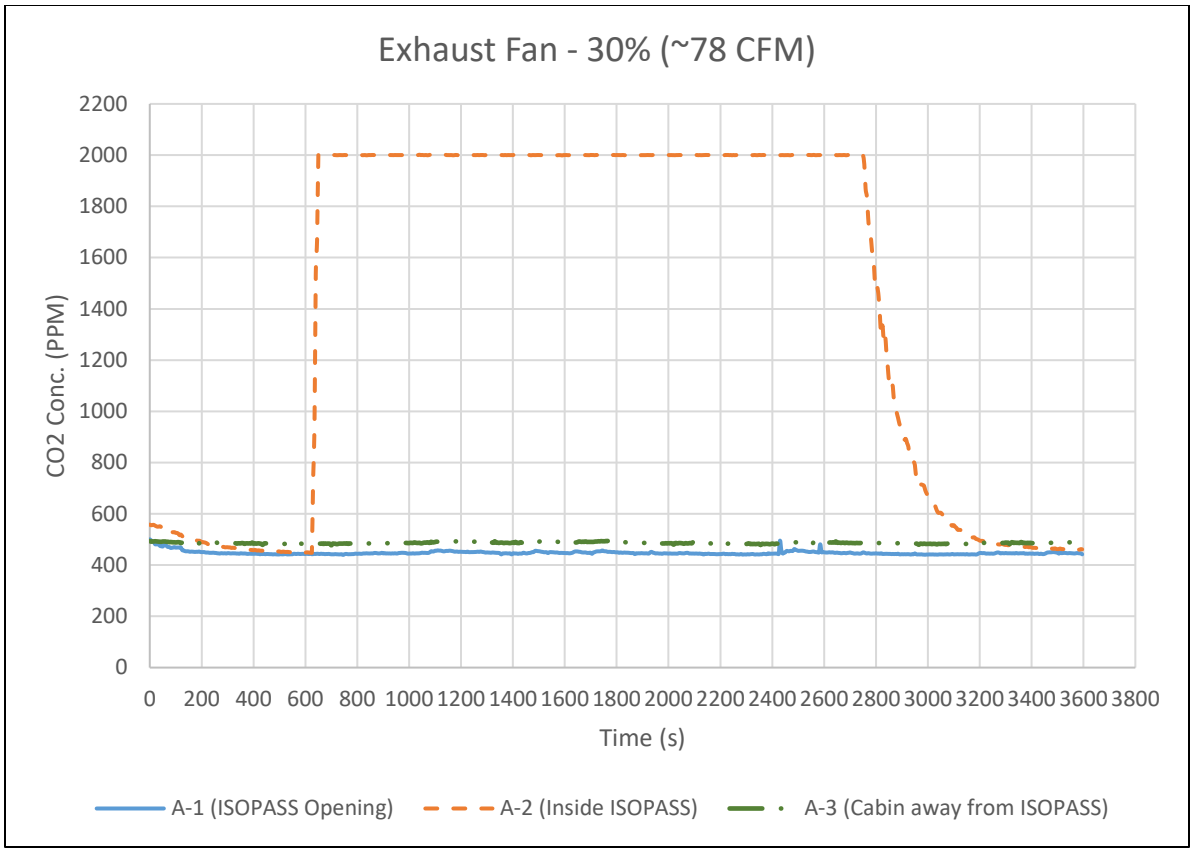

Figure 4.17: Gaspers Off Minimum Exhaust Fan Speed - 30%

Starting from 30%, there is no longer any observable leakage either at the controlled leak point or in the cabin. Percent increase in average CO_2 concentration is essentially identical to the ISOPASS-on tests with the exhaust fan set to 60%, with the ISOPASS opening seeing a percent difference of -1% and the cabin seeing no difference, at ±0%.

From this point, higher exhaust fan speeds provide the same results that we observe at 30%. Full results for 40% and 60% are included in the electronic appendix.

4.5.2 Gaspers On

The 20%, 30%, and 40% tests were repeated for the gaspers-on condition, each test performed twice as before. The 0% test was then added to provide some perspective for the results of the other tests.

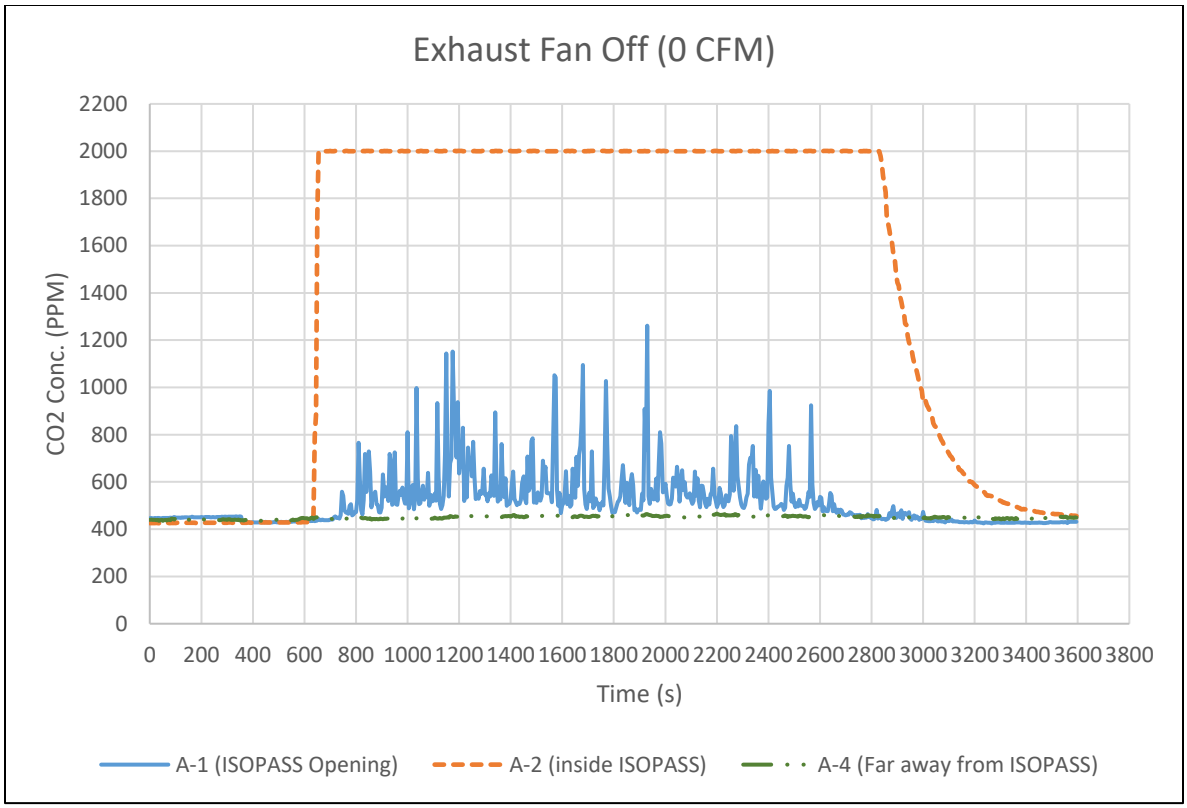

Figure 4.18: Gaspers On Minimum Exhaust Fan Speed - No Flow

With the gaspers on and the exhaust fan off, we observe leakage at the controlled opening and a very slight increase in the concentration inside the cabin, although to a much lesser degree than with gaspers off. The percent increase in average CO_2 concentration at the ISOPASS opening is +32%, and the increase in the cabin is +4%. This is comparable to the results of the gaspers-off condition at 20% fan speed. Smoke visualization tests were conducted and confirmed that above approximately 15% fan speed, the ISOPASS begins to draw air in.

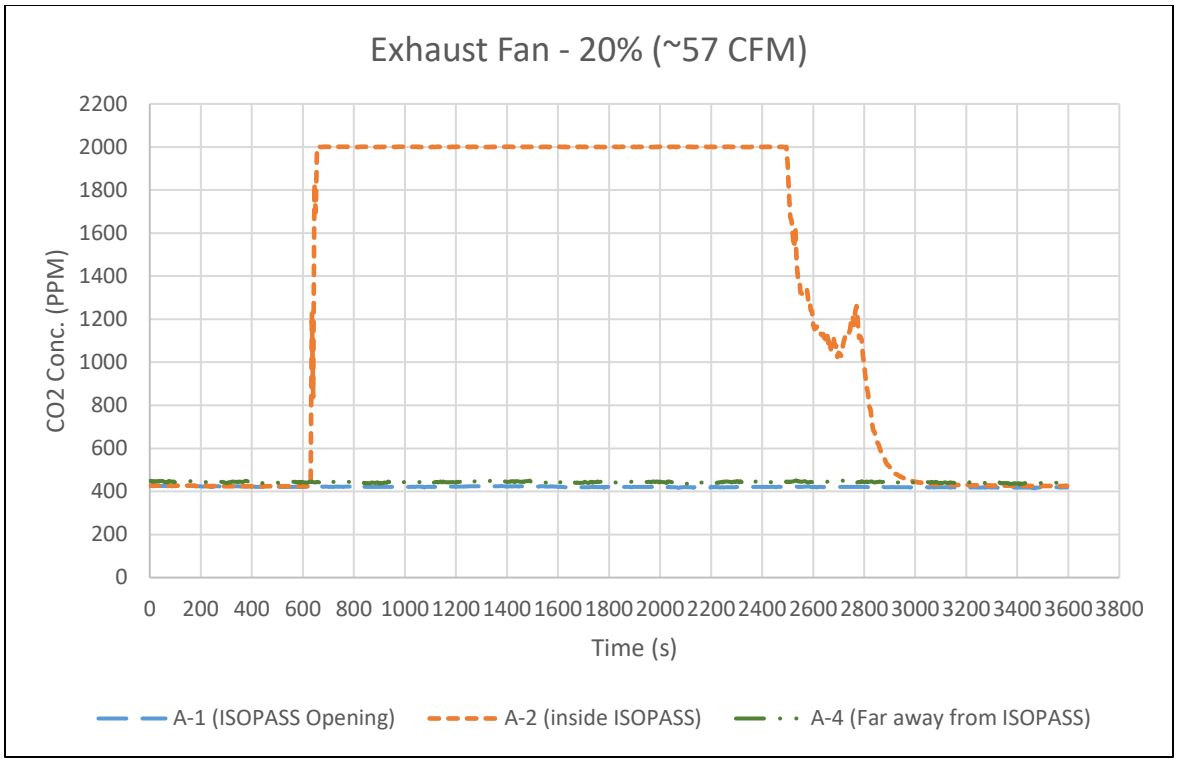

Figure 4.19: Gaspers On Minimum Exhaust Fan Speed - 20%

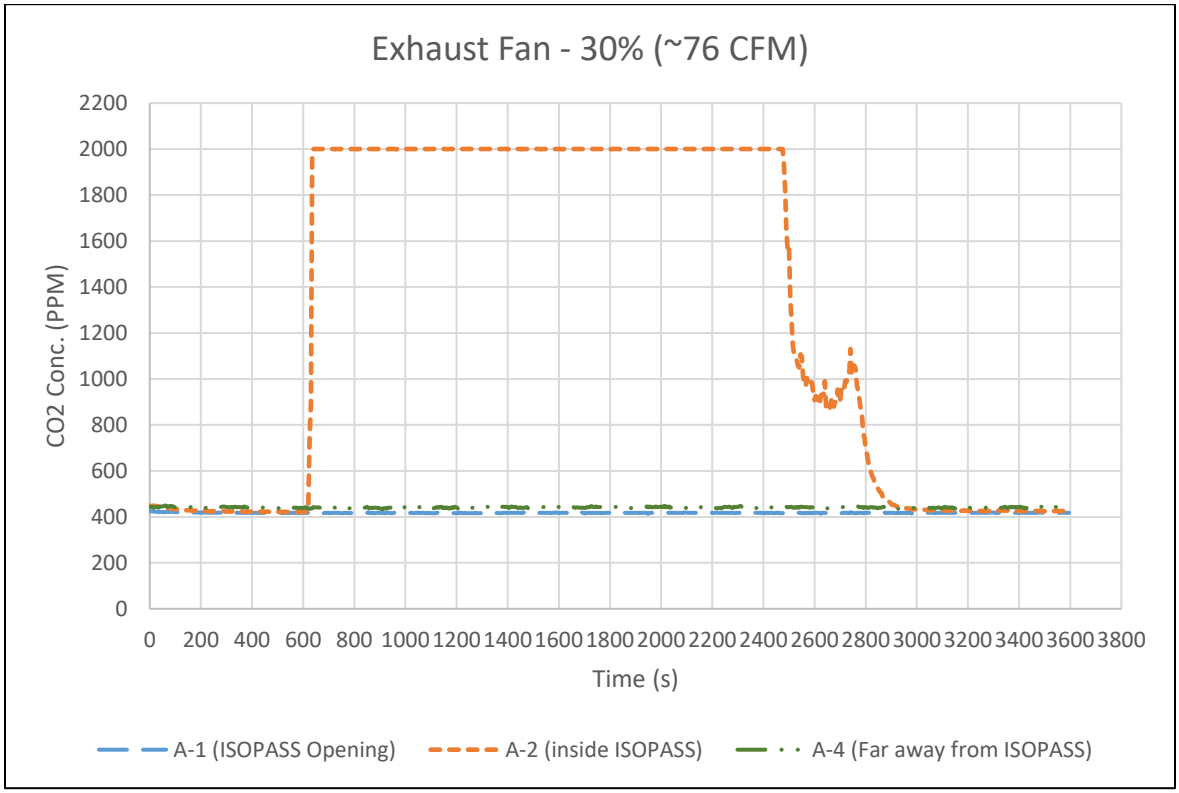

Figure 4.20: Gaspers On Minimum Exhaust Fan Speed - 30%

From 20% fan speed, the results match the same test taken at 30% with the gaspers off. There is no measurable tracer gas leakage at or above this point.

4.6 Mass Balance Problem Overview

While testing minimum exhaust fan speed for no-leakage with a 3-inch hole placed in the opening, it was observed that the expected theoretical no-leakage CO2 concentration in the ISOPASS exhaust was lower than the actual value measured in the exhaust. A series of subsequent tests in which the CO2 injection rate was lowered to a point where the measured concentration in the exhaust would be less than 2000 ppm for different fan speeds verified the discrepancy when the measured data was plotted against the theoretical. The theoretical concentration was determined at five points during the tests, reading the variable area flow meter at each point to verify the actual injection rate, converting from the scale using the provided correlations for CO2, and corrected using the provided correction equation for the temperature and pressure at operating conditions. This problem grabbed our attention, since it is important to verify that our tests are recorded correctly, and to confirm whether any of the injected CO2 escapes from the ISOPASS.

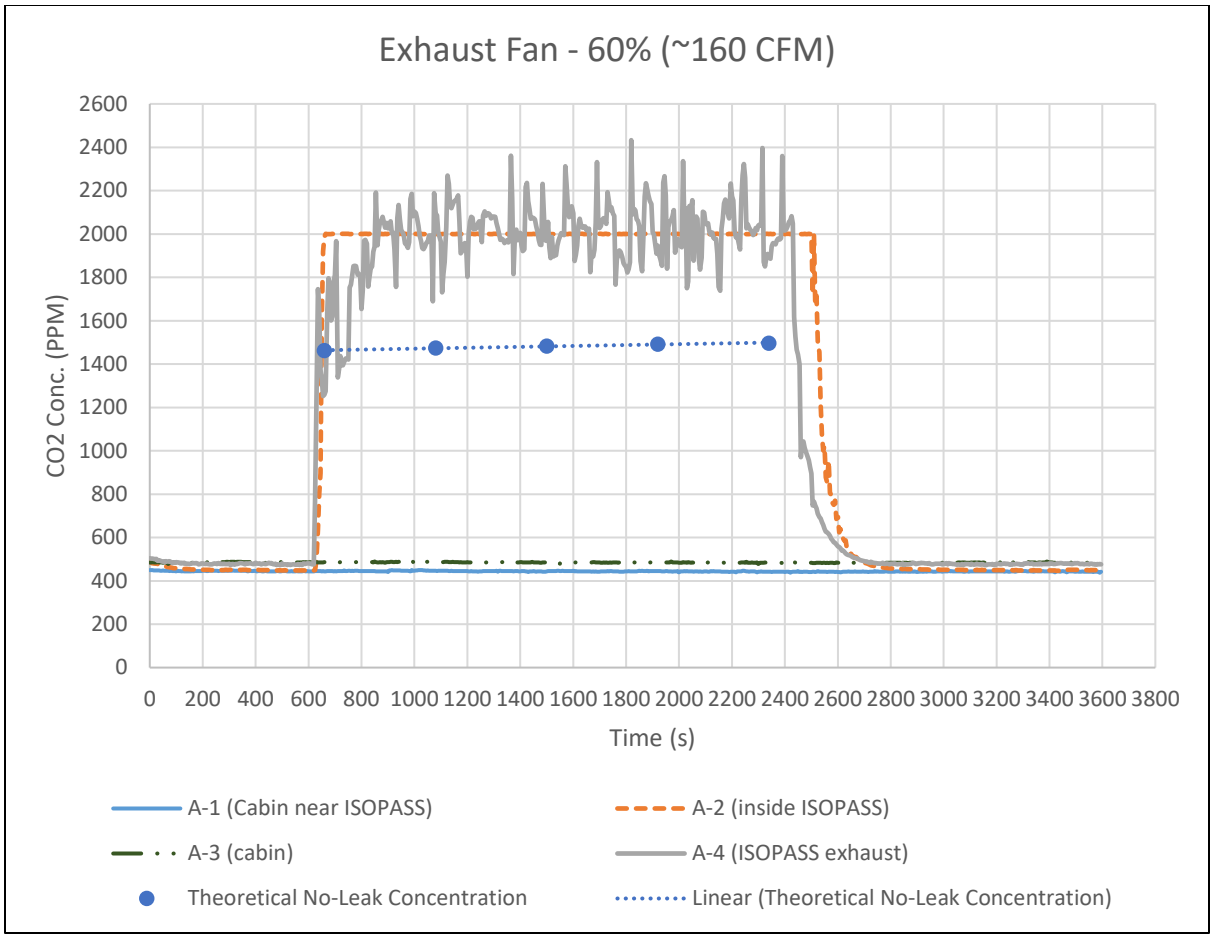

Figure 4.21: Theoretical Concentration vs. Actual

4.7.1 Mass Balance in ISOPASS

To calculate the expected no-leak concentration in the ISOPASS exhaust, the following mass balance equation was derived:

$$C_{exh} = \left[\dot{V}_{inj,CO_2} * \left(1 - \frac{C_{cabin}}{10^6}\right) + \left(\dot{V}_{exh} - \dot{V}_{inj,He}\right) * \frac{C_{cabin}}{10^6}\right] * \frac{10^6}{\dot{V}_{exh}}$$

Which can be further reduced to:

$$C_{exh} = \frac{\left[\dot{V}_{inj,CO_2} * 10^6 + \left(\dot{V}_{exh} - \dot{V}_{inj,CO_2} - \dot{V}_{inj,He}\right) * C_{cabin}\right]}{\dot{V}_{exh}}$$

Where C represents concentration of CO_2 in parts per million (ppm), $\dot{V}_{exh}$ represents the volumetric flowrate of the ISOPASS exhaust, and $\dot{V}_{inj,CO_2}$ and $\dot{V}_{inj,He}$ represent the volumetric flowrates of the CO_2 injection and Helium injection, respectively. A similar equation was derived for the 767 cabin system in previous research (Lebbin, 2006). For this equation, however, density is considered to be constant. Additionally, the concentration of CO_2 in the CO_2 injection is assumed to be pure at 10^6 ppm, and the concentration of CO_2 in the helium injection is assumed to be 0.

While there are many potential explanations for why the theoretical no-leak concentration would be higher than the measured concentration, there were not many factors that could make the theoretical concentration lower. Having made sure that there were no other sources of CO2 in the ISOPASS, and having verified that the no-leak mass balance calculations were correct, we determined these potential causes:

1) The exhaust flowrate measured by the vane anemometer is incorrect
2) The CO2 injection rate measured by the flowmeter is incorrect
3) The CO2 gas analyzers being used to measure the concentration in the exhaust are incorrect
4) The flow through the ISOPASS exhaust is stratified, and the concentration where we were measuring happened to be especially high

4.7.2 Vane Anemometer

To verify the flow rate of the vane anemometer being used to measure the exhaust fan speed, the exhaust assembly was taken out and attached to a flow hood. Measurements were recorded from the flow hood and the vane anemometer simultaneously and plotted together. To distribute the flow inside the hood better, a piece of cardboard with holes was placed across the

center of the hood in the path of the exhaust flow. The baffle made the data less consistent, so we ran the test again without the baffle and got better results.

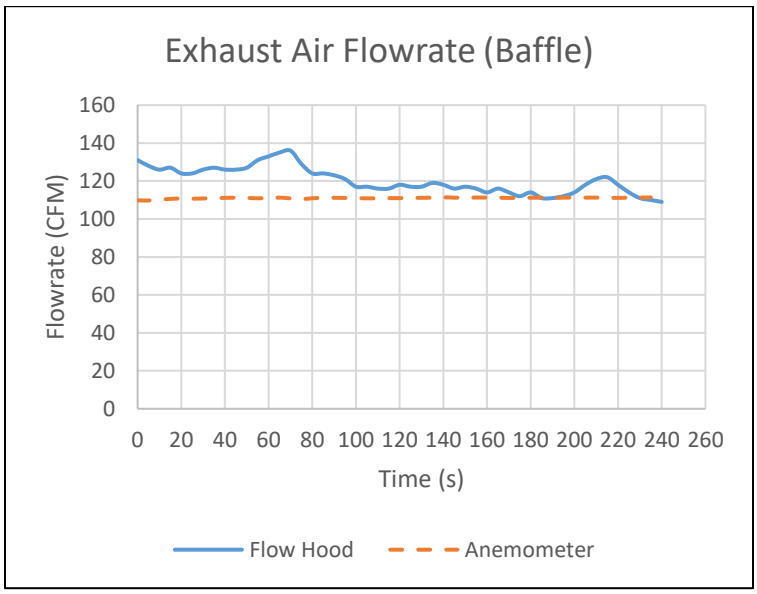

Figure 4.22: Anemometer / Flow Hood Comparison with Baffle

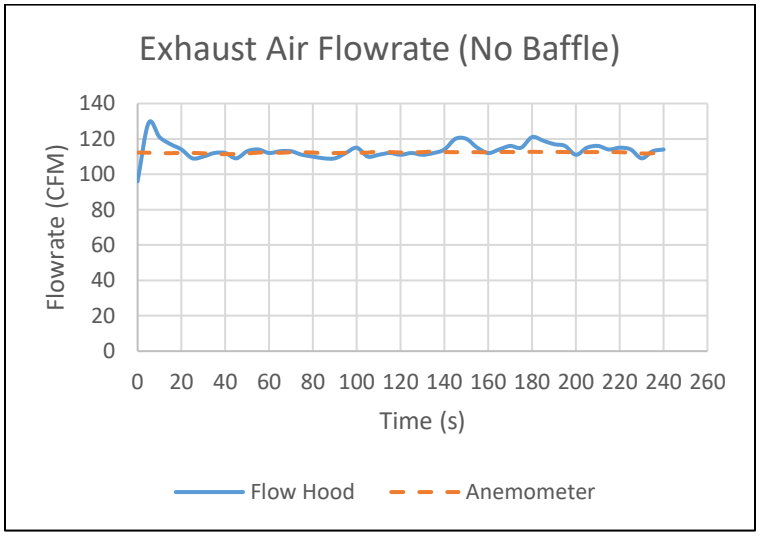

Figure 4.23: Anemometer / Flow Hood Comparison without Baffle

It was determined from these results that the anemometer being used to measure the flowrate in the ISOPASS exhaust was accurate well within the limits of uncertainty for the system, and therefore could not be the issue.

4.7.3 Variable Area Flowmeter

To verify the readings from the variable area flowmeter being used in the mass balance to determine the theoretical CO2 concentration, air was pulled through the flowmeter in series with a digital flowmeter and the results compared for several different flowrates. The measured flowrates from the variable area flowmeter were corrected for the actual operating conditions as usual.

Table 4.2 Omega Variable Area Flow Meter / TSI Digital Flow Meter Comparison for Air

(Reading 1)	Rotameter	TSI Flowmeter
Temperature (k)	297.75	
P_atm (psi)	14.12667565	
dV	5	
P_flow (psi)	1	
Reading	66	
Corresponding Flowrate (table) (lpm)	5.10	
Actual Flowrate (lpm)	**4.790**	**4.65**
(Reading 2)	Rotameter	TSI Flowmeter
Temperature (k)	297.75	
P_atm (psi)	14.12667565	
dV	5	
P_flow (psi)	1	
Reading	46	
Corresponding Flowrate (table) (lpm)	3.45	
Actual Flowrate (lpm)	**3.240**	**3.04**
(Reading 3)	Rotameter	TSI Flowmeter
Temperature (k)	297.75	
P_atm (psi)	14.12667565	
dV	5	
P_flow (psi)	1	
Reading	33	
Corresponding Flowrate (table) (lpm)	2.44	
Actual Flowrate (lpm)	**2.287**	**2.01**

Note that the differential pressure transducer used to measure the pressure drop in the variable area flowmeter maxed out at 1 psi, so the pressure correction may be slightly low.

A subsequent test was also conducted to verify the accuracy of the previous tests, with a pressure

drop below 1 psi, and the result was closer than before, confirming that the variable area flowmeter was within expected tolerances and did not appear to be the issue either.

Additionally, it was later found that the flowmeter was missing a seal on the input side, which may have caused some discrepancy in the results if CO2 leaked around the sides of the flowmeter's enclosure. The seal was placed back into its correct position and another mass balance test was ran, with the same results as before. This showed that the missing seal had negligible effect on the mass balance in the ISOPASS.

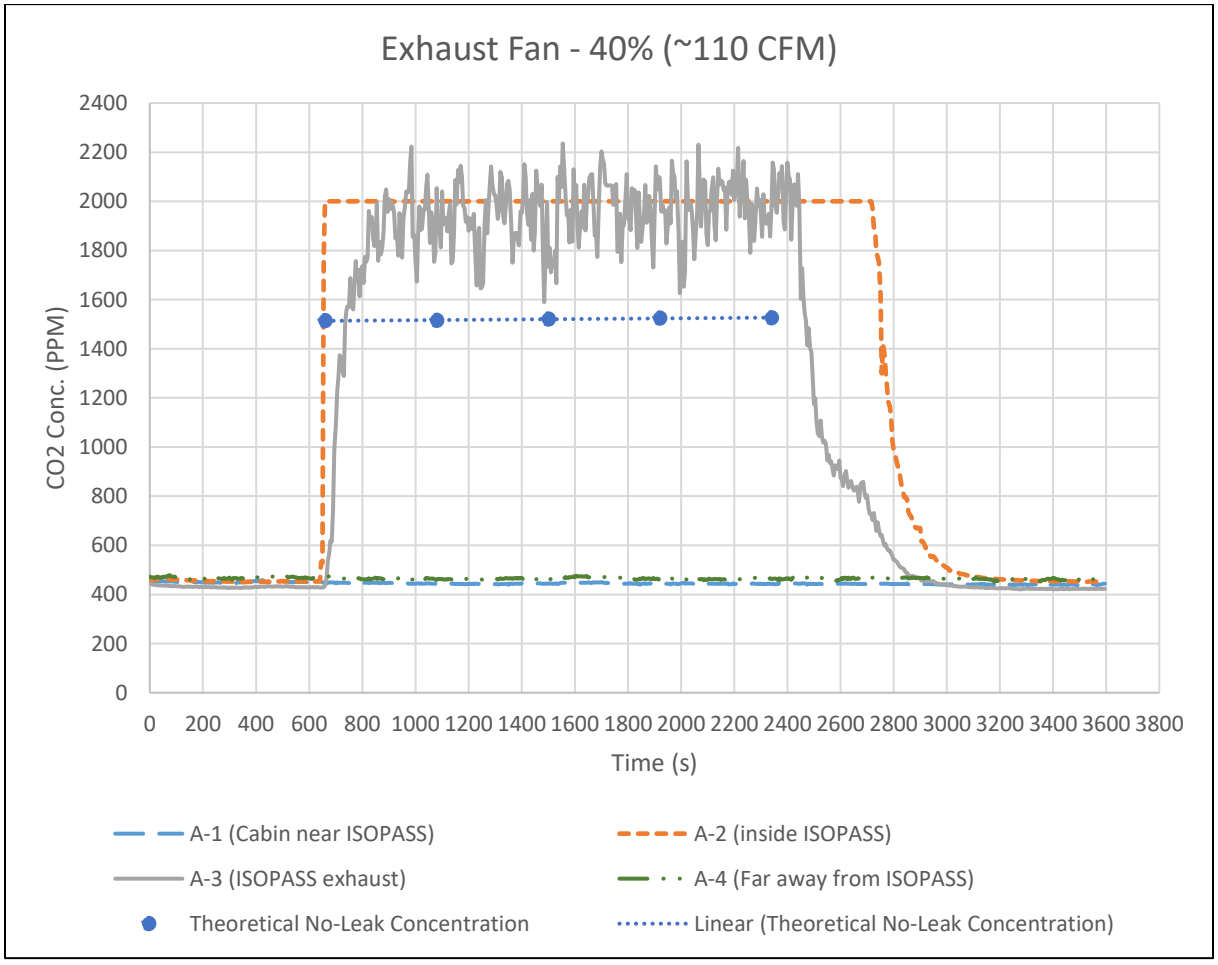

Figure 4.24: Mass Balance for Resealed Flowmeter

4.7.4 CO2 Gas Analyzers

It was observed during previous testing that the gas analyzer being used to measure the CO2 concentration in the ISOPASS exhaust was inaccurate above 2000 ppm, and may have been inaccurate below that. To be sure it wasn't an analyzer issue, this analyzer was swapped out with a different analyzer that was also calibrated to 2000 ppm but with a higher voltage range. Upon testing, this yielded similar results. The troublesome analyzer was sent out for recalibration and repair, and a brand new analyzer with a calibration range of 0-3000 ppm was installed in its place. Another mass balance test with the new analyzer with the higher range yielded the same results as the previous analyzers.

While testing the stratification theory a second time, a test was run with all four CO2 analyzers in as near as possible to the same position in the exhaust stream, and all read virtually the same. This demonstrates conclusively that the analyzer used to measure the exhaust concentration made no significant difference.

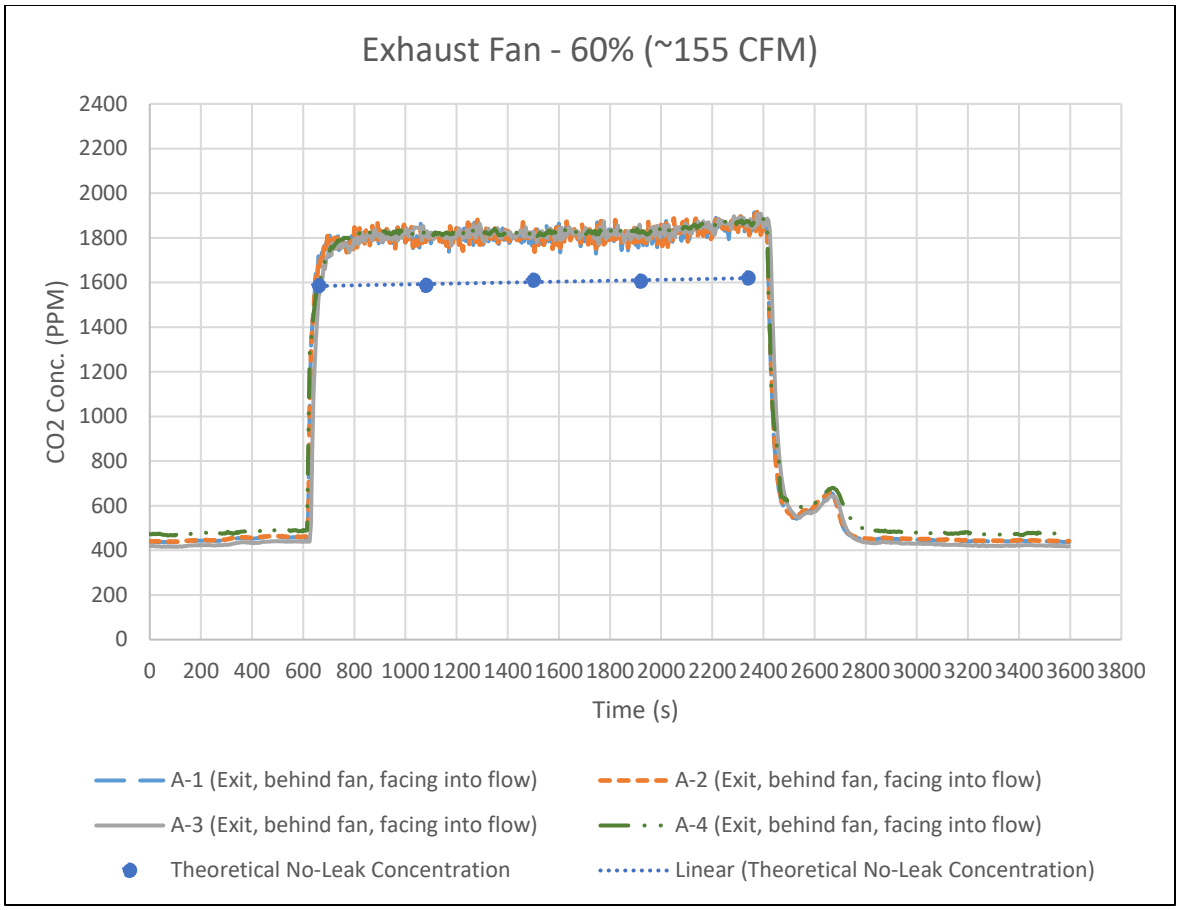

Figure 4.25: All Four Analyzers in the Same Location

4.7.4.1 Injecting CO2 Directly into ISOPASS Exhaust

To bypass the ISOPASS and isolate the problem to the CO2 injection and exhaust flow alone, the exhaust pipe was extended into the aisle of the 767 cabin, outside of the ISOPASS, and CO2 source was placed directly into the exhaust pipe a few inches into the pipe from the opening. The total length of the extended duct was 101 inches, which corresonds to approximately 25 diameters and should be adequate to provide thorough mixing of the incoming air. Concentration was measured in the usual location, between the anemometer and the fan. Tests were conducted with the fan at 60% power and again at 40%. The test duration was reduced, since achieving steady state and returning to ambient did not take as long. As a result, the axis for the following graphs are shorter, and the legend is formatted differently.

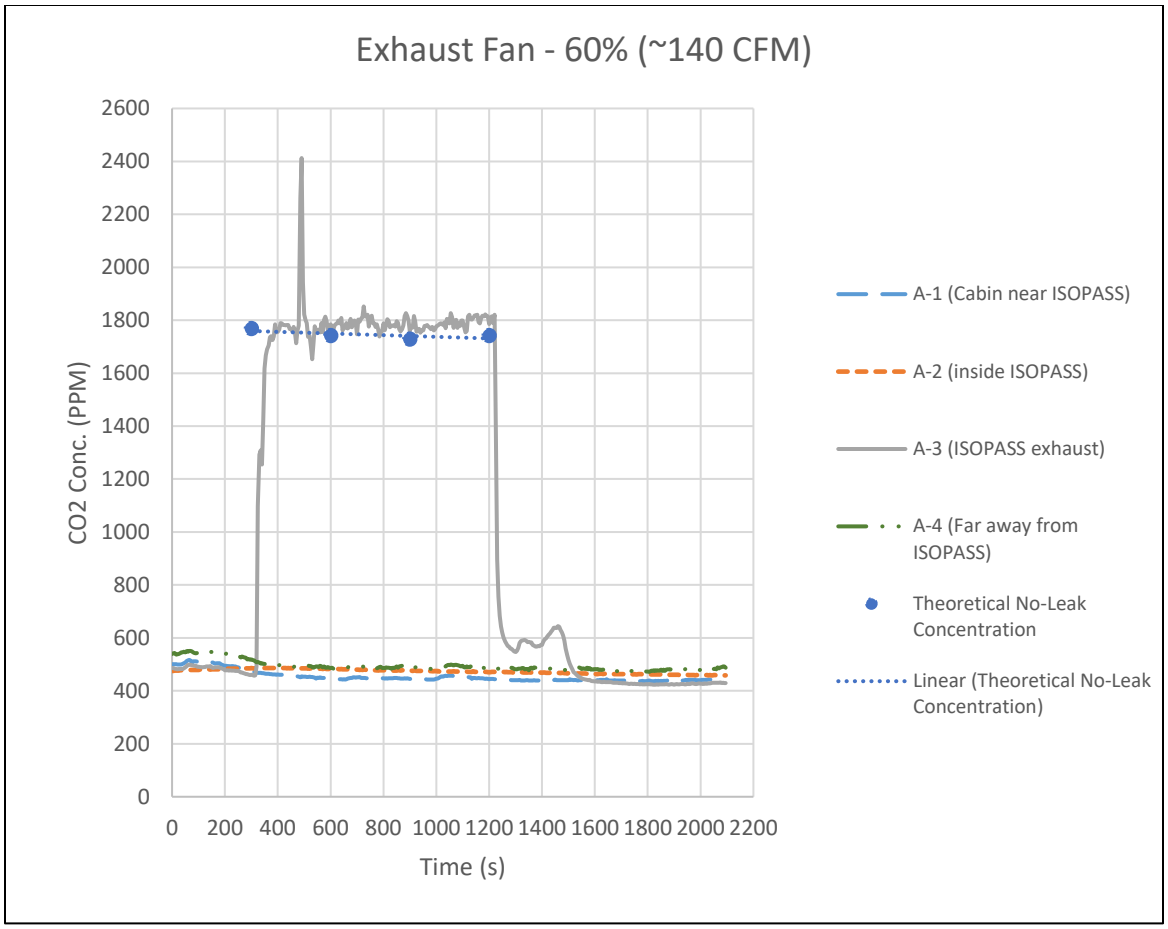

Figure 4.26: CO2 Directly into Exhaust, 60% Fan Power

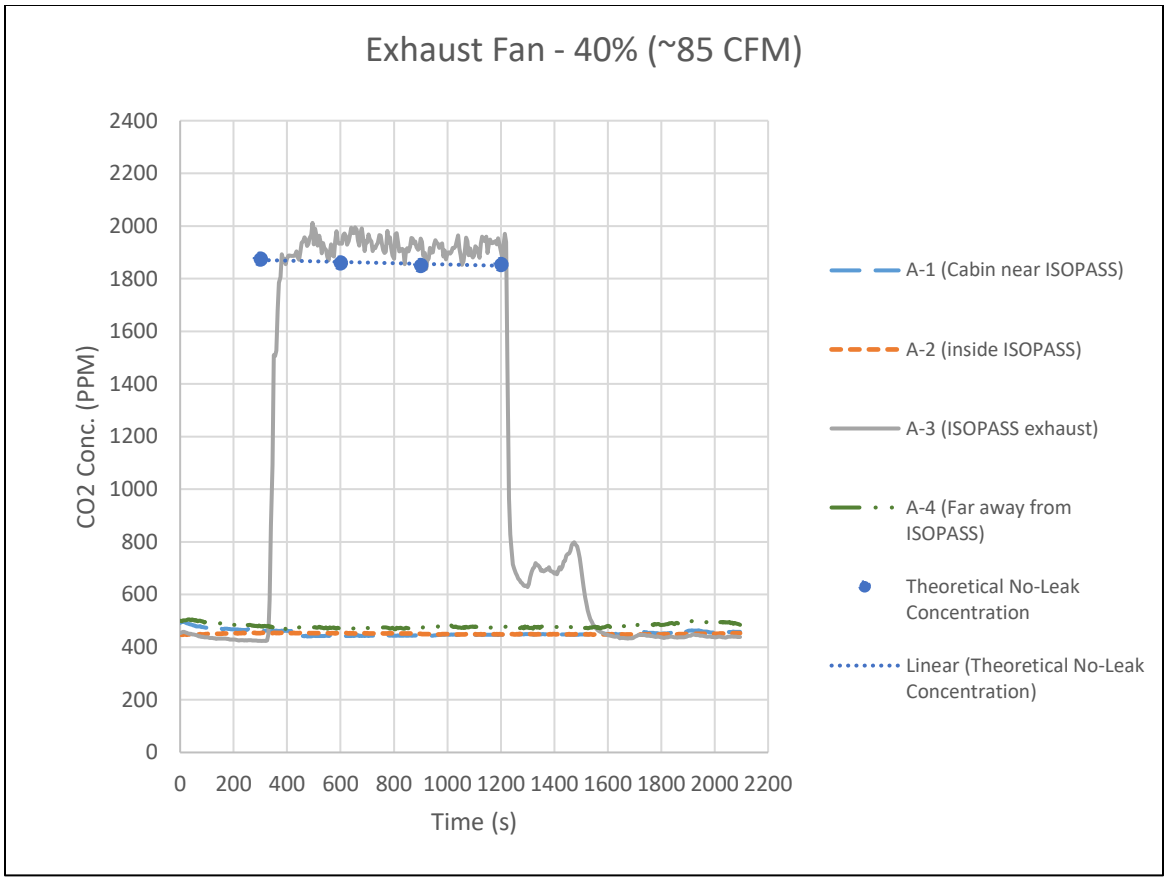

Figure 4.27: CO2 Directly into Exhaust, 40% Fan Power

Note that the large, brief spike in CO2 concentration in the 60% test occurred when the helium canister was opened later than usual.

These tests make it clear that, when the ISOPASS itself is taken out of the picture, the mass balance matches the measured concentration in the exhaust within the limits of uncertainty for the system. This fact lead us to reconsider the possibility of stratified flow in the exhaust stream of the ISOPASS.

4.7.5 Stratification of CO2 Concentration in Exhaust Flow

The ISOPASS exhaust is set on the floor in the passenger feet area, and the CO2 injection source is set at approximately breathing level in the opposite seat. The ISOPASS is clearly not air tight, nor is it designed to be, and the exhaust pulls in air from small openings in the

ISOPASS. These openings include many on the ground level, such as where the ISOPASS drapes over the exhaust pipe itself, places where the gas injection tube and CO2 analyzer tubes enter the ISOPASS, and where the ISOPASS drapes over electrical outlet cables. Since the exhaust entrance is near the floor, it draws much of its air from these leak points. Meanwhile, the CO2 concentration builds up in the breathing space of the ISOPASS and eventually enters the exhaust in a fairly thin stream near the top of the exhaust pipe. Thus, most of the airflow bypasses the occupied zone and goes directly to the exhaust at floor level, producing a stratified flow in the exhaust and potentially poor ventilation for passengers at breathing level (at least for no gaspers on).

Early on while trying to determine the cause of the discrepancy between the theoretical no-leak exhaust concentration and the actual exhaust concentration, stratification of the CO2 concentration was considered. An additional test was performed with the analyzer's sampling tube at the bottom of the exhaust pipe in the same axial location as previously tested, and the concentration was found to be in the same range as in the top and middle positions. Thus, this stratification theory was dismissed and the previously mentioned theories were tested. However, having shown that the other potential causes could not be the actual problem, the stratification theory was revisited more thoroughly.

For this test, the four CO2 analyzers were each placed in the exhaust stream, in four different locations:

1) Bottom, facing opposite of the flow, about 5" from the entrance
2) Right at the entrance, around the center of the cross section, facing down
3) Between the anemometer and the fan, near the top of the cross section, facing down
4) At the exit, behind the fan, facing into the flow

Additional tests were performed with a small desk fan placed in the feet area, about 16” away from the exhaust, facing directly upward. Once the first test was completed, the same test was performed again with the analyzers swapped around the same locations. Figures 4.29 - 4.32 show the placement of the analyzers for these tests:

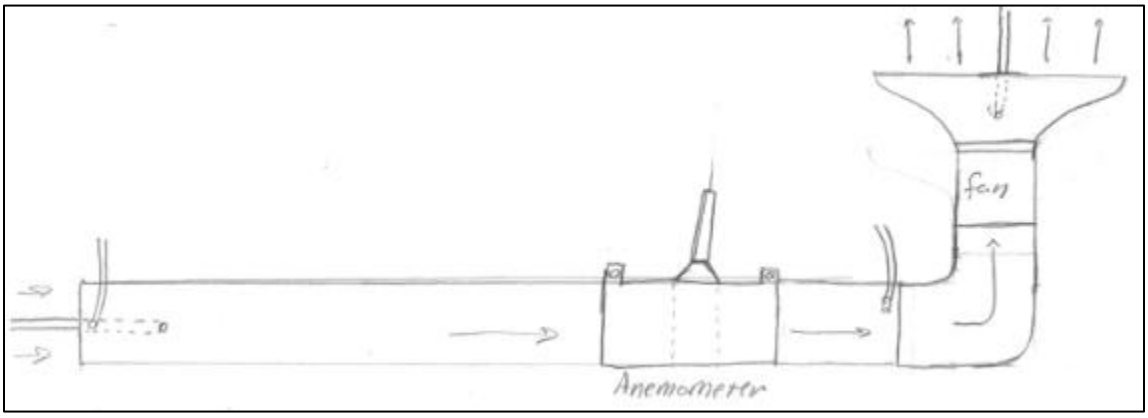

Figure 4.28: Overview of ISOPASS exhaust and Analyzer Locations

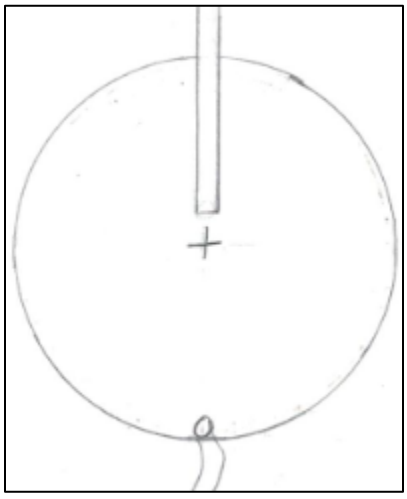

Figure 4.29: Exhaust Entrance Analyzer Location

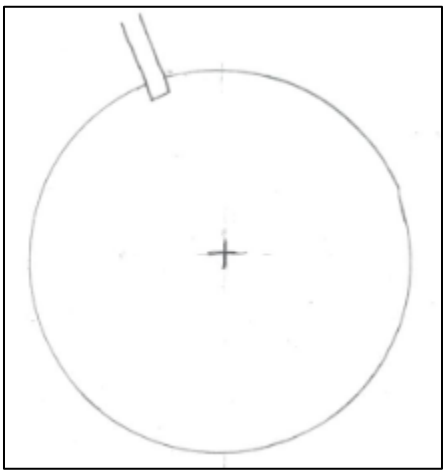

Figure 4.30: Between Anemometer and Fan

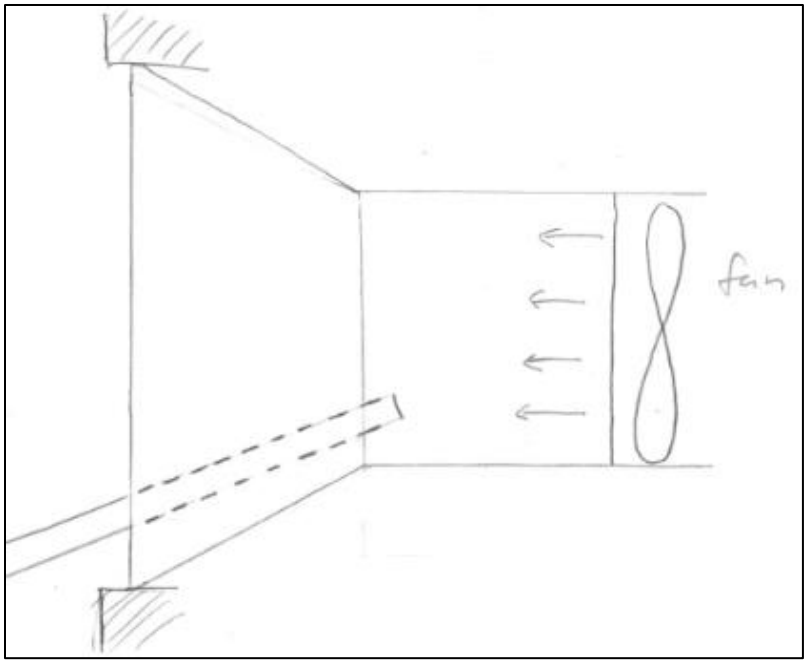

Figure 4.31: Exhaust Exit Analyzer Location

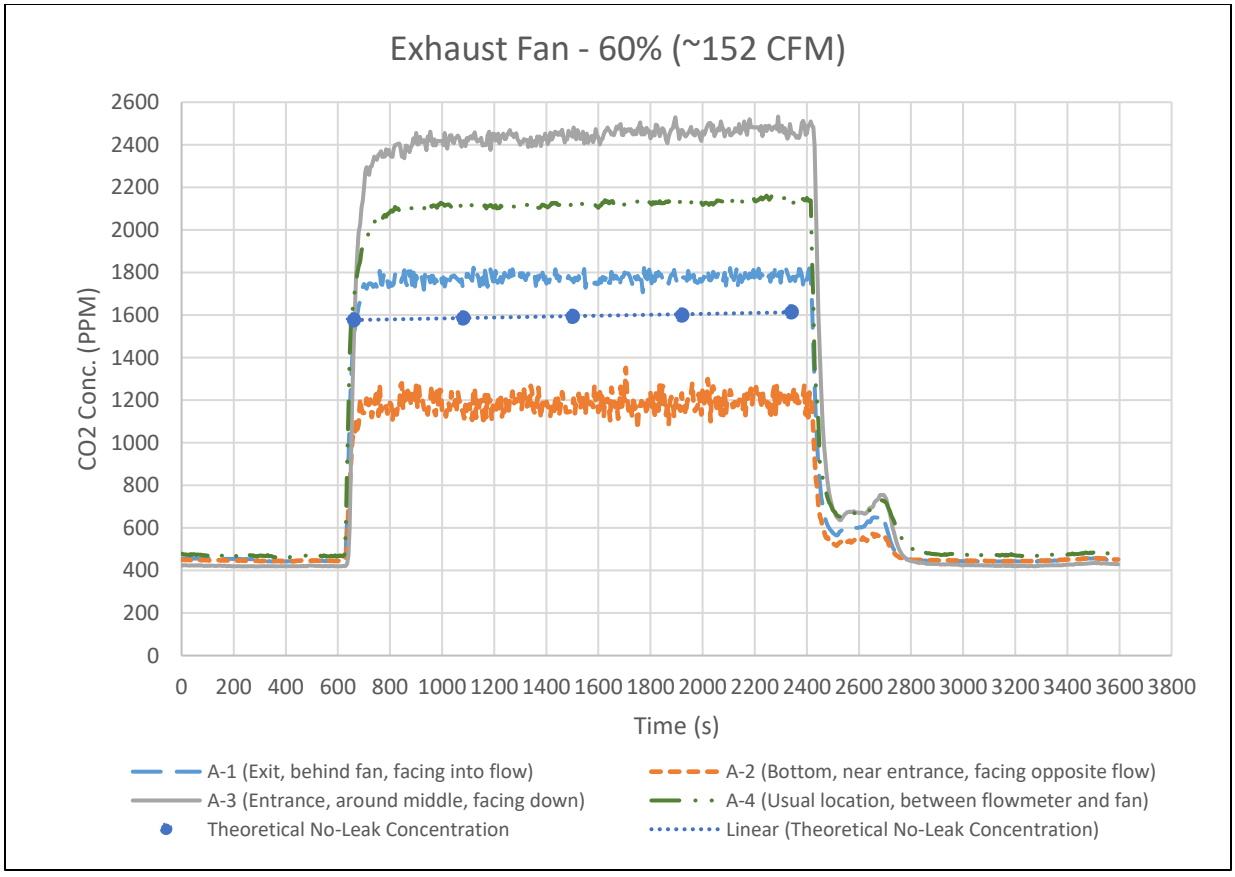

Figure 4.32: Stratification of CO2 Concentration in the ISOPASS Exhaust

These tests revealed stratification of the CO2 concentration in the exhaust, with the analyzer at the bottom below the theoretical no-leak concentration, and higher analyzers being above. As mentioned previously, this test was conducted a third time with all four analyzers at the same location (at the exit of the exhaust) and each measured virtually the same concentration (Fig. 4.28).

To attempt to break up the stratification at the entrance of the exhaust, the small desk fan was directed to blow across the entrance perpendicular to the flow. A test was then conducted with the fan off for the first 20 minutes of the CO2 injection, and then turned on for the next 20 minutes of CO2 injection.

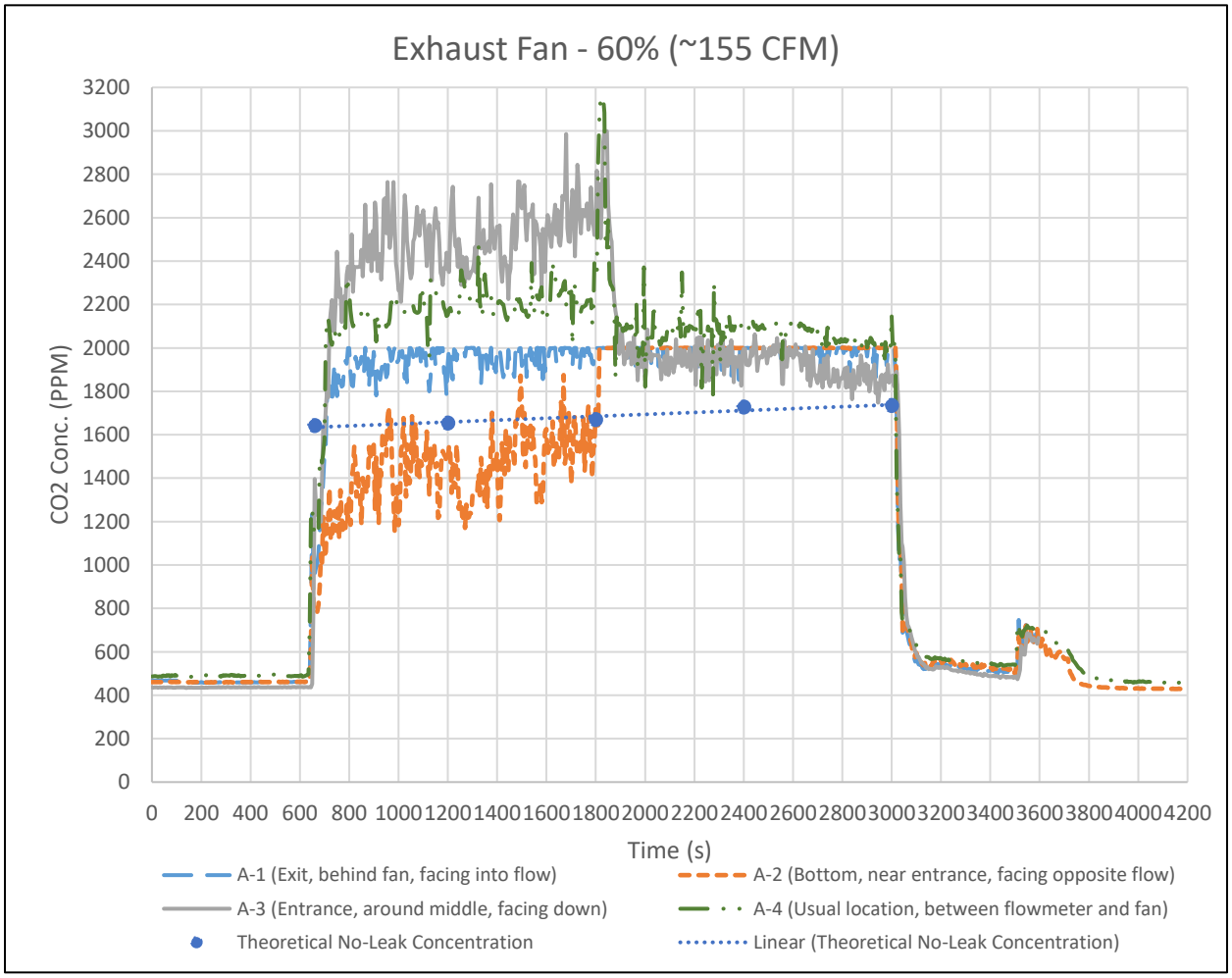

Figure 4.33: Fan Across Exhaust Entrance Halfway Through Injection

Note that the A-2 analyzer is peaking out at 2000 ppm (5 volts) at the computer, but the display on the analyzer itself was reading between 2000 ppm and 2100 ppm.

With the floor fan turned off, we again see the same stratification in the ISOPASS exhaust stream as we'd seen in previous tests. Once the floor fan was turned on, however, we observe that the lower concentration areas increase in concentration and the higher concentration areas drop down, approaching each other in the middle. While the concentrations do not come down to the theoretical no-leak concentration by the end of the test, they are approaching. While the floor fan makes a clear difference in the mixing of the CO2/air mixture entering the exhaust, it likely does not do a perfect job of it, which may explain this slight discrepancy. Additionally, if the fan had been used since the beginning of the test rather than halfway through, or if it had been given longer to reach steady state, the concentrations would likely reach closer to the theoretical concentration. In any case, these tests are sufficient to verify stratification in the exhaust stream as the primary cause for the high measured concentration compared to the theoretical.

4.7.6 Mass Balance and Stratification Conclusion

When comparing the actual CO_2 concentration in the ISOPASS exhaust to the expected no-leak concentration based on the mass balance for the system, it was observed that the experimental concentration was higher than the calculated. At first, this did not make much sense, as the tracer gas injection was the only source of CO_2 inside the ISOPASS. After verifying the mass balance equations, exhaust flowrate, variable area flowmeter reading for the injection rate, and the accuracy and calibration of the CO_2 analyzers, several tests were completed to check for stratification in the ISOPASS exhaust. This stratification was determined to be the issue, and we were able to demonstrate that the mass balance in the ISOPASS is, in fact, correct.

The stratification does make the concentration measurements in the exhaust less valuable in the subsequent ISOPASS containment effectiveness tests, although ISOPASS exhaust data provides a good reference for when steady state is achieved.

4.8 Procedure Overview – Containment Effectiveness in Boeing 737 Mock-up

Containment effectiveness of the ISOPASS was tested in the 737 in the same manner as in the 767, with tracer gas being injected through a point source at breathing level inside the ISOPASS. To occupy a similar space as the coughing mannequin that was inside the ISOPASS during the 767 tests, an inflatable mannequin was placed in the seat next to the injection source. Since the coughing mannequin was not heated, the inflatable mannequin was also left unheated. Matched ISOPASS on, ISOPASS off pairs were used once again to eliminate statistical problems for repeatability. Tests were conducted both with gaspers on and gaspers off. As in the 767, each matched pair was completed three times; 3 repetitions x 2 gasper conditions for a total of 6 matched pairs, or 12 individual tests. A new speed controller was used with the exhaust fan for all the 737 tests, and as a result the flowrate at 60% did not match the flowrate used in the 767 tests. Instead, the level was set to approximately match the 767 test flowrates, about 160 CFM on average.

Ventilation air entered the 737 cabin at a rate of 600 CFM, corresponding to 20 CFM per seat. The ventilation airflow pattern inside the Boeing 737 cabin is documented and reviewed in previous research (Patel, 2017). Gasper flow is taken from the supply flow and does not change the total ventilation flow to the cabin.

Concentration measurements were taken inside the ISOPASS in the seat next to the injection source, in the seat across the aisle adjacent to the ISOPASS, and far away from the ISOPASS near the front of the cabin. Each of the sampling tubes were positioned at

approximate breathing level. The radial distances between the injection point and the sampling tubes were 16", 60", and 123", as shown in Figure 4.35. The uncertainty of the CO_2 analyzers is 1% of the range of the analyzer. This corresponds to 20 ppm for the A-1, A-2, and A-4 analyzers, and 30 ppm for the A-3 analyzer.

ISOPASS exhaust concentration data was collected for all the 737 tests. However, due to the stratification of the tracer gas in the ISOPASS exhaust stream as discussed previously, this data is inconsistent and not useful for the purposes of this analysis. For the sake of clarity and comparison, the exhaust concentration will be left off the graphs presented here. Full results including ISOPASS exhaust concentration will be included in the electronic appendix.

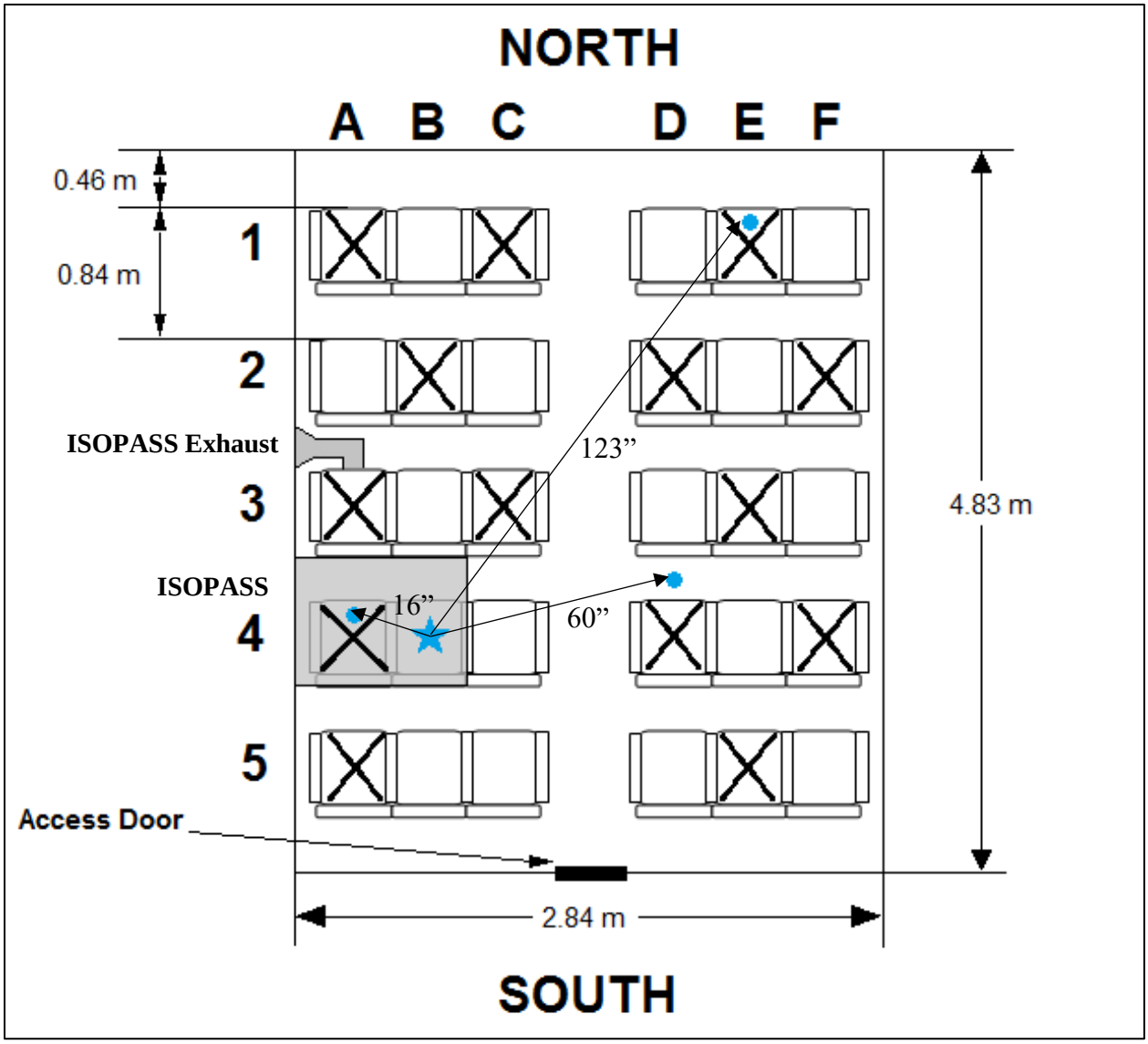

Figure 4.34 737 Cabin Layout, Sampling and Mannequin Locations

4.9 Representative Results and Analysis – Boeing 737 Mock-up Cabin

Presented here are the results of the matched pair tests inside the Boeing 737 aircraft cabin. Representative test results are given for ISOPASS on and ISOPASS off, and for each gasper condition, gaspers on and gaspers off. Full results for each test are available in the electronic appendix.

The ISOPASS on tests were conducted with the ISOPASS in place over two seats, with the curtain fully closed. The ISOPASS off tests were conducted with the ISOPASS completely removed from the cabin. The ISOPASS exhaust pipe remained in place, with the exhaust fan off. The ISOPASS location is specified in Figure 4.35. As with the 767 tests, the injection and analyzer locations remain the same between ISOPASS on and ISOPASS off conditions, and are referred to with respect to the ISOPASS whether it is in place or not.

The tracer gas injection is composed of a mixture of CO_2 and Helium to achieve neutral buoyancy. To preserve similarity between the 767 and 737 tests, the injection rates were kept the same. The CO_2 injection rate is approximately 5.0 liters per minute, and the helium injection rate is a corresponding 3.07 liter per minute. Because the 767 cabin was half-loaded with thermal mannequins, the 737 cabin is also half-loaded to maintain similar conditions. Mannequin locations are presented on Figure 4.35 as X's.

4.9.1 ISOPASS Off

The ISOPASS off condition is useful to provide a baseline from which to compare the effectiveness of the ISOPASS prototype.

4.9.1.1 Gaspers Off

The ISOPASS off, gaspers off condition eliminates the less-predictable flow patterns generated by the gaspers in the cabin. The only major factor affecting airflow patterns in this baseline, in addition to the central ventilation air itself, is the heat from the mannequins. Since the use or inclusion of gaspers is not required for commercial aircraft, this is a realistic and important baseline to consider in addition to the gaspers on condition. The gaspers off tests are conducted with the gasper fan shut off and the individual gasper vents fully closed.

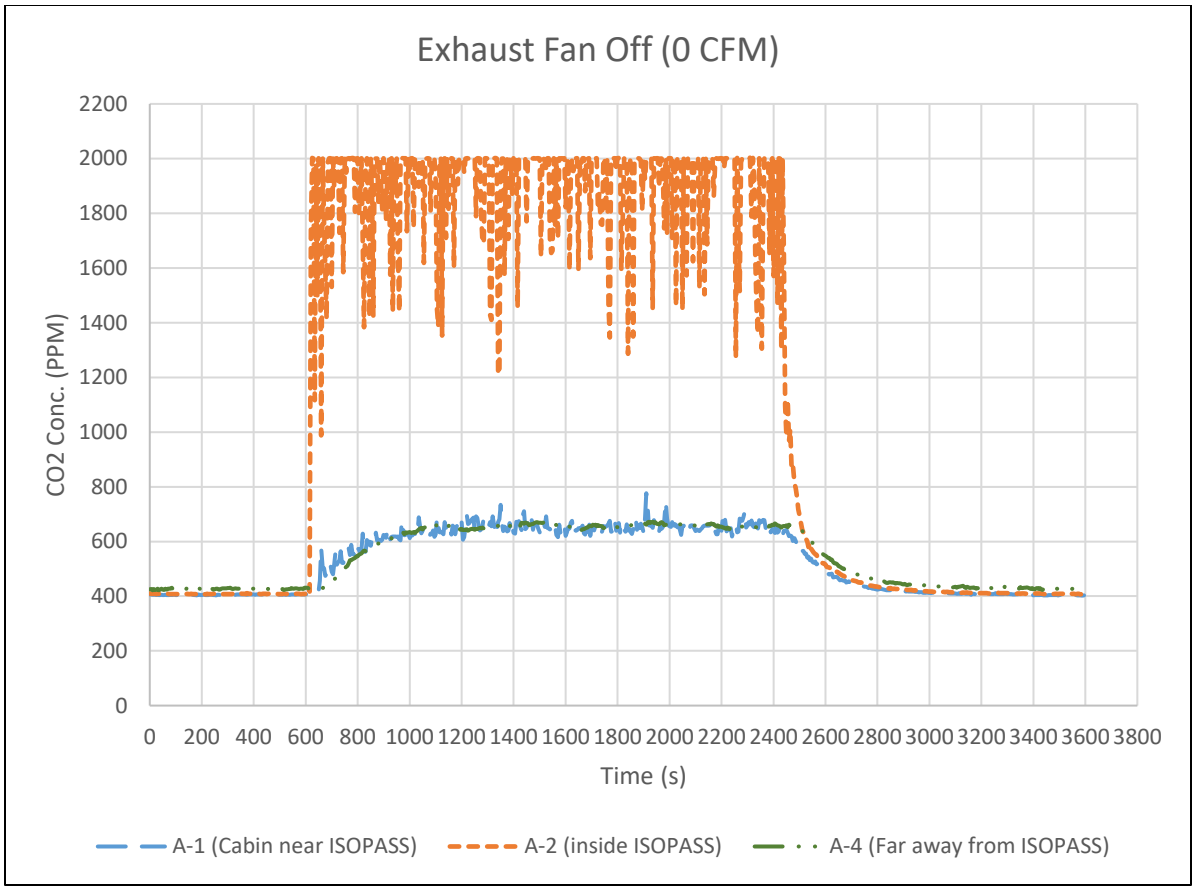

Figure 4.35 ISOPASS Off, Gaspers Off

The average background CO_2 levels at each sampling location before the tracer gas injection for this test were as follows:

A-1 (Cabin near ISOPASS): 405 ppm

A-2 (Inside ISOPASS): 408 ppm

A-4 (Cabin Away from ISOPASS): 427 ppm

With the tracer gas injection on, the average steady state CO_2 concentration at each sampling location became:

A-1 (Cabin near ISOPASS): 655 ppm

A-2 (Inside ISOPASS): 1906 ppm

A-4 (Cabin Away from ISOPASS): 659 ppm

We can see that the CO_2 concentration increases throughout the cabin with the ISOPASS off. This result is expected, and matches the data from the tests completed in the 767 cabin. The A-2 and A-3 concentrations increase significantly more in the 737 than in the 767, however, despite the radial distances from the source being similar. This higher concentration was expected as the same CO2 injection rate was used for both the 737 and 767 cabins but the 737 cabin is smaller and has less total ventilation airflow. This difference becomes more apparent when comparing the percent difference between the pre-test background and the steady state gas on concentrations. The percent difference for each sampling location for the 737 ISOPASS off, gaspers off test are as follows:

A-1 (Cabin near ISOPASS): +62%
A-2 (Inside ISOPASS): +367%
A-4 (Cabin Away from ISOPASS): +54%

In comparison, the 767 ISOPASS off and gaspers off results are as follows:

A-1 (Cabin near ISOPASS): +62%
A-2 (Inside ISOPASS): +142%
A-4 (Cabin Away from ISOPASS): +17%

4.9.1.2 Gaspers On

With the gaspers on, the airflow patterns throughout the aircraft cabin may be disrupted, altering the distribution of the tracer gas. Because testing for the 737 was done in a section of an actual 737 aircraft, gaspers were present for each seat in every row, unlike the 767 mock-up. Like the 767 gaspers on tests, each gasper was fully opened and directed straight down. Gasper pressure was maintained at 2" H_2O.

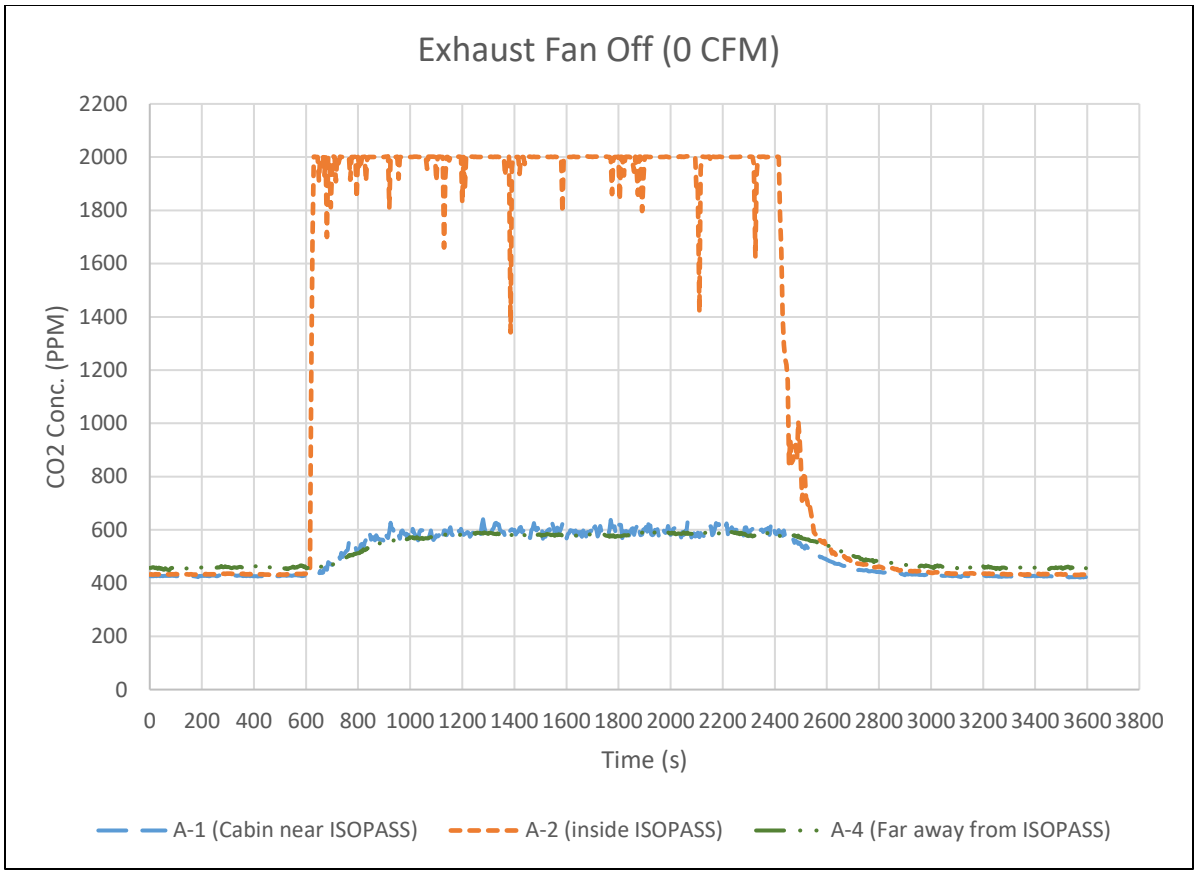

Figure 4.36 ISOPASS Off, Gaspers On

The average background CO_2 levels at each sampling location before the tracer gas injection for this test were as follows:

A-1 (Cabin near ISOPASS):	427 ppm
A-2 (Inside ISOPASS):	433 ppm
A-4 (Cabin Away from ISOPASS):	458 ppm

With the tracer gas injection on, the average steady state CO_2 concentration at each sampling location became:

A-1 (Cabin near ISOPASS):	597 ppm
A-2 (Inside ISOPASS):	1988 ppm
A-4 (Cabin Away from ISOPASS):	584 ppm

With gaspers at each seat for the entire length of the 737 cabin section, more mixing of the tracer gas throughout the cabin occurs with the gaspers on compared to gaspers off. This is especially evident when comparing the percent difference values:

A-1 (Cabin near ISOPASS):	+40%
A-2 (Inside ISOPASS):	+359%
A-4 (Cabin Away from ISOPASS):	+28%

We did not see a significant difference between gaspers on and off in the 767 cabin with the ISOPASS off. The larger impact of the gaspers in the 737 cabin is likely due to the fact that every seat has a gasper in the 737 while only three of the eleven rows of seats had gaspers in the 767.

4.9.2 ISOPASS On

As with the testing in the 767 cabin, the ISOPASS was installed and fully closed, with the tracer gas injection inside the ISOPASS at breathing level. We expect the same performance from the ISOPASS regardless of the size and geometry of the cabin.

Because a different speed controller was used for the ISOPASS exhaust fan, the set percentages did not entirely line up with the flowrate of the previous controller. The fan speed was adjusted for each test to return an average flowrate of 160 CFM, as measured by the 4” vane anemometer placed in the exhaust stream. The metal honeycomb was removed from the exhaust stream as the shortened pipe required for the 737’s layout caused complications with the honeycomb interfering with the anemometer.

4.9.2.1 Gaspers Off

With the gaspers off, all of the ventilation to the passenger in the ISOPASS comes through leak points around the ISOPASS. As a result, the passenger's head space gets relatively little ventilation compared to the feet area.

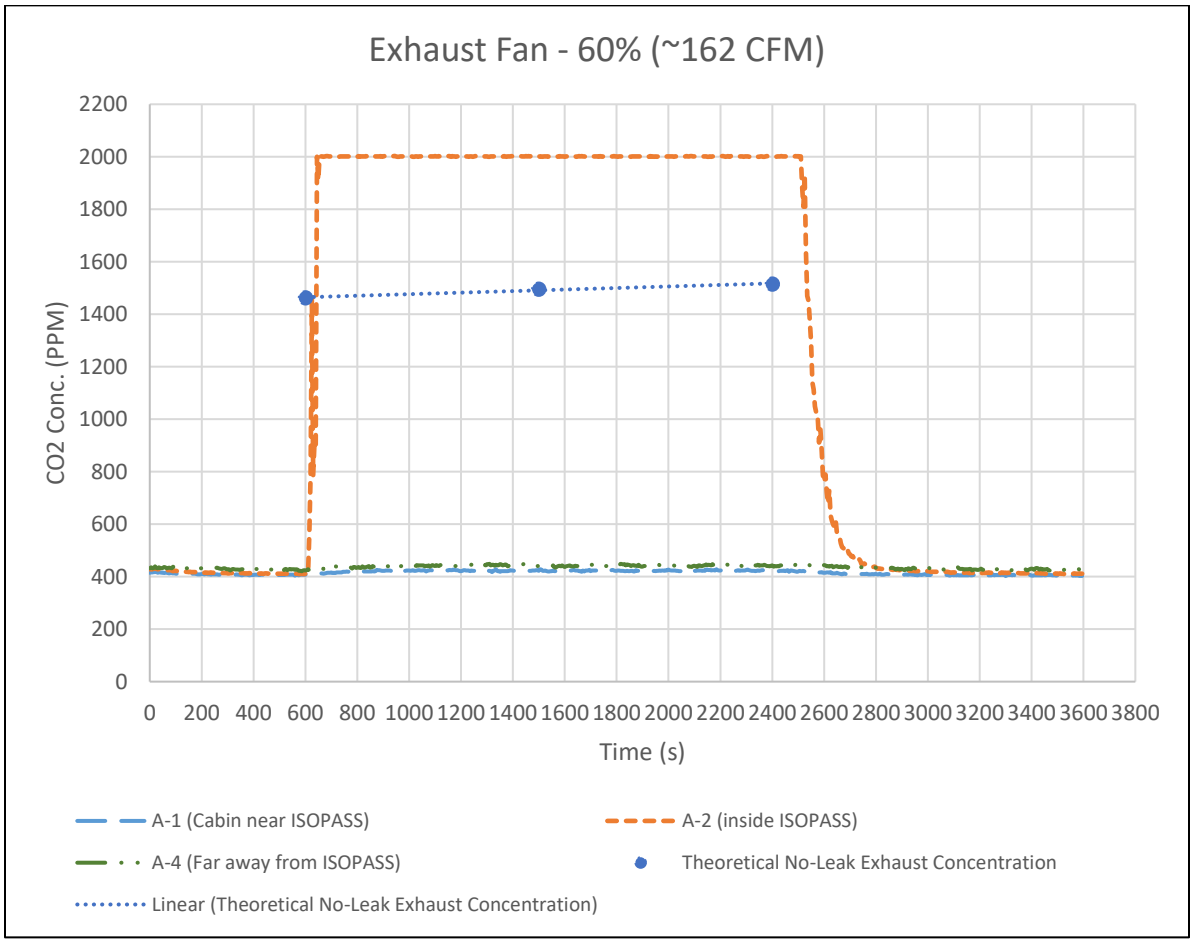

Figure 4.37 ISOPASS On, Gaspers Off

The average background CO_2 levels at each sampling location before the tracer gas injection for this test were as follows:

A-1 (Cabin near ISOPASS):	409 ppm
A-2 (Inside ISOPASS):	416 ppm
A-4 (Cabin Away from ISOPASS):	430 ppm

Upon reaching steady state concentration in the cabin with tracer gas injection on, the average CO_2 concentrations at each sampling location became:

A-1 (Cabin near ISOPASS):	423 ppm
A-2 (Inside ISOPASS):	2001 ppm (at least)
A-4 (Cabin Away from ISOPASS):	442 ppm

The A-1, A-2, and A-4 analyzers are calibrated to a 2000 ppm range. A-1 and A-2 have a corresponding 5 volt range. Since the concentration exceeds this range inside the ISOPASS enclosure, the received data peaks at 5V (2000 ppm).

A-1 (Cabin near ISOPASS):	+3%
A-2 (Inside ISOPASS):	+381% (at least)
A-4 (Cabin Away from ISOPASS):	+3%

This result is reasonably consistent for each test, showing a slight increase in the concentration outside the ISOPASS. Additionally, during the post-test period with the tracer gas injection switched off, the background concentration returns to the pre-test levels. This led us to consider possible recirculation of the ISOPASS exhaust back into the 737 cabin. This topic is explored further in the section titled "ISOPASS Exhaust Recirculation and Leakage".

4.9.2.2 Gaspers On

Although the combined flowrate of the gaspers inside the ISOPASS is far lower than the flowrate of the ISOPASS exhaust, they may be useful in providing better ventilation to the passenger's head space and increase passenger comfort. As in the 767, we do not expect the use of the gaspers to affect the containment effectiveness of the ISOPASS in any significant way while it remains in the fully closed position.

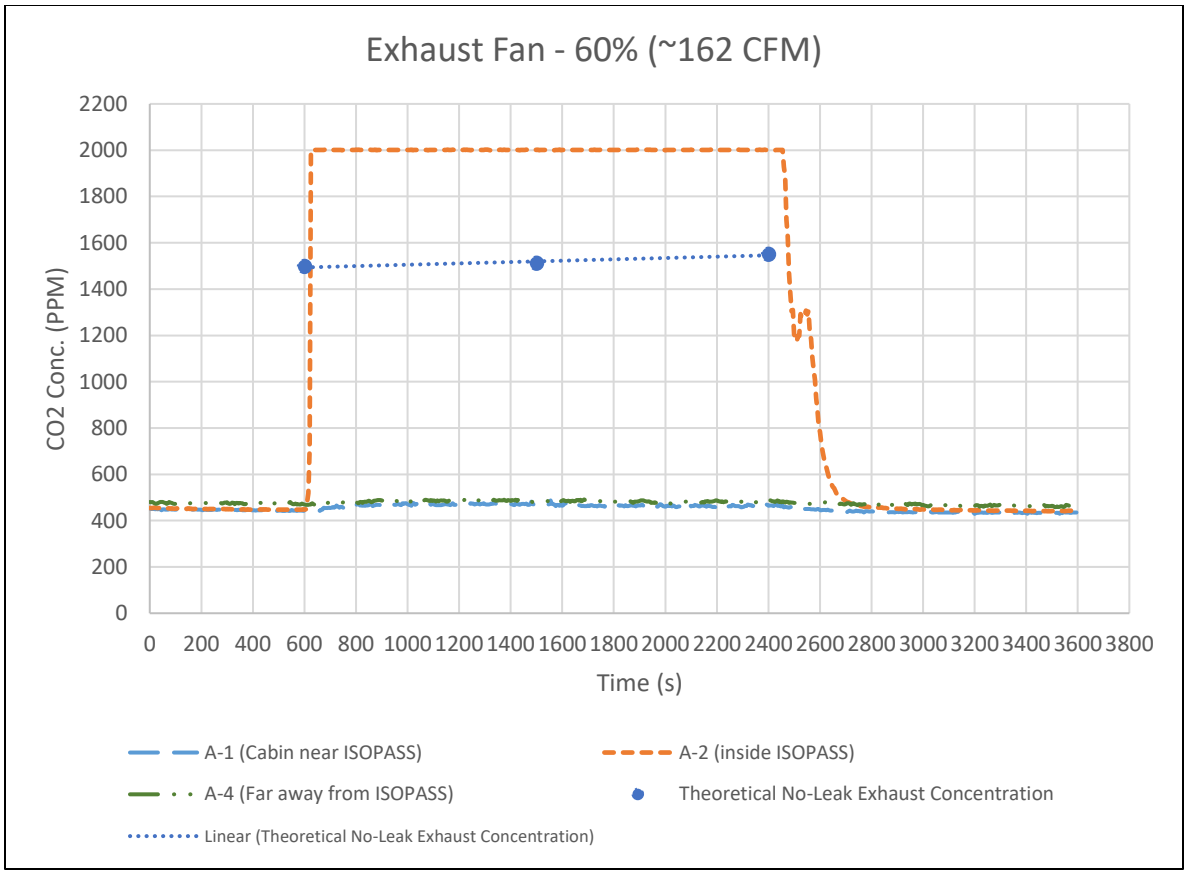

Figure 4.38 ISOPASS On, Gaspers On

The average background CO_2 levels at each sampling location before the tracer gas injection for this test were as follows:

A-1 (Cabin near ISOPASS):	446 ppm
A-2 (Inside ISOPASS):	450 ppm
A-4 (Cabin Away from ISOPASS):	475 ppm

At steady state concentration with the tracer gas injection on:

A-1 (Cabin near ISOPASS):	465 ppm
A-2 (Inside ISOPASS):	2001 ppm (at least)
A-4 (Cabin Away from ISOPASS):	483 ppm

Making the percent difference between the pre-test and the steady state gas on state approximately:

A-1 (Cabin near ISOPASS):	+4%
A-2 (Inside ISOPASS):	+345% (at least)
A-4 (Cabin Away from ISOPASS):	+2%

The results with the gaspers on closely resemble the results with the gaspers off. This was observed in the 767 testing and is confirmed for the 737 cabin as well, as expected. Again, we notice that the CO_2 concentrations outside of the ISOPASS increase very slightly during the tracer gas injection. As with the gaspers off tests, the CO_2 concentrations return to their pre-test values or even slightly lower, indicating that the increase in the concentrations during the test cannot likely be attributed to fluctuations in the atmosphere.

4.10 ISOPASS Exhaust Recirculation and Leakage

Upon reviewing the data for the ISOPASS on tests in the 737 cabin, it appeared that the CO_2 concentration in the cabin outside of the ISOPASS was increasing by 15 to 20 parts per million during the tracer gas injection consistently for each test. This increase is within the accuracy of the CO2 analyzers but, because it was consistent for all tests and both analyzers, the increase was judged to be real and not due to measurement uncertainty. It was suspected that this increase may have been due to some recirculation of the ISOPASS exhaust back into the cabin through adjacent exhaust vents. Layout and locations of these vents in the 737 cabin with respect to the ISOPASS and the ISOPASS exhaust are shown here in Figure 4.40:

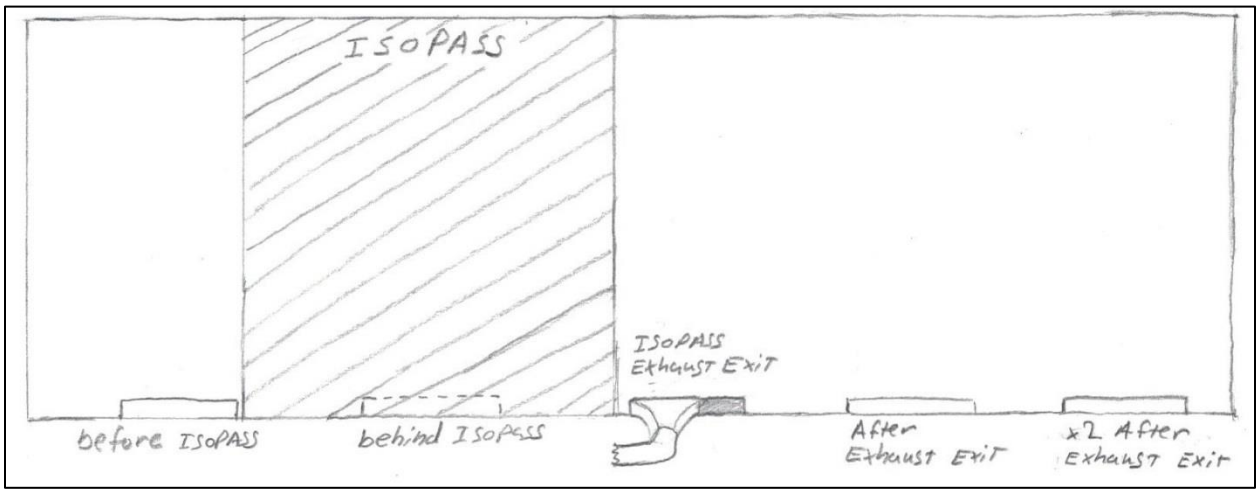

Figure 4.39 737 Vent Diagram

To test for recirculation, the sampling tubes that were previously placed at the front of the cabin and inside the ISOPASS were relocated to the exhaust vent before the ISOPASS and the exhaust vent after the ISOPASS exhaust exit. Please refer to Fig. 4.41 and Fig. 4.42 for photographs of the sampling locations for these recirculation and leakage tests.

Figure 4.40 Vent Before ISOPASS, 737 Cabin

Figure 4.41 Vent After ISOPASS Exhaust Exit, 737 Cabin

Once the sampling tubes had been placed in front of their respective exhaust vents, the test was conducted in the same manner as before.

4.10.1 Recirculation at 60% Fan Speed

Recirculation tests were completed once with gaspers off and once with gaspers on. Both tests were conducted with the ISOPASS exhaust fan set to approximately 160 CFM as before.

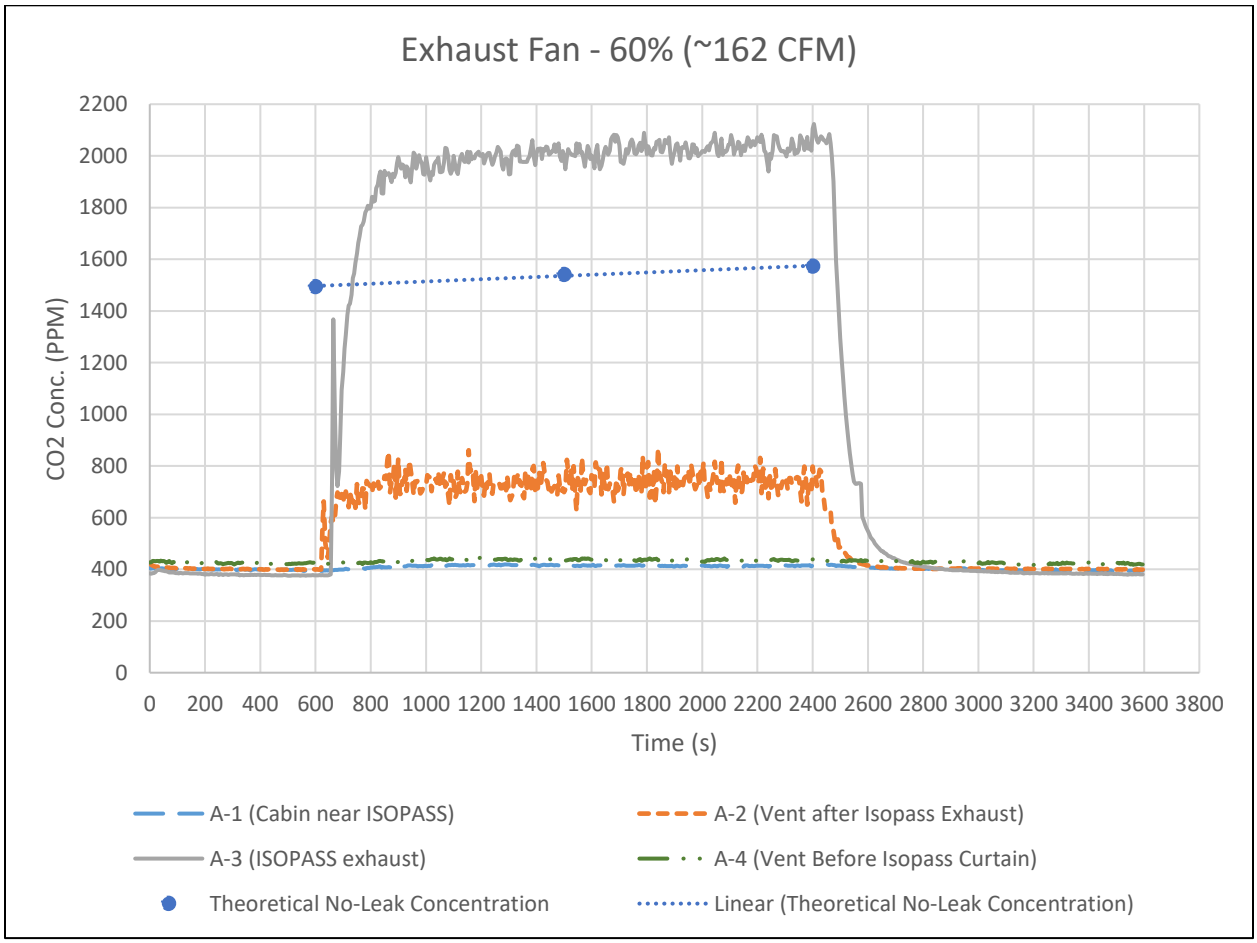

Figure 4.42 737 Recirculation Test, Gaspers Off, 60%

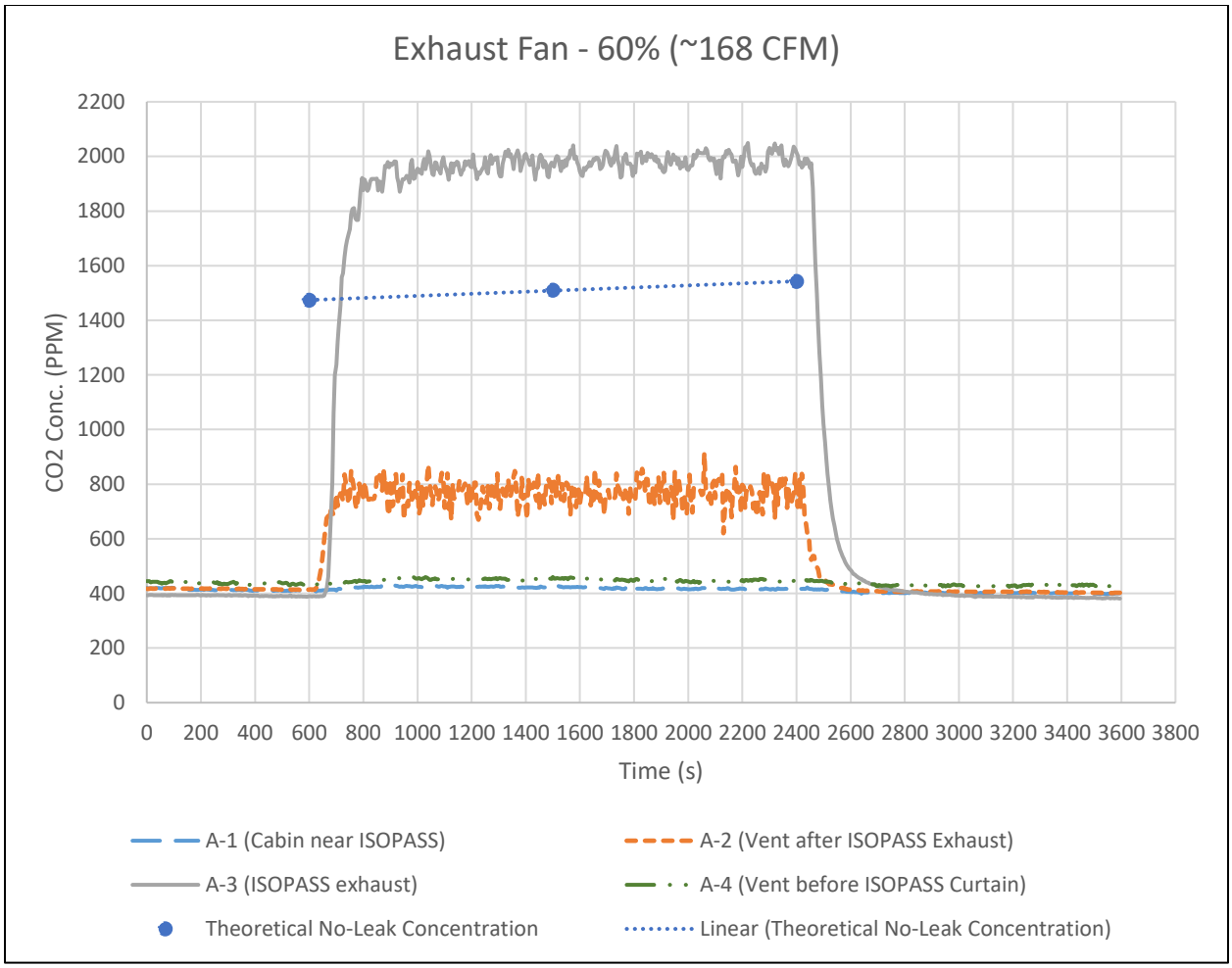

Figure 4.43 737 Recirculation Test, Gaspers On, 60%

For both the gaspers off and gaspers on conditions, we observe a significant rise in CO_2 concentration at the vent adjacent to the ISOPASS exhaust exit. This increase is essentially equal for each case, with the percent difference compared to ambient being 84% with gaspers off and 85% with gaspers on. Likewise, the concentration at the vent before the ISOPASS curtain increased by 2.6% for both gasper conditions. Distribution throughout the cabin differed slightly, with the concentration at the seat adjacent to the ISOPASS increasing by 3.6% with the gaspers off, and just 1.2% with the gaspers on.

After this, the ISOPASS exhaust flowrate was reduced to approximately 80 CFM to see if this would reduce or eliminate the recirculation. Measurements were made only in the gaspers on configuration as it was determined that the gasper condition did not affect the outcome of the test.

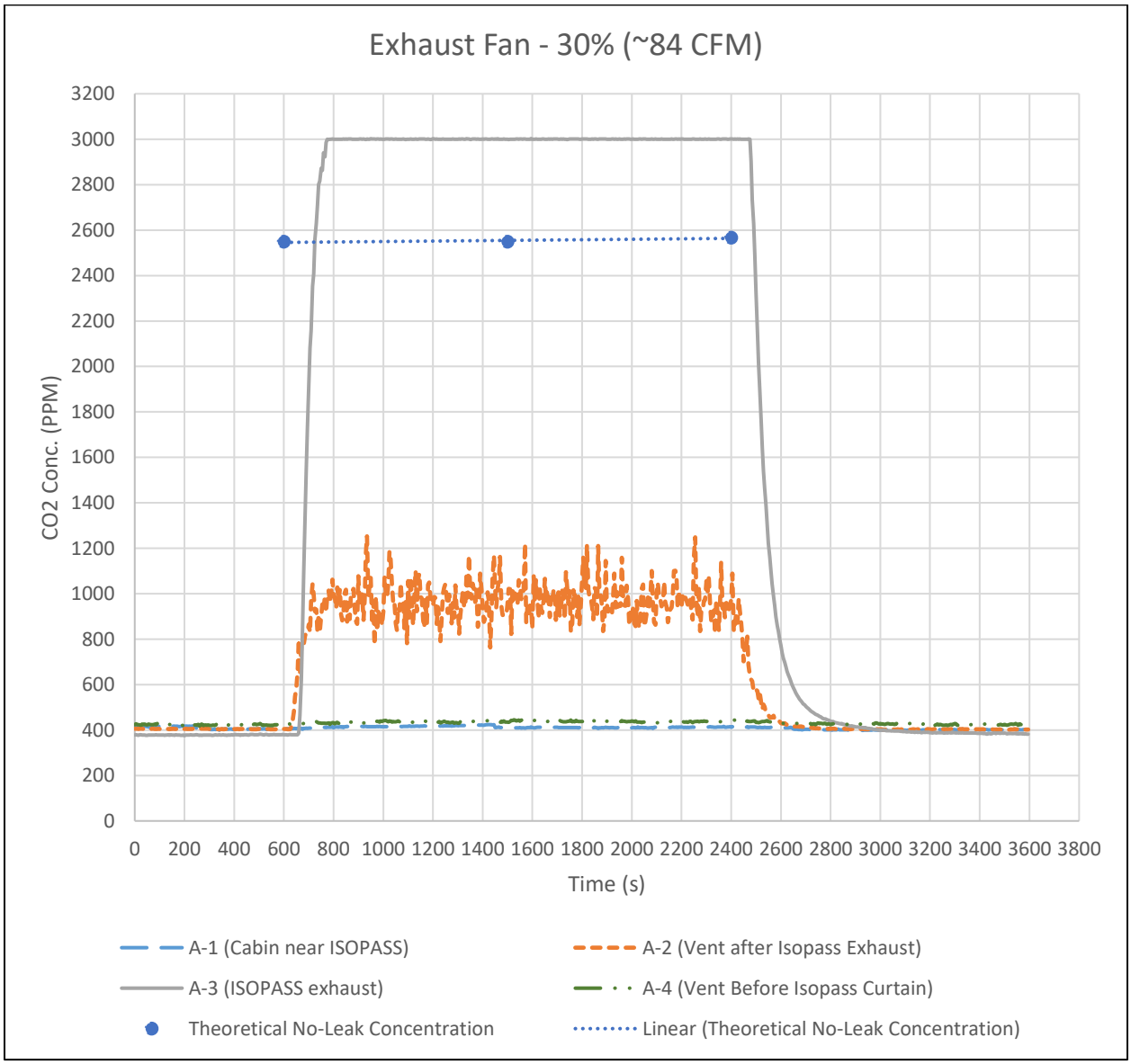

Figure 4.44 737 Recirculation Test, Gaspers On, 30%

Because the exhaust flowrate was lowered without lowering the tracer gas injection rate, the CO_2 concentration in the exhaust stream at 30% fan speed was higher than the concentration

at 60% fan speed. Because of this, the concentrations at the exhaust vents were also higher than in the 60% tests. The flowrate of any air returning through the exhaust vents was not measured during these tests, so the actual volume of the recirculation was not clear. The concentration at the exhaust vent after the ISOPASS exhaust increased by 140%, and the concentration at the vent before the ISOPASS curtain increased by 3.6%.

As evidence of the reduced volume of recirculation, the concentration at the seat adjacent to the ISOPASS increased by just 0.7%, essentially no change in concentration compared to the ambient.

4.10.2 Recirculation at 30% Fan Speed

An additional experiment was run at 30% fan speed with the exhaust vent sampling locations relocated to the vent behind the ISOPASS curtain, and to the vent x2 after the ISOPASS exhaust exit. The locations are shown in Fig. 6. Refer also to Fig. 12 and Fig. 13 for photographs of the sampling locations.

Figure 4.45 Vent Behind ISOPASS, 737 Cabin

The vent behind the ISOPASS is photographed from the top down perspective, with the curtain moved away from the wall for clarity. During the tests, the ISOPASS curtain rests against the wall.

Figure 4.46 Vent x2 After ISOPASS Exhaust Exit, 737 Cabin

The vent x2 after the ISOPASS exhaust exit did not have the metal mesh and housing present.

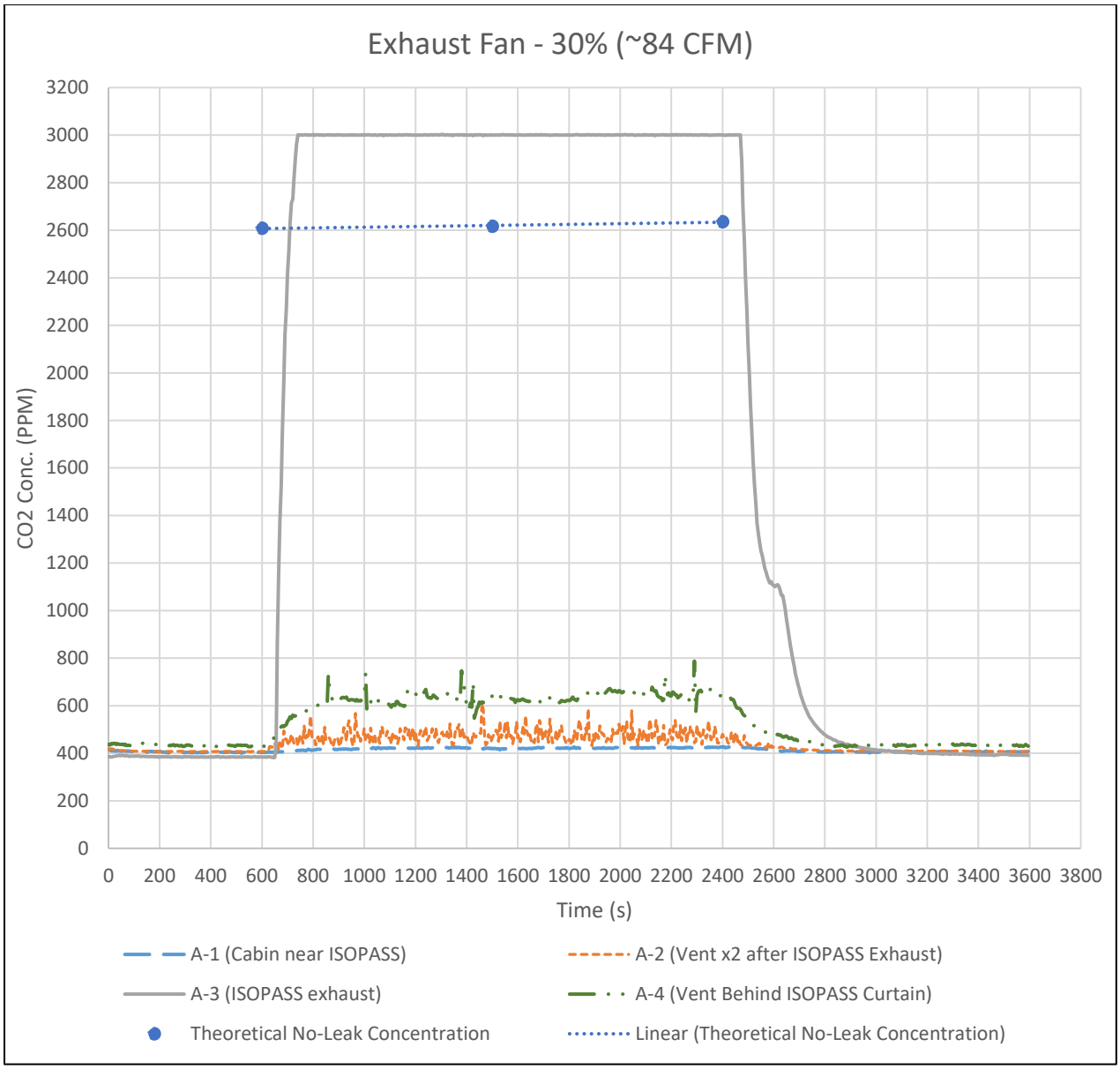

Figure 4.47 Relocated Recirculation Test, Gaspers On, 30%

Like previous tests, we observe a substantial increase in the CO_2 concentration in the exhaust vent adjacent to the ISOPASS exhaust exit. This concentration increase at the adjacent vent is less than previous tests, however, and the concentration two over from the ISOPASS exhaust exit is higher; with the vent behind the ISOPASS curtain (adjacent to the ISOPASS

exhaust exit) seeing an increase of 48% and the vent x2 after the ISOPASS exhaust exit increasing by 17%.

4.10.3 Smoke Visualization and Resealed Exhaust Exit

The initial assessment based on the concentration measurements made at the adjacent vents was that there was communication between exhaust vents, with the high flow from the ISOPASS exhaust forcing reverse flow in the adjacent vents. However, the results of the measurement for the additional vents led us to question that assessment. In order to better determine the flow characteristics, smoke visualization was employed.

During the smoke visualization, we did not notice any smoke coming into the cabin from any of the previously tested exhaust vents. Once the laser was directed at the ISOPASS exhaust exit itself, we noticed large quantities of smoke coming from around the connection to the exhaust vent. The connection between the ISOPASS exhaust at the exhaust vent was sealed up further with duct tape as best as possible and a final tracer gas test was conducted with the resealed ISOPASS exhaust exit. For this test, the two sampling tubes were both placed in the exhaust vents directly adjacent to the ISOPASS exhaust exit, where we had observed the highest concentration increases previously.

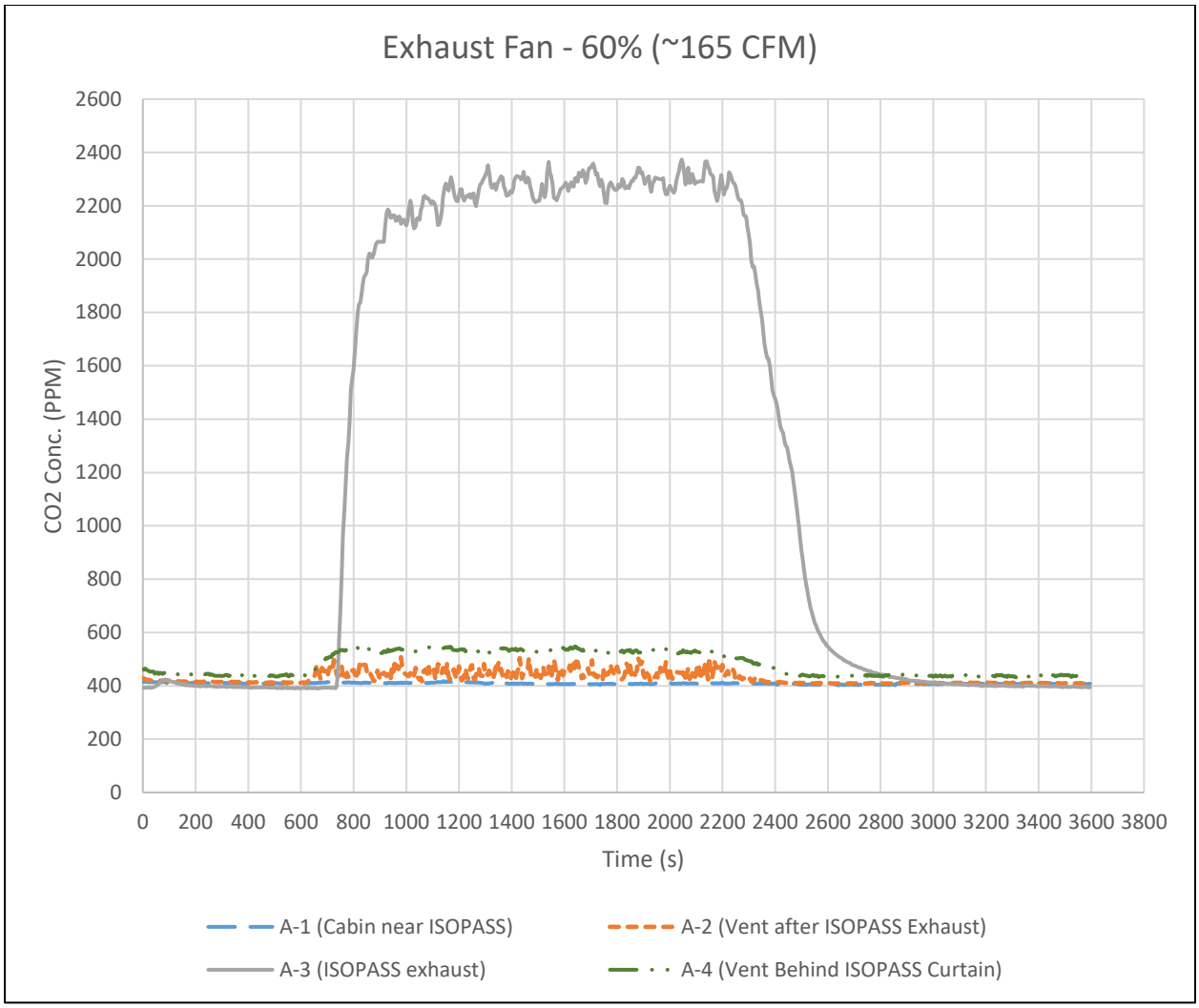

Figure 4.48 Recirculation Test, Resealed Exhaust Exit, 737 Cabin, 60%

With the resealed exit, the concentration at the vent after the ISOPASS exhaust exit increases by just 7.5% compared to the 85% increase before re-taping the exhaust exit. The concentration at the exhaust vent behind the ISOPASS curtain increased by 18%. The higher concentration behind the ISOPASS curtain compared to the vent after the ISOPASS exhaust exit may be due to extra accumulation behind the curtain.

4.10.4 ISOPASS Exhaust Leakage Conclusion and Recommendations

The results of this test suggest that the 'recirculation' we observed during the matched pair tests in the 737 cabin was in fact leakage from the connection between the ISOPASS exhaust and the 737's exhaust vent. Because the increase in the CO_2 concentration in the cabin during the matched pair tests was within the accuracy of the instrumentation, it was determined that this issue does not require any additional testing.

This experience shows that how the ISOPASS exhaust is ducted from the cabin is important. Typical aircraft cabin ventilation flows are about 15-20 cfm per seat. If there is approximately one vent row per seat, then the normal flow per vent would be about 45-60 cfm per vent. This flow will vary depending upon the number of seats per row and the spacing of the vents, but the 45-60 cfm flow is a representative value. At approximately 160 cfm, the ISOPASS exhaust will overwhelm the normal cabin exhaust flow and it will be important that the ISOPASS exhaust be sealed to the cabin exhaust vent to avoid leakage into the cabin. From an engineering perspective, this leakage is probably of minimal consequence as the reduction in concentration is complete within the measurement accuracy. However, from a psychological perspective, having some of the ISOPASS exhaust end up in the cabin may not be acceptable.

Even though it turned out that the ISOPASS exhaust was not being forced back into the cabin through adjacent exhaust vents as initially thought, it is entirely possible that it could have occurred given the flow path from the vents to the cabin "knee-space" in the 737 aircraft had the ISOPASS exhaust been connected in a slightly different manner. Thus, it is also important that the flow path of the cabin exhaust for a given make and model of aircraft be known and that the

ISOPASS exhaust be connected or vents blocked off to prevent flow of the ISOPASS exhaust back into the cabin through adjacent vents.

Chapter 5 - Summary and Conclusions

Tests were conducted in a mock-up of a section of a Boeing 767 aircraft cabin and a section of an actual Boeing 737 aircraft cabin to evaluate of the containment effectiveness of the ISOPASS negative pressure isolation system prototype. These tests were conducted in matched pair sets with the ISOPASS on and off. Gaspers on and gaspers off conditions were also tested. The containment effectiveness of the ISOPASS was tested by injecting a neutrally buoyant mixture of CO_2 and helium as a tracer gas at the ISOPASS location and measuring the CO_2 concentration at several locations inside and outside of the ISOPASS location. In the process, several other factors were considered, such as the observed stratification of CO_2 in the ISOPASS exhaust stream and potential recirculation and leakage of the ISOPASS exhaust in the 737 cabin. Additionally, an initial evaluation of the ISOPASS with a coughing mannequin was performed.

5.1 767 Mock-up Conclusions

With the ISOPASS on, ISOPASS off matched pair tests performed in the 767 cabin, it is clear that the ISOPASS prototype is entirely effective at containing the tracer gas and preventing its spread in the cabin. Additionally, the matched pair tests were conducted for both gaspers-on and gaspers-off conditions and it was determined that the inclusion or exclusion of gaspers in the ISOPASS makes no perceivable difference in the performance of the ISOPASS with an exhaust fan speed of 60%. The representative results discussed in this thesis are summarized in Table 5.1.

Table 5.1 767 Mock-up Matched Pair Results Summary

Analyzer	Pre-Injection	Steady State Tracer Gas Injection	Percent Difference
ISOPASS Off, Gaspers Off			
A-1	441 ppm	715 ppm	+62%
A-2	434 ppm	1050 ppm	+142%
A-4	446 ppm	524 ppm	+17%
ISOPASS Off, Gaspers On			
A-1	432 ppm	698 ppm	+61%
A-2	436 ppm	894 ppm	+105%
A-4	455 ppm	536 ppm	+18%
ISOPASS On, Gaspers Off			
A-1	443 ppm	433 ppm	-2%
A-2	437 ppm	2000+ ppm	+358%
A-4	462 ppm	459 ppm	-1%
ISOPASS On, Gaspers On			
A-1	424 ppm	421 ppm	-1%
A-2	428 ppm	2000+ ppm	+368%
A-4	452 ppm	449 ppm	-1%

We also found that, with gaspers off, the exhaust fan speed can be reduced to 30% without seeing any leakage from the ISOPASS. With gaspers on, the exhaust fan speed can be reduced to 20% with the same results. A cursory evaluation of the coughing mannequin was also completed. The results of the matched pair are largely comparable to those of the continuous

injection matched pair tests, suggesting that the force and direction associated with coughing does not affect the containment effectiveness of the ISOPASS. However, the coughing mannequin does appear to somewhat affect the distribution and flow pattern of the tracer gas around the cabin without the ISOPASS in place.

5.2 737 Cabin Conclusions

The results of the matched pair tests in the 737 cabin are comparable to the matched pair tests performed in the 767 mock-up. The ISOPASS prototype is entirely effective at containing the tracer gas and preventing its spread in the 737 cabin. The use of gaspers makes no perceivable difference in the containment effectiveness of the ISOPASS. Some differences between the 737 and the 767 testing were revealed during the ISOPASS off experiments. The ISOPASS off, gaspers on condition has greater mixing in the 737 cabin section compared to the 767 mock-up due to the smaller volume of the 737 section and higher number of gaspers in the 737 section compared to the 767 mock-up. With the ISOPASS off, the concentration near the front of the cabin increases much more during the tracer gas injection in the 737 compared to the 767 despite similar radial distances from the injection source for each cabin. The representative results discussed in this thesis are summarized in Table 5.2.

Table 5.2 737 Cabin Matched Pair Results Summary

Analyzer	Pre-Injection	Steady State Tracer Gas Injection	Percent Difference
ISOPASS Off, Gaspers Off			
A-1	405 ppm	655 ppm	+62%
A-2	408 ppm	1906+ ppm	+367%
A-4	427 ppm	659 ppm	+54%
ISOPASS Off, Gaspers On			
A-1	427 ppm	597 ppm	+40%
A-2	433 ppm	1988+ ppm	+359%
A-4	458 ppm	584 ppm	+28%
ISOPASS On, Gaspers Off			
A-1	409 ppm	423 ppm	+3%
A-2	416 ppm	2001+ ppm	+381%
A-4	430 ppm	442 ppm	+3%
ISOPASS On, Gaspers On			
A-1	446 ppm	465 ppm	+4%
A-2	450 ppm	2001+ ppm	+345%
A-4	475 ppm	483 ppm	+2%

Chapter 6 - Recommendations

Further research may be done on the effect of coughing on the containment effectiveness of the ISOPASS at containing airborne contaminants. The initial evaluation using the coughing mannequin is very positive, but only one matched pair set was completed. Additional matched pair tests and gaspers on and off conditions, matching the point source injection tests from this study, should be conducted to thoroughly evaluate the ISOPASS with the coughing mannequin.

The experiments conducted with the ISOPASS in this study were limited primarily to testing with the ISOPASS fully installed with the entrance flap closed, and the ISOPASS fully removed. However, in actual practice, the entrance flap may be opened and closed on occasion while attending the sick passenger. To further evaluate the ISOPASS, further testing should be conducted with the ISOPASS installed and the entrance open. Testing may also be done with the ISOPASS opened and then closed again part way through the experiment to study the effect that opening and closing the ISOPASS has on the concentration inside the cabin compared to the control with the ISOPASS off.

Finally, further consideration should be given to the connection between the ISOPASS and the aircraft's ventilation system while finalizing the design of the ISOPASS. To prevent any possible recirculation of contaminated air into the passenger compartment of the aircraft, it is important that the flow path of the cabin exhaust for a given make and model of aircraft be known and the ISOPASS exhaust be connected securely, with vents blocked off where there might be recirculation.

Chapter 7 - References

Patel, J. 2017. Experimental investigation of ventilation effectiveness and dispersion of tracer gas in aircraft cabin mockups. Master's Thesis, Kansas State University.

Shehadi, M. 2015. Airflow distribution and turbulence analysis in the longitudinal direction of a Boeing 767 Mockup Cabin. PhD diss., Kansas State University.

Anderson, M. 2012. Effect of gaspers on airflow patterns and the transmission of within an aircraft cabin environment. Master's Thesis, Kansas State University.

Trupka, A. 2011. Tracer gas mapping of beverage cart wake in a twin aisle aircraft cabin simulation chamber. Master's Thesis, Kansas State University.

Beneke, J. 2010. Small diameter particle dispersion in a commercial aircraft cabin. Master's Thesis, Kansas State University.

Jones, B. 2009. Advanced models for predicting contaminants and infectious disease virus transport in the airliner cabin environment (part 2). *Proceedings of the Transportation Research Board, Research on the Transmission of Disease in Airports and Aircrafts, Washington, D.C.*

Lebbin, P. 2006. Experimental and numerical analysis of air, tracer gas, and particulate movement in a large eddy simulation chamber. PhD diss., Kansas State University.

FAA. 2010. Environmental control and life support systems for flight crew and space flight participants in suborbital space flight, Version 1, Guide for 14 CFR § 460.11. Federal Aviation Administration, Washington, D.C.

NASA. 1994. Design for Human Presence in Space: An Introduction to Environmental Control and Life Support Systems. National Aeronautics and Space Administration, Washington D.C.

ASHRAE. 2018. ASHRAE standard: air quality in commercial aircraft (ANSI/ASHRAE 161-2018). Atlanta: ASHRAE.

ASHRAE. 2016. ASHRAE guideline: air quality in commercial aircraft (ASHRAE 28-2016). Atlanta: ASHRAE.

ASHRAE. 2007. Chapter 10, Aircraft. In *ASHRAE Handbook – Heating, Ventilating and Air-Conditioning Applications*. Atlanta: ASHRAE.

Madden, M. 2015. The effects of passenger loading and ventilation air on airflow patterns within an aircraft cabin. Master's Thesis, Kansas State University.

CDC. 2017. https://www.cdc.gov/quarantine/air/managing-sick-travelers/commercial-aircraft/infection-control-cabin-crew.html. Center for Disease Control, Washington, D.C.

WHO. 2008. http://www.who.int/tb/features_archive/aviation_guidelines/en/. World Health Organization, Geneva, Switzerland.

ICAO. 2009. Guidelines for states concerning the management of communicable disease posing a serious public health risk. International Civil Aviation Organization, Montreal, Canada.

Melikov, A.K., & Dzhartov, V. 2012. Advanced air distribution for minimizing airborne cross infection in aircraft cabin. In Proceedings of Healthy Buildings 2012 (3A.5) International Society of Indoor Air Quality and Climate.

Mo, H. 2002. Experimental and computational study of interactions of airflow inside aircraft cabin with human body. Master's Thesis, Kansas State University.

ASHRAE. 2013. Chapter 16, Ventilation and Infiltration. In *ASHRAE Handbook-Fundamentals*. Atlanta: ASHRAE.

Appendix A - Uncertainty Analysis

Many instruments are used throughout the ACER lab to measure and control parameters involved in testing. These instruments each have their own uncertainties. To analyze the uncertainty, the instruments are grouped into three sub-systems: the air supply system, the tracer gas injection, and the tracer gas sampling. The uncertainty of each sub-system is calculated and then combined to determine the overall uncertainty of the total system.

A.1 Experiment Repeatability

The accuracy of the measurements can only be as accurate as the overall experiment itself. To demonstrate the accuracy of the experiments, we will look at the standard deviation of the average at each different measurement location in the mock-up. From this, we can examine the repeatability of the experiments, as the airflow patterns may change from one test to the next. Because the ISOPASS-on experiments show negligible deviation, it is useless to compare these results. Instead, this section will focus on the ISOPASS-off experiments, which have much greater deviations and may be affected by slight air pattern changes more significantly.

To determine the standard deviation of the mean at each analyzer location, the regular standard deviation is taken over the same period as the average. The average is taken over a 200 – point section at steady state with the gas on, with a point taken every five seconds. The standard deviation over this period is calculated in Microsoft Excel. Once the standard deviation (σ_x) is calculated, the standard deviation of the mean can be calculated using equation A.1.

$$\sigma_{\bar{x}} = \frac{1}{\sqrt{n}} \cdot \sigma_x \tag{A.1}$$

With the standard deviation of the mean, the 95% confidence interval can also be calculated by multiplying $\sigma_{\bar{x}}$ by the 95% confidence factor, 1.960.

To assess the repeatability of the experiment, we can look at the pooled standard deviation of the mean for each analyzer over the three tests conducted for each condition (gaspers on and gaspers off, for the 767 cabin and the 737 cabin). This is calculated using Equation (A.2). The pooled standard deviation of the mean for each analyzer in the 767 mock-up cabin is given in Table A.1 and Table A.2.

$$\sigma_{\bar{x},pooled} = \sqrt{\frac{(n_1 - 1) \cdot {\sigma_{\bar{x}1}}^2 + (n_2 - 1) \cdot {\sigma_{\bar{x}2}}^2 + \cdots + (n_k - 1) \cdot {\sigma_{\bar{x}k}}^2}{(n_1 - 1) + (n_2 - 1) + \cdots + (n_k - 1)}} \qquad \text{(A.2)}$$

Table A.1 ISOPASS Off Gaspers Off Deviations, 767 Mock-up

$\sigma_{\bar{x}}$ **(ppm) ISOPASS Off, Gaspers Off**			
	A-1	**A-2**	**A-4**
Test 1	25.49	46.85	2.07
Test 2	32.34	34.84	3.55
Test 3	10.74	80.49	1.55
Pooled $\sigma_{\bar{x}}$	24.57	57.41	2.54

Table A.7.2 ISOPASS Off Gaspers On Deviations, 767 Mock-up

$\sigma_{\bar{x}}$ **(ppm) ISOPASS Off, Gaspers On**			
	A-1	**A-2**	**A-4**
Test 1	25.17	60.91	1.59
Test 2	20.26	59.07	1.1
Test 3	15.12	88.48	1.04
Pooled $\sigma_{\bar{x}}$	20.60	70.78	1.27

Recall that the A-1 analyzer was in the cabin near the ISOPASS location, the A-2 analyzer was inside the ISOPASS location, and the A-4 analyzers was in the cabin far away from the ISOPASS. As expected, the pooled standard deviation becomes smaller as the analyzer gets further away from the injection source.

Likewise, the pooled standard deviations are calculated for the 737 cabin and are given in Table A.3 and Table A.4.

Table A.3 ISOPASS Off Gaspers Off Deviations, 737 Cabin

$\sigma_{\bar{x}}$ **ISOPASS Off, Gaspers Off**			
	A-1	**A-2**	**A-4**
Test 1	7.01	77.17	0.99
Test 2	4.79	39.97	1.59
Test 3	3.27	47.7	2.27
Pooled $\sigma_{\bar{x}}$	5.25	57.24	1.70

Table A.4 ISOPASS Off Gaspers On Deviations, 737 Cabin

$\sigma_{\bar{x}}$ **ISOPASS Off, Gaspers On**			
	A-1	**A-2**	**A-4**
Test 1	5.90	9.45	0.98
Test 2	5.49	92.05	1.02
Test 3	3.31	12.9	1.03
Pooled $\sigma_{\bar{x}}$	5.03	53.94	1.01

The pooled standard deviation of each analyzer in the 737 cabin is smaller than in the 767 cabin. Similarly, the pooled standard deviation decreases as the analyzer gets further away from the injection source, as expected. However, note that the concentration at the A-2 analyzer during Gaspers On tests 1 and 3 peaks out at the 2000 ppm limit for significant periods, and thus the averages and standard deviations are not accurate. These values are denoted in red in Table A.4.

A.2 Air Supply Uncertainty

The air supply sub-system provides 1400 CFM of conditioned air to the 767 mock-up cabin, or 600 CFM of conditioned air to the 737 cabin. The flowrate, temperature, and pressure of the conditioned air is controlled by an Agilent DAQ using temperature sensors, pressure transducer, and flow meter. The range and uncertainty of each instrument is give below in Table A.5.

Table A.5 Supply Air Instrument Uncertainties (Madden, 2015)

Instrument	Uncertainty	Range
Agilent 34970A DAQ	0.06° C (RTD)	49Ω – 2.1kΩ
NI Field Point AI-110	0.07% of reading +0.0007% of range	0 – 5 V
PCI FE-1500 Flow Meter	2%	100-10000 fpm
Omega PX 653	0.25% F.S.	1” Water Column
	0.05% F.S. Repeatability	0 – 5 V
Omega 3-wire RTD	±(0.30 + 0.005*T) ℃	-50 – 250 ℃, Class B

In order to calculate the uncertainty of the flow rate of the supply air, the uncertainty of the two variables related to the supply air flow rate, temperature and pressure, must be

calculated. The uncertainty of the supply air temperature is calculated using Equation A.3 through A.6 below (Patel, 2017), where 'U' represents uncertainty. The uncertainty for the temperature is the same for both the 767 mock-up and the 737 mock-up.

$$\left(\frac{U_{temp}}{T_{supply}}\right)^2 = \left(\frac{U_{RTD}}{T_{Supply}}\right)^2 + \left(\frac{U_{DAQ}}{T_{supply}}\right)^2 \tag{A.3}$$

$$\left(\frac{U_{temp}}{T_{supply}}\right)^2 = \left(\frac{(0.30 + 0.005 * 15.6)\,°C}{288.8\,K}\right)^2 + \left(\frac{0.06\,°C}{288.8\,K}\right)^2 \tag{A.4}$$

$$\frac{U_{temp}}{T_{supply}} = 0.134\% \tag{A.5}$$

$$U_{temp} = T_{supply} * \ 0.134\ \% = 0.39\ °C = 0.70\ °F \tag{A.6}$$

Likewise, the uncertainty for the supply air pressure can be calculated. The pressure uncertainty for the 767 mock-up cabin's flow rate was previously calculated (Trupka, 2011). This is given in Equation A.7 and A.8.

$$U_{press} = \sqrt{U_{PCI}^2 + U_{omega}^2 + U_{NI}^2} \tag{A.7}$$

$$U_{press,1400cfm} = \sqrt{2\ \%^2 + 0.803\ \%^2 + 0.08\ \%^2} = 2.16\ \% \tag{A.8}$$

The pressure uncertainty for the 737 cabin's flow rate was previously calculated by Patel (2017). These calculations are given in Equation A.9 and A.10, below.

$$U_{press} = \sqrt{U_{PCI}^2 + U_{omega}^2 + U_{NI}^2} \tag{A.9}$$

$$U_{press,1400cfm} = \sqrt{2\ \%^2 + 0.0029\ \%^2 + 0.14\ \%^2} = 2.0\ \% \tag{A.10}$$

The overall supply air uncertainty can now be calculated using the root sum squared method. From Bernoulli's Equation, the pressure is related to the square of the velocity. Because

we are trying to find the uncertainty of the supply air velocity, the uncertainties of the temperatures and pressures must be divided by two before being squared, from the principle of partial derivatives. The total uncertainty for the supply air for each flow rate was previously calculated by Patel (2017), using Equations A.11 through A.14.

$$U_{suppy\ air@1400cfm} = \sqrt{\left(\frac{1}{2}U_{temp}\right)^2 + \left(\frac{1}{2}U_{press@1400cfm}\right)^2} \quad \text{(A.11)}$$

$$U_{suppy\ air@1400cfm} = \sqrt{\left(\frac{1}{2} * 0.134\ \%\right)^2 + \left(\frac{1}{2} *\ 2.16\%\right)^2} = 1.08\ \% \quad \text{(A12)}$$

$$U_{suppy\ air@600cfm} = \sqrt{\left(\frac{1}{2}U_{temp}\right)^2 + \left(\frac{1}{2}U_{press@600cfm}\right)^2} \quad \text{(A.13)}$$

$$U_{suppy\ air@600cfm} = \sqrt{\left(\frac{1}{2} * 0.134\%\right)^2 + \left(\frac{1}{2} * 2\right)^2} = 1.0\ \% \quad \text{(A.14)}$$

A.3 Tracer Gas Injection Uncertainty

The tracer gas injection sub-system involves the purity of the gases used for calibrating the CO_2 gas analyzers and the purity of the CO_2 and He used in the tracer gas, along with the mass flow controllers used to control the flow rate of the helium and carbon dioxide gases used in the tracer gas. The purity and uncertainty of each gas is given in Table A.6, below (Trupka, 2011).

Table A.6 Calibration Gas and Tracer Gas Uncertainties

Gas	Uncertainty/Purity
CO_2	0.5% / 99.5% pure
He	0.003% / 99.997% pure
500 ppm CO_2 – Air Mixture	2%
1000 ppm CO_2 – Air mixture	1%
2000 ppm CO_2 – Air Mixture	1%

The calibration gas uncertainty is again calculated using the root rum square method. This calculation was done by Patel (2017) using Equations A.15 and A.16.

$$U_{calib} = \sqrt{U_{500}^2 + U_{1000}^2 + U_{2000}^2} \tag{A.15}$$

$$U_{calib} = \sqrt{2\ \%^2 + 1\ \%^2 + 1\%^2} = 2.45\ \% \tag{A.16}$$

In addition to the calibration and tracer gas uncertainties, the tracer gas injection system also includes the CO_2 and He mass flow controllers and the PR 4000 power supply that controls them. The PR 4000 has 16-bit uncertainty and is considered to be negligible for this study. The uncertainties of the mass flow controllers are given in Table A.7.

Table A.7 Mass Flow Controller Uncertainties

Instrument	Uncertainty	Rated Flow
CO_2 **Mass Flow Controller**	1.0% F.S. (accuracy)	100 SLM
	±0.5% of reading (repeatability)	
	0.1% F.S. (resolution)	
	10 to 50 °C (operation)	
He Mass Flow Controller	1.0% F.S. (accuracy)	10,000 SCCM
	0.2% F.S. (repeatability)	
	0.1% F.S. (resolution)	
	0 to 50 °C (operation)	

The gas injection rates used in this study are 5 lpm for CO_2 and 3.07 lpm for He. The same injection rate was used in every test. Knowing this, the gas injection uncertainties can be calculated. The CO_2 injection uncertainty is calculated using Equations A.17 and A.18, and the He injection uncertainty is calculated using Equations A.19 and A.20.

$$U_{rep,CO_2} = \frac{0.2\% * 100\ LPM}{5\ LPM} = 4.00\ \% \tag{A.17}$$

$$U_{CO_2} = \sqrt{U_{rep,CO_2}^2 + U_{CO_2,purity}^2} = 4.03\ \% \quad \text{(A.18)}$$

$$U_{rep,He} = \frac{0.2\% * 10\ LPM}{3.07\ LPM} = 0.651\% \quad \text{(A.19)}$$

$$U_{He} = \sqrt{U_{rep,He}^2 + U_{He,purity}^2} = 0.651\ \% \quad \text{(A.20)}$$

A.4 Tracer Gas Sampling Uncertainty

Four CO_2 gas analyzers are used throughout the cabin during testing. These measure the concentration of the CO_2 in the air at each location and output the concentration in volts to an Agilent 34970 DAQ unit. The DAQ relays the voltage readings to the LabVIEW program on the computer. The DAQ and each analyzer have corresponding uncertainties. The range and uncertainty of each is given in Table A.8.

Table A.8 Tracer Gas Sampling Uncertainties

Model/Instrument	Uncertainty	Range
Edinburgh Gas card NG	2% of Range (accuracy)	0 – 3000 ppm
	0.3@zero, 1.5%@span (repeatability)	
PP Systems WMA-4	<1%@span (repeatability)	0 – 2000 ppm
	20 ppm (accuracy)	
PP Systems WMA-5	<1%@span (repeatability)	0 – 3000 ppm
	30 ppm (accuracy)	
Agilent 34970A DAQ	0.0035% of reading + 0.0005% of range	10V

From the previous studies conducted by Patel (2017) and Madden (2015), the linearity uncertainty of the CO_2 analyzers is shown to be very low, with the worst case in Patel's study being 0.0015%. Additionally, the uncertainties introduced to the system by the DAQ (Table A.4) and the instrument repeatability are shown to be negligible compared to the uncertainty of the calibration gasses. Thus, the total uncertainty of the tracer gas sampling system is dominated by

only the uncertainty of the calibration gas. Because the same or very similar analyzers were used in this study as in Patel's study, the same linearity and repeatability data will be used to calculate the total tracer gas sampling uncertainty here.

Table A.9 Linearity Uncertainty (Patel, 2017)

Calibration Date	A-1 Sensor	A-2 Sensor	A-3 Sensor	A-4 Sensor
08-24-2016	0.99998517	0.99998970	0.99999411	0.99999995
09-13-2016	0.99998001	0.99998207	0.99999840	0.99997675
10-24-2016	0.99998980	0.99999964	0.99999992	0.99999977
Average R-Squared Values	0.99998499	0.99999047	0.99999748	0.99999216
Linearity Uncertainty	0.00150%	0.00095%	0.00025%	0.00078%

Table A.10 Repeatability Uncertainty of Sampling System (Patel, 2017)

Sensor	CO_2 Concentration(ppm)	Output Voltage (V)	Repeatability (%)
A-1	518.56	1.28	0.26
A-2	608.63	1.52	0.30
A-3	500.13	0.51	0.25
A-4	398.97	0.61	0.50

Combining the data from Tables A.9 and A.10, along with the uncertainties calculated for the calibration and the data acquisition system, the total uncertainty for each analyze (U_{sensor}) can be calculated. As mentioned previously, the calibration uncertainty dominates the total uncertainty of the analyzer.

Table A.11 Total Sensor Uncertainty (Patel, 2017)

Sensor	$U_{calibration}$	$U_{linearity}$	$U_{repeatability}$	U_{DAQ}	U_{sensor}
A-1	2.45	0.00150	0.26	0.0095	2.46
A-2	2.45	0.00095	0.30	0.0103	2.47
A-3	2.45	0.00025	0.25	0.0068	2.46
A-4	2.45	0.00078	0.50	0.0071	2.50

A.5 Overall Uncertainty

Because the concentration data used in this study is not normalized, the overall uncertainty of the concentration measurements is a function of the tracer gas injection and the tracer gas sampling uncertainties only. The overall uncertainty can be found using Equation A.21.

$$U_{Concentration} = \sqrt{{U_{sample}}^2 + {U_{injection}}^2} \quad \text{(A.21)}$$

Thus, plugging in the uncertainties calculated previously, the overall concentration uncertainty becomes:

$$U_{Concentration} = \sqrt{2.47^2 + 4.03^2} = 4.73\% \quad \text{(A.22)}$$

Appendix B - Electronic Appendix Instructions

The full results for each experiment is included in the electronic appendix. The electronic appendix is included with this thesis in a folder titled “Electronic Appendix.zip”. In order to preserve the links between spreadsheets, it is recommended that the entire folder be extracted locally. The electronic appendix contains three subfolders labeled “Boeing 767”, “Boeing 737”, and “Uncertainty” These subfolders are explained in further detail in this section.

B.1 Boeing 767 Folder Directory

The “Boeing 767” folder contains five subfolders: “767 Matched Pair Tests”, “Calibration”, “Coughing Mannequin initial test”, “Minimum Exhaust Speed Tests”, and “Stratification Tests”. Each one of these subfolders contains the test data associated with that portion of the thesis.

The “767 Matched Pair Tests” folder contains the additional subfolders “767 ISOPASS Off” and “767 ISOPASS On”. Each of these folders is split between “Gaspers On” and “Gaspers Off” results. Within each gasper condition folder are subfolders for “Test 1 Data”, Test 2 Data”, etc. and a folder labeled “Analysis”. The data folders contain the raw data for the corresponding test, while the “Analysis” folder contains the fully analyzed results for each test, with the voltage to ppm conversions and graphs.

The “Calibration” folder contains the data and analysis for the calibration of the CO_2 analyzers performed before beginning the matched pair tests. The “Coughing Mannequin initial test” folder contains two subfolders “ISOPASS Off” and “ISOPASS On”. These folders contain the raw test data files along with an analysis file in the form “Coughing Isopass Off test1 Analysis”. The “Minimum Exhaust Speed Tests” folder has two subfolders, one for each gasper condition. Each of these subfolders contains subfolders for each fan speed tested. Each fan speed

subfolder is organized similarly to the matched pair tests, with “Test X Data” folders containing the raw data taken from the computer and an “Analysis” folder containing the concentration conversions and plots. Finally, the “Stratification Tests” folder contains three subfolders “CO2 directly into exhaust”, “Mass Balance with Resealed Rotameter”, and “Strat and Mixing Tests”. Each of the “CO2 directly into exhaust” and “Strat and Mixing Tests” folders contain subfolders for each test as before. Inside each of these folders are the raw data files and the analysis file for that test. Because the “Mass Balance with Resealed Rotameter” has only one test, there are no additional subfolders, but rather just the raw data files and analysis file.

B.2 Boeing 737 Folder Directory

The “Boeing 737” folder contains two subfolders “737 Matched Pair Tests” and “737 Recirculation Tests”. The “737 Matched Pair Tests” is organized in the same way as in the “Boeing 767” folder, with subfolders for ISOPASS off and ISOPASS on, each having additional subfolders for gaspers off and gaspers on. Like the “Boeing 767 Matched Pair Tests” section, each gasper condition has a folder for the raw data for each test, and a folder containing the analysis files.

The “737 Recirculation Tests” folder contains five subfolders, one for each testing condition, labeled “Recirculation Gaspers Off Isopass On 60%”, “Recirculation Gaspers On Isopass On 60%”, “Recirculation Gaspers On Isopass On 30%”, “Recirculation Relocated Analyzers”, and “Resealed Exhaust Exit”. Each one of these subfolders contains an analysis file and a folder labeled “Data”, which contains all the raw data files for that test.

B.3 Uncertainty Folder Directory

The “Uncertainty” folder contains a file named “Standard Deviations and Distribution”, which is used for calculations related to the uncertainty (Appendix A). Because this file is used for both the 767 and 737 experiments, it is under its own folder.